



---

University Federico II of Napoli

Electrical Engineering Department

PhD in Electrical Engineering  
XX course

METHODS AND TECHNIQUES FOR THE EVALUATION OF  
LIGHTNING INDUCED OVERVOLTAGES ON POWER LINES.  
APPLICATION TO MV DISTRIBUTION SYSTEMS FOR IMPROVING  
THE QUALITY OF POWER SUPPLY

PhD Thesis of  
FABIO MOTTOLA

Tutor  
PROF. AMEDEO ANDREOTTI

PhD Coordinator  
PROF. GUIDO CARPINELLI

---

NOVEMBER 2007



# INDEX

Charter 1: Introduction .....	pag. 1
1.1    A survey on the investigations on Lightning Induced Overvoltages .....	pag. 2
1.2    Contents and Contribution of the Thesis .....	pag. 4
Chapter 2: Numerical Methods for Lightning	
Induced Overvoltages Calculations .....	pag. 8
2.1    Introduction .....	pag. 8
2.2    Return Stroke Models .....	pag. 10
2.2.1    The Lightning Mechanism .....	pag. 10
2.2.2    Return Stroke Models .....	pag. 13
2.2.3    Channel Base Current .....	pag. 21
2.2.4    Mode Validation .....	pag. 30
2.3    Calculation of lightning return stroke fields .....	pag. 34
2.4    Propagation effect .....	pag. 38
2.5    Field to Line Coupling .....	pag. 40
2.6    Indirect Lightning Induced Voltages Calculation ....	pag. 47
Chapter 3: Analytical Formulations for Lightning	
Induced Overvoltages Calculations .....	pag. 54
3.1    The Rusk Formulae .....	pag. 55
3.1.1    The Lightning Electromagnetic Field .....	pag. 56
3.1.2    Field to Line coupling .....	pag. 64

3.2	Chowdhuri and Gross Formulae .....	pag. 67
3.2.1	Electromagnetic field .....	pag. 68
3.2.2	Field to Line coupling .....	pag. 70
3.2.3	Induced Voltage: Step Current along the lightning channel .....	pag. 71
3.2.4	Induced Voltage: Linearly rising front current along the lightning channel ....	pag. 74
3.3	Liew and Mar Formulae .....	pag. 76
3.3.1	Induced Voltage: Lightning Step Current along the lightning channel .....	pag. 77
3.3.2	Induced Voltage: Linearly rising front current along the lightning channel .....	pag. 78
3.4	Hoidalén Formulae .....	pag. 81
3.4.1	Electromagnetic Field over a lossless ground ...	pag. 81
3.4.2	Effect of lossy ground .....	pag. 82
3.4.3	Induced Voltage .....	pag. 83
3.5	Exact Closed Form Solution .....	pag. 87
3.5.1	Lightning Electromagnetic Field appraisal .....	pag. 89
3.5.2	Field to Transmission Line coupling .....	pag. 102
3.5.3	Induced Voltages appraisal .....	pag. 105
3.6	Analysis of closed form .....	pag. 115
3.6.1	Rusck Formulae .....	pag. 115
3.6.2	Chowdhuri and Gross Formulae .....	pag. 117
3.6.3	Liew and Mar Formulae .....	pag. 118
3.6.4	Hoidalén Formulae .....	pag. 119

#### Chapter 4: Application to MV Distribution Systems

	for improving the Quality of Power Supply .....	pag. 124
4.1	Lightning parameters .....	pag. 126
4.2	The IEEE Method .....	pag. 130

4.3	Method Based on Monte Carlo Technique .....	pag. 133
4.4	Application to operating condition of MV Distribution Network .....	pag. 135
	Conclusions .....	pag. 142
	Appendix A.1 .....	pag. 143
	A.1.1 Integral (3.115) .....	pag. 143
	A.1.2 Integral (3.116) .....	pag. 145
	A.1.3 Integral (3.129) .....	pag. 146
	A.1.4 Integral (3.130) .....	pag. 147
	Appendix A.2 .....	pag. 149
	A.2.1 Derivation of the Rusck Formula .....	pag. 149

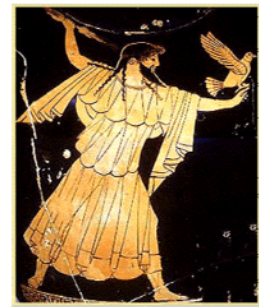
## List of symbols

$c$	Free space light velocity
$c'$	per-unit-length capacitance
$d$	Horizontal distance between the lightning channel and the line
$e_r$	Electric field radial component
$e_x$	Electric field line axial component
$e_z$	Electric field vertical component
$h$	Line height
$h_y$	Magnetic field y-component
$h_\varphi$	Magnetic field azimuthal component
$i(x, t)$	Current along the line
$I_0$	Return stroke peak current
$l'$	per-unit-length inductance
$L$	Line length
$q$	Charge distribution
$R$	Observation point to source point distance
$T$	$L / c$
$u(t)$	Heaviside function
$v$	Return stroke velocity
$v(x, t)$	Voltage along the line
$z'$	Source point vertical abscissa
$Z_c$	Line characteristic impedance
$\beta$	$v / c$
$\gamma$	$1 / \sqrt{1 - \beta^2}$
$\delta$	$\sqrt{d^2 + x^2} / \gamma$
$\delta_l$	$\sqrt{d^2 + x_l^2} / \gamma$
$\epsilon_0$	Permittivity of free space
$\mu_0$	Permeability of free space
$\tau$	$\beta ct - h$
$\tau_m$	$\beta(ct - x) - h$
$\tau_p$	$\beta(ct - x) + h$
$\zeta_0$	Free space characteristic impedance

# CHAPTER 1

## INTRODUCTION

Lightning is one of the natural phenomena that have amazed the human beings since the beginning of the civilization. In the history of almost all societies there are records that relate lightning to a punishment from a powerful god. In ancient times, some important personalities of the public life tried to protect themselves against it by techniques based on myths. For example, Julius Caesar used to wear a laurel crown and the Romans emperors used to wear a skin striped from a cow under their robes during thunderstorms. But with time, people started questioning these techniques and started wondering whether this phenomena arising in the sky was an act of god or a natural phenomenon.



In 1752 Benjamin Franklin proposed its kite experiment to show that a lightning flash is a result of electricity and movement of charges. Since then, the scientific community has tried to understand the

physical mechanism and the consequences of lightning flashes.

Nowadays, in the field of the power system, the lightning activity is one of the main causes of a-periodic disturbances on distribution networks which seriously affect the power quality and in particular the so-called *lightning indirect activity*.



Due to the limited height of distribution lines of medium and low voltage distribution networks as compared to that of the structures in their vicinity, indirect lightning return strokes are more frequent events than direct strokes, and for this reason we shall focus on such a type of lightning event.

## **1.1 A survey on the investigations on Lightning Induced Overvoltages**

In 1908, K.W. Wagner [1] carried out the first theoretical investigation of induced lightning surges on power transmission lines. He assumed the following conditions. A charged thunder cloud situated above a power transmission line will induce charges with opposite polarity in the line. On the assumption that free charges can move to earth via the leakage resistance of the line during the time when the field is determined by the fact that the resulting potential of the line should be equal to zero. If the charge of the thunder-cloud, and with it also the inducing field, suddenly disappears, the induced charges will be free to move out on the line is given by the product of the height of the conductor above the ground and the inducing electrical field strength prior to the lightning discharge. The

fronts and half-value times of the waves are given by the variation along the line of the inducing field strength, which implies very flat surges.

In 1929, Bewley [2] improved Wagner's theory by taking account of the fact that the inducing field cannot disappear instantaneously but must have a limited time derivative.

An article written by Aigner in 1935 [3] is interesting considering that it is the first time in the literature on the present topic that the inducing effect of the vertical lightning path of a lightning stroke to ground is taken into account.

In 1942, C.F. Wagner and McCann [4] published a paper which must be considered fundamental to the modern conception of the nature of the induced overvoltages. In this paper, it is the first time, excepting the above mentioned attempt by Aigner, that the influence of the charge and current in the lightning channel during the return stroke is introduced and it is shown that it is the field of the lightning path which is of a dominating importance in comparison with the field of the thunder-cold.

In a paper published in 1948 Szpor [5] has calculated the induced voltages caused by a vertical lightning stroke using other, and more complicated, assumptions than Wagner and McCann. Szpor takes account of the magnetic as well as the electrostatic induction, but treats the problem as quasi-stationary, stating that the results are valid only in the immediate vicinity of the lightning stroke.

In 1954 Golde [6] published an investigation dealing with the influence of the induced voltages on the fault frequency of power-distribution lines. In his calculations of the induced voltages his assumptions are somewhat different from those of Wagner and McCann. The influence of the different assumptions on the maximum value of the induced voltages may, however, not be great.. In Golde's calculations, which are carried out by a numerical integration method, only the scalar potential is computed.

In 1955, R. Lundholm [7] computed the induced voltages on short and long high-voltage transmission lines with approximately the same assumptions of

Wagner and McCann. The new point in Lundholm's treatment are principally a new theory for the relation between the velocity of the return stroke and the lightning current and a definition of the induced voltage. In deducing the formula of the induced voltage, Lundholm neglects the magnetic field, which implies that the result at last from the theoretical point of view is not quite satisfactory.

In 1958 Rusck [8] computed the induced voltages on short and long low-voltage transmission lines by means of a closed form expression which is still used in important international standard [9].

In 1967 [10] Chowdhuri and Gross proposed two closed form expressions for computing the induced overvoltages in the same hypothesis of Rusck, obtaining different results.

In 1986 [11] Liew and Mar, modifying the Chowdhuri-Gross approach, have proposed also closed form solutions.

In 2001 [12] Hoidalén has proposed a closed form which accounts for finite ground conductivity.

In addition, starting from the early '90s, the more and more increasing request of power quality has pushed many other researches to focus on the indirect lightning phenomenon solving the problem by means of more and more sophisticated numerical approaches.

## **1.2 Contents and Contribution of the Thesis**

In recent years, in literature many efforts have been directed to improve the knowledge of the lightning phenomenon and its effects on power circuits. In particular, many numerical approaches have been proposed for the evaluation of the overvoltages induced on an overhead line by indirect lightning. Also closed form solutions have been proposed and it is important to underline that they are very important both in the design phase and in parametric evaluation and sensitivity analysis. Closed form solutions provide considerable insight into the phenomenon, which is often obscured in numerical approaches. All the closed

form proposed so far in literature are approximated and/or incomplete as we will show in the thesis. The first significant contribution of the present work is that of obtaining the *exact closed form solution*, overcoming errors and/or approximations in the closed form solutions so far available in literature. Another contribution will be that of using our exact formulation to check the accuracy of the other closed form solutions, which is still object of an international debate [13, 14]. The work will carry on with the analysis of the effects of the indirect lightning on distribution network and on the methods used for improving the quality of power supply.

The thesis is organised as follows:

- o chapter 2 will be devoted to introductive aspects of the lightning phenomenon and to summarise the numerical approaches used to calculate the induced overvoltage due to indirect lightning;
- o chapter 3 will be devoted to the analytical formulation of the indirect lightning problem. An exact closed form solution will be presented and used to discuss the other formulae adopted in literature;
- o chapter 4 will be devoted to the analysis of the effects of indirect lightning on power quality. A method based on the Monte Carlo technique will be used to improve the commonly used IEEE method [9]. The results will be analysed and discussed in order to obtain methods to improve distribution network design and operational control.

***Acknowledgments***

*It has been an honour and great pleasure to pursue my PhD studies at the Electrical Engineering Department of University Federico II of Napoli. During these last three years, I had the opportunity to cooperate with a large number of people that have made this moment possible to happen.*

*I would like to express my gratitude chiefly to Prof. Amedeo Andreotti for his fundamental guide all along the three years of PhD and his constant and helpful support.*

*I am also grateful to Prof. Luigi Verolino for him helpful and valuable comments and advice.*

## References

- [1] K.W. Wagner, “Elektromagnetische ausgleichsvorgange in freileitungen und kabeln”, (in German), par. 5, Leipzig, 1908.
- [2] L. W. Bewley “Traveling Waves due to lightning”, AIEE Trans. 48, pp. 1050 – 1064, 1929.
- [3] V. Aigner, “Induzierte Blitzuberspannungen und ihre Beziehung zum ruck wartigen”, Überschlag, ETZ 56, pp. 497-500, 1935.
- [4] C.F. Wagner, G.D. Mc Cann, “Induced Voltages on Transmission Lines”, AIEE Transactions, Vol. 61, pp. 916- 930, 1942.
- [5] S. Szpor, “A new theory of the induced overvoltages“, Cigré Report 308, 1948.
- [6] R. H. Golde, “Indirect lightning Surges on overhead distribution lines”, The electrical research associations, S/T 75, Leatherhead, 1954.
- [7] R. Lundholm, “Induced Overvoltages on Transmission lines and their bearing on the lightning performance of medium voltage networks”, Duplic Goteborg, 1955.
- [8] S. Rusck, “Induced Lightning over-voltages on power transmission lines with special reference to the overvoltage protection of low-voltage networks”, Trans. Royal Inst. of Tech., no. 120, pp.1-118, 1958.
- [9] IEEE Guide for improving the lightning performance of electric power overhead distribution, IEEE Standard 1410, 2004.
- [10] P. Chowdhuri and E.T.B. Gross, “Voltage surges induced on overhead lines by lightning strokes”, Proc. IEE, Vol. 114, no.12, pp. 1899-1907, Dec. 1967.
- [11] A.C. Liew, S.C. Mar, “Extension of the Chowdhuri – Gross Model for Lightning Induced Voltage on Overhead Lines”, IEEE Trans. Power Systems, Vol. 1, no. 2, pp240-247, 1986.
- [12] H.K. Høidalen, “Analytical Formulation of Lightning-Induced Voltages on Multiconductor Overhead Lines Above Lossy Ground”, IEEE Trans. Electromagnetic Compatibility, vol.45, no.1, pp.92-100, Feb. 2003.
- [13] C.A. Nucci, F. Rachidi, M. Ianoz, C. Mazzetti, “Comparison of two coupling models for lightning-induced overvoltage calculations”, IEEE Transactions on Power Delivery, vol.10, no.1, pp.330-339, Jan. 1995.
- [14] P. Chowdhuri S. Li, P. Yan, “Review of research om lightning-induced voltages on an overhead line”, IEE Proc. Generation, Transmission, Distribution, Vol. 148, No. 1, January 2001.

## **CHAPTER 2: NUMERICAL METHODS FOR LIGHTNING INDUCED OVERVOLTAGES CALCULATIONS**

In literature, many numerical approaches have been proposed for the evaluation of the overvoltages induced on an overhead line by indirect lightning. These approaches are based on different models which will be presented and discussed in this chapter. In what follows the focuses will be on:

- 1) introduction to the indirect lightning problem;
- 2) lightning return stroke models;
- 3) lightning electromagnetic field evaluation;
- 4) coupling between lightning electromagnetic field and power line.

In the final part of the chapter the lightning induced voltages predicted by some numerical methods will be presented and discussed.

### **2.1 Introduction**

Since the early years of the past century, many researchers activities focused on the estimation of lightning induced overvoltages. K.W. Wagner [1] in 1908, Bewley [2] in 1929 and Norinder [3] in 1936, stated that the overvoltages

produced by indirect lightning were produced, basically, via electrostatic induction by charged clouds. According to K.W. Wagner [1], when the lightning discharge occurs, the charge bound to the line is released in form of travelling waves of voltage and current. Wagner did not consider the electromagnetic field radiated by the lightning discharge. In the early 1940's C.F. Wagner and McCann [4], based on Schonland's [5] investigations on the nature of the lightning discharge, published a paper in which the overvoltage was considered due to a phase of lightning named return stroke phase. Also in recent years, in literature many efforts have been directed to improve the knowledge of the lightning phenomenon and its effects on power circuits. In particular, many numerical approaches have been proposed for the evaluation of the overvoltages induced on an overhead line by indirect lightning. In all these approaches, the overvoltage calculations deal with three main phases involving the lightning phenomenon and its effects:

- 1) the return stroke phase generating the electromagnetic field;
- 2) the field propagation;
- 3) interaction between the field and the line conductors.

In figure 2.1 these three phases are depicted. The lightning return stroke electromagnetic field is evaluated by employing a lightning return-stroke current model. This model describes the waveform of the return stroke current as a function of height and time along the vertical channel. To this aim, the return stroke channel is generally considered as a straight vertical antenna (as depicted in fig. 2.1). The electromagnetic field is then evaluated and, by considering also the propagation effects, the field is used to calculate the induced overvoltages by means of a coupling model which describes the field to line conductors interaction.

In the next paragraph 2.2 the return stroke models, along with a brief description of the basics behind a lightning flash, will be presented and discussed.

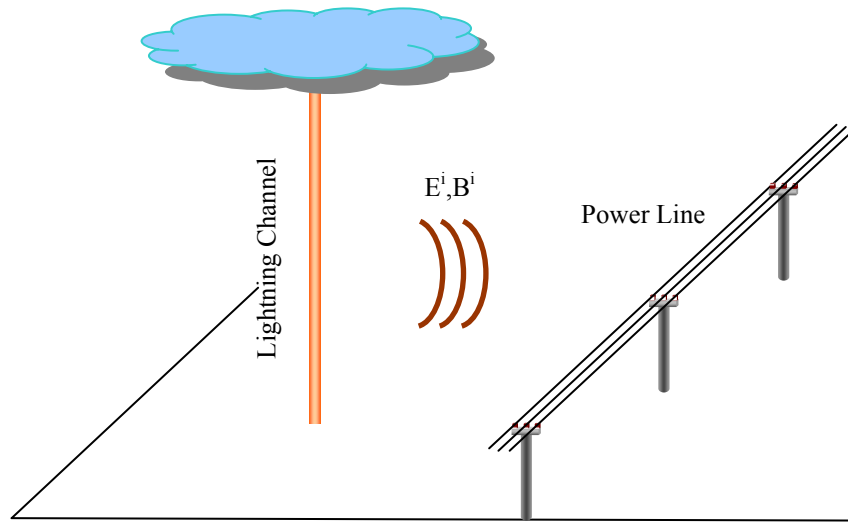


Figure 2.1: Pictorial representation of the three main phases of the lightning event for the induced overvoltages calculations.

The paragraph 2.3 will be devoted to the evaluation of the electromagnetic field radiated by a return stroke and, in the paragraph 2.4 the propagation of the field will be discussed. The field to line coupling models will be discussed in paragraph 2.5.

## 2.2. Return Stroke Models

Lightning electromagnetic field is generally calculated making use of a return stroke current model which specifies the spatial-temporal distribution of the lightning current along the channel. In this paragraph the return stroke models, along with a brief description of the basics behind a lightning flash, will be summarised and discussed. Obviously, most attention will be given to the mathematical models constructed to represent the return stroke electromagnetic fields.

### 2.2.1 The Lightning Mechanism

Lightning flashes can produce three types of electrical discharge: between two clouds (inter-cloud flashes), within the same cloud (intra-cloud flashes) or

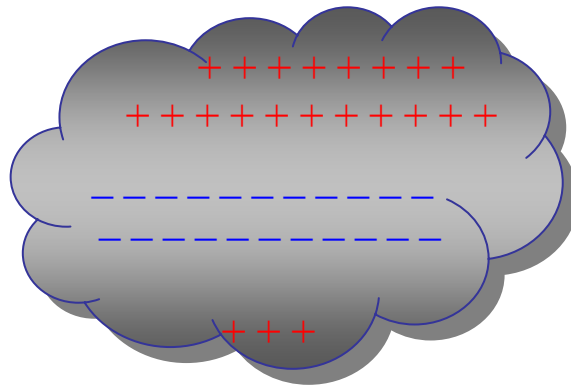


Figure 2.2: Charge distribution in a thunder cloud

between cloud and ground. In literature, traditionally, the most severe induced overvoltages are considered due to the cloud to ground flashes. Then, in the following the mechanism of the cloud to ground flashes is described more in details.

A thundercloud has three charge centres as shown in figure 2.2: one large positive charge centre at the top of the cloud, one negative charge centre in the middle of the cloud, and one small positive charge pocket at the base of the cloud [6].

Normally, a cloud to ground flash takes place either from the negative charge centre or the positive charge centre to ground. The former leads to a negative ground flash where the latest leads to a positive ground flash. Researchers have observed from the electromagnetic field signatures of lightning flashes that a cloud to ground flash has an initial stage that takes place in the cloud. This electrical breakdown process is called preliminary breakdown [7]. This process leads to the formation of a conductive channel propagating, from the cloud towards the ground, in a stepped manner. This is called a stepped leader. In many cases all this process, the initial electrical breakdown and the stepped leader are termed as preliminary breakdown. In this chapter, the initial electrical discharge that takes place inside the cloud will be termed preliminary breakdown and the stepping process will be named as the stepped leader. In the negative stepped leader, the length of each step is around 50 m [7].

When the negative stepped leader is propagating towards the ground, it will induce charges of the opposite polarity at the surface of the ground. When the stepped leader is about 100 meters from the ground level, the intense electric field at the ground level will be able to initiate upward electrical discharges from the tip of the tall objects at ground level. Such discharges are called upward connecting leaders. Several of these upward connecting leaders will be launched from different objects, but only one will be able to join the stepped leader with the ground via an upward connecting leader. After this connection between the stepped leader and the ground is made, a wave of zero potential will propagate along the stepped leader channel to neutralize the charges deposited along it [7]. This will result in a luminous event that propagates from the ground to cloud with a speed close to the speed of light. This is called a return stroke. Once the channel is established between the cloud and ground several such strokes can take place along the same conductive channel. Typically a ground flash may last for about 0.5 s with a mean number of strokes between four and five.

There is not much information available on the mechanism of the positive flashes. However, available information indicates that its mechanism is similar to the negative with some differences. For instance, observations show that the positive stepped leader propagates more or less continuously towards the ground [7]. Moreover, positive flashes may contain a single return stroke while the negatives may contain several.

As can be seen, all the processes associated with either the positive or the negative ground flashes involve the movement of electrical charges. This will result in an electromagnetic field that will propagate in air. In the following subparagraph some details will be presented on the different return stroke models utilized to generate electromagnetic fields similar to those generated by lightning return strokes.

### ***2.2.2 Return Stroke Models***

A comprehensive review of the return stroke models to represent lightning return stroke could be found in the literature [7,8]. Rakov and Uman, in [8], have been defined four classes of return stroke models:

- 1) gas dynamic or “physical” models, which are primarily concerned with the radial evolution of a short segment of the lightning channel and its associated shock wave;
- 2) electromagnetic models that are usually based on a lossy, thin-wire antenna approximation to the lightning channel. These models involve a numerical solution of Maxwell’s equations to find the current distribution along the channel from which the remote electric and magnetic fields can be computed;
- 3) distributed-circuit models that can be viewed as an approximation to the electromagnetic models described above and that represent the lightning discharge as a transient process on a vertical transmission line characterized by resistance (R), inductance (L), and capacitance (C) per unit length;
- 4) Engineering models in which a spatial and temporal distribution of the channel current (or the channel-charge density) is specified based on such observed lightning return-stroke characteristics as current at the channel base, the speed of the upward propagating front, and the channel luminosity profile.

The gas dynamic model are primarily used to reproduce physical parameters of the return stroke. The other models are mainly used to reproduce the electromagnetic field from a return stroke. In this chapter we shall limit the discussion to the engineering models. Infact most of the methods for induced overvoltages calculations are based on engineering models.

An engineering model for return stroke current is a mathematical specification of the spatial-temporal distribution of the lightning current along the discharge channel  $i(z',t)$ , or the channel line charge density  $\rho(z',t)$ . Such a mathematical specification includes the return stroke wavefront velocity, which is generally one of the model inputs [9], the charge distribution along the channel, and a number of adjustable parameters related, to a certain extent, to the discharge phenomenon [7] and which should be inferred by means of model comparison with experimental results [10]. Outputs can be directly used for computation of electromagnetic fields. In these models the lightning channel is generally assumed to be straight, vertical and perpendicular to the conducting ground plane, as shown in figure 2.3, where the geometry of the problem is also defined.

From an engineering point of view, the models of main interest are those in which the return stroke current  $i(z',t)$  can be related to the specified channel-base current  $i(0,t)$ , since only the channel-base current can be measured directly and for which experimental data are available. For this reason, the most used engineering models presented in literature give the mathematical specification of the spatial-temporal distribution of the lightning current along the discharge channel  $i(z',t)$  as follows [11]:

$$i(z',t) = u(t - z'/v_f) P(z') i(0,t - z'/v) \quad (2.1)$$

where  $u$  is the Heaviside function,  $v_f$  is the return stroke wavefront velocity,  $v$  is the propagation velocity of the return stroke current, and  $P(z')$  is the attenuation function of the return stroke current along the channel, which was proposed by Rakov and Dulzon [12]. The next subparagraph will be devoted to the main models of channel-base current  $i(0,t)$  presented in literature.

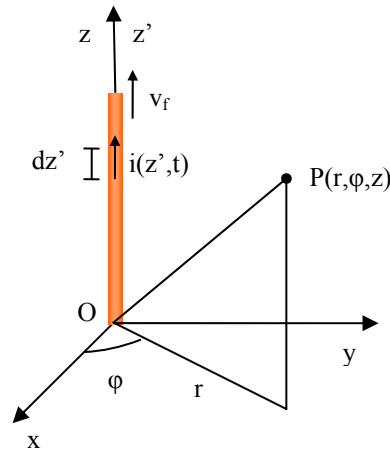


Figure 2.3: Return stroke channel.

The most commonly adopted return stroke models for lightning induced overvoltages calculations are:

- the Bruce and Golde model (BG), proposed in [13];
- the Travelling Current Source model (TCS), proposed by Heidler [14];
- the Transmission Line model (TL), proposed by Uman and McLain [9];
- the Modified Transmission Line model, with a linearly decay current (MTLL), proposed by Rakov and Dulzon [12];
- the Modified Transmission Line model, with an exponential decay current (MTLE), proposed by Nucci et al. [15].

These five main models are summarised in table 2.1. In this table, according with expression (2.1), both the propagation velocity of the return stroke current  $v$  and the attenuation function of the return stroke current along the channel  $P(z')$  are specified for each model. In particular, in table 2.1  $H$  is the channel length,  $\lambda$  is the decay constant of the current along the channel and  $c$  is the free space light velocity. For sake of completeness other two return stroke engineering models will

also be presented at the end of this subparagraph: the Master, Uman, Lin and Standler (MULS) model reported in [16] and the Diendorfer and Uman (DU) model [17].

Model	$P(z')$	$v$
BG (Bruce and Golde [13])	1	$\infty$
TCS (Heidler [14])	1	$-c$
TL (Uman and McLain [9])	1	$v_f$
MTLL (Rakov and Dulzon [12])	$1 -  z' /H$	$v_f$
MTLE (Nucci et al. [15])	$\exp(- z' /\lambda)$	$v_f$

Table 2.1: Return stroke model summarization according [11]

### 1) Bruce and Golde (BG) Model

Bruce and Golde proposed a simple model of return stroke in which the channel-base current propagates along the channel undistorted and unattenuated. The expression of this current model reads:

$$i(z', t) = \begin{cases} i(0, t) & z' \leq v_f t, \\ 0 & z' > v_f t, \end{cases} \quad (2.2)$$

An equivalent expression in terms of the line charge density  $\rho(z', t)$  on the channel was proposed by Thottappillil et al. in [18] by means of the continuity equation:

$$\rho(z', t) = \lim_{\Delta z' \rightarrow 0} \frac{1}{\Delta z'} \left[ \int_0^t i(z' + \Delta z', \tau) d\tau - \int_0^t i(z', \tau) d\tau \right] \quad (2.3)$$

An initial charge distribution, which takes into account the effects of the charges stored in the corona sheath of the leader, is instantaneously removed by the current. By combining the expressions (2.2) and (2.3) the instantaneously removed charge is obtained and reads [18]:

$$\rho(z', t) = \frac{i(0, z'/v_f)}{v_f} \quad (2.4)$$

According with the hypothesis of instantaneous charge removal, the removed charge (2.4) is time independent.

## 2) Travelling Current Source (TCS) model

This model was proposed by Heidler in [14]. In this type of model, the return stroke current may be viewed as generated at the upward-moving return stroke front and propagating downward. In the TCS model, current at a given channel section turns on instantaneously as this section is passed by the front. Channel current may be viewed as a downward-propagating wave originating at the upward-moving front, and the expression reads:

$$i(z', t) = \begin{cases} i(0, t + z'/c) & z' \leq v_f t \\ 0 & z' > v_f t \end{cases} \quad (2.5)$$

The equivalent formulation of this model in terms of charge distribution reads:

$$\rho(z', t) = -\frac{i(0, z'/v)}{c} + \frac{i(0, z'/v^*)}{v^*} \quad (2.6)$$

with  $v^* = v_f / (1 + v_f / c)$ . Eventually, the TCS model reduces to the BG model if the downward current propagation speed is set equal to infinity instead of the speed of light.

### 3) *Transmission Line (TL) model*

In this model, proposed by Uman and McLain [9], the current is assumed to travel undistorted and unattenuated upwards the lightning channel at a constant velocity  $v$ . The expression of this model is:

$$i(z', t) = \begin{cases} i(0, t - z'/v) & z' \leq v_f t, \\ 0 & z' > v_f t. \end{cases} \quad (2.7)$$

The transfer of charge takes place only from the bottom of the leader channel to the top; thus no net charge is removed from the channel, i.e.  $\rho(z', t) = 0$ . This being an unrealistic situation with respect to the present knowledge of lightning physics [20]. However, in [19] the authors show that the TL model is in fairly good agreement with measurements. Moreover in [19] the authors show that the early time field prediction of the TL model is very similar to that of the more physically reasonable models.

Eventually, one can note if  $v = \infty$ , the TL model reduces to the BG model.

### 4) *Modified Transmission Line Linear (MTLL) model*

The Transmission Line model, with a linear decay current, was proposed by Rakov and Dulzon [12]. This model can be viewed as incorporating a current source at the channel base, which injects a specified current wave into the channel, that wave propagating upward without distortion but with specified linear attenuation as seen from the corresponding current expression which reads:

$$i(z', t) = \begin{cases} i(0, t - z'/v)(1 - z'/H) & z' \leq v_f t, \\ 0 & z' > v_f t. \end{cases} \quad (2.8)$$

with  $H$  the specified channel height. The equivalent formulation of this model in terms of charge distribution reads:

$$\rho(z', t) = \frac{1 - z'/H}{H} \frac{i(0, t - z'/v_f)}{v_f} + \frac{1}{H} Q(t) \quad (2.9)$$

whit  $Q(t)$  the total charge transfers from the ground to the channel at the time  $t$ . It is given by:

$$Q(t) = \int_{z'/v}^t i(0, \tau - z'/v) d\tau \quad (2.10)$$

### 5) *Modified Transmission Line Exponential (MTLE) model*

This model was proposed by Nucci et al. [15] and it is similar to the MTLL one. This model can be viewed as incorporating a current source at the channel base, which injects a specified current wave into the channel, that wave propagating upward without distortion but with specified exponential attenuation as seen from the corresponding current expression which reads:

$$i(z', t) = \begin{cases} i(0, t - z'/v) \exp(-z'/\lambda) & z' \leq v_f t \\ 0 & z' > v_f t \end{cases} \quad (2.11)$$

The equivalent formulation of this model in terms of charge distribution reads:

$$\rho(z', t) = \exp(-z'/\lambda) \frac{i(0, t - z'/v)}{v} + \frac{\exp(-z'/\lambda)}{\lambda} Q(t) \quad (2.12)$$

with  $Q(t)$  the total charge transfers from the ground to the channel at the time  $t$ , still given by expression (2.10).

The two modified transmission line models MTLL and MTLE represent a modification of the TL model, in which the attenuation is not considered. This attenuation was introduced to take into account the effect of the charges stored in the corona sheath of the leader, and subsequently discharged during the return stroke phase via the upwards current [15]. Thus, the fields predicted by these two models result in a better agreement with experimental results. However, if one considers that for lightning induced overvoltages calculations it is the early time region of the field that plays the major role [22], it follows that the TL model, for the problem of interest, can be considered a useful and relatively simple engineering tool.

#### 6) *Master, Uman, Lin and Standler (MULS) model*

The Master, Uman, Lin and Standler model (MULS) [16] results from physic considerations and from experimental tests. Originally proposed by Uman, Lin e Standler (LUS) it was modified by Master (MULS). According to this model, the return stroke current is composed by three terms: a uniform current  $i_u$  which is the sequel of the leader current, an impulsive current  $i_p$  propagating upwards, to take in account the collapse of the return stoke wavefront, and a current  $i_c$  due to the removal of the charges stored in the corona sheath of the leader. For the latter term the surge current is assumed distributed along the channel with a double exponential mathematical form with an exponential decay with the cannel height.

#### 7) *The Diendorfer and Uman (DU) model*

In the Diendorfer and Uman model [17], the return-stroke current may be viewed as generated at the upward-moving return stroke front and propagating

downward. The current at a given channel section turns on exponentially as this section is passed by the front. The expression of the DU model reads:

$$i(z', t) = \begin{cases} i(0, t + z'/c) - i(0, z'/v^*) \exp[-(t - z'/v_f)/\tau_D] & z' \leq v_f t \\ 0 & z' > v_f t \end{cases} \quad (2.13)$$

where  $v^* = v_f / (1 + v_f / c)$  and  $\tau_D$  is the decay time constant of the current. The current expression (2.13) involves two terms: the first is a downward-propagating current as in the TCS model that exhibits an inherent discontinuity at the upward-moving front, and the second term being an opposite polarity current which rises instantaneously to the value equal in magnitude to the current at the front and then decays exponentially with a time constant  $\tau_D$ .

The equivalent formulation of this model in terms of charge distribution reads:

$$\rho(z', t) = -\frac{i(0, t + z'/c)}{c} - \left[ \frac{i(0, z'/v^*)}{v_f} + \frac{\tau_D}{v^*} \frac{di(0, z'/v^*)}{dt} \right] \exp[-(t - z'/v_f)/\tau_D] + \frac{i(0, z'/v^*)}{v^*} + \frac{\tau_D}{v^*} \frac{di(0, z'/v^*)}{dt} \quad (2.13)$$

Eventually if  $\tau_D = 0$  the DU model reduces to the TCS model.

### **2.2.3 Channel-base current**

Channel-base current measurements have been performed by means of instrumented towers in some countries, and statistical elaboration of lightning current data have been presented (e.g. [23, 24]). Usually, positive flash occurrences are less frequently than the negative ones and have also a lower peak

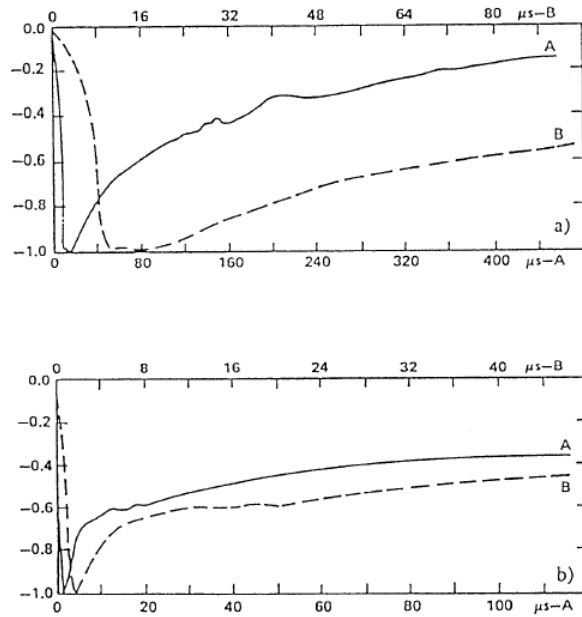


Figure 2.4: Typical channel-base current wave shapes for the first negative return strokes a) and for subsequent negative return strokes b) adapted from [23].

current-derivative. For this reason only lightning with negative charge to ground will be considered.

Typical channel-base current wave shapes for negative return strokes is reported in figure 2.4. This figure, as reported by Berger et al. [23], shows both the first (fig. 2.4a) and subsequent (fig. 2.4b) strokes. The statistics of lightning current parameters which are most significant for the evaluation of induced overvoltages (peak value and front steepness) are shown in table 2.2.

Stroke	95 %		50 %		5 %	
	First	Subs	First	Subs	First	Subs
$I_{\text{peak}}$ [kA]	14	4.6	30	12	80	30
Time to crest [ $\mu\text{s}$ ]	1.8	0.2	5.5	1.1	18	4.5
$\left(\frac{di}{dt}\right)_{\text{max}}$ [kA/ms]	5.5	12	12	40	32	120

Table 2.2 Statistics of peak amplitude, time to crest and maximum front steepness for first and subsequent negative return strokes [23].

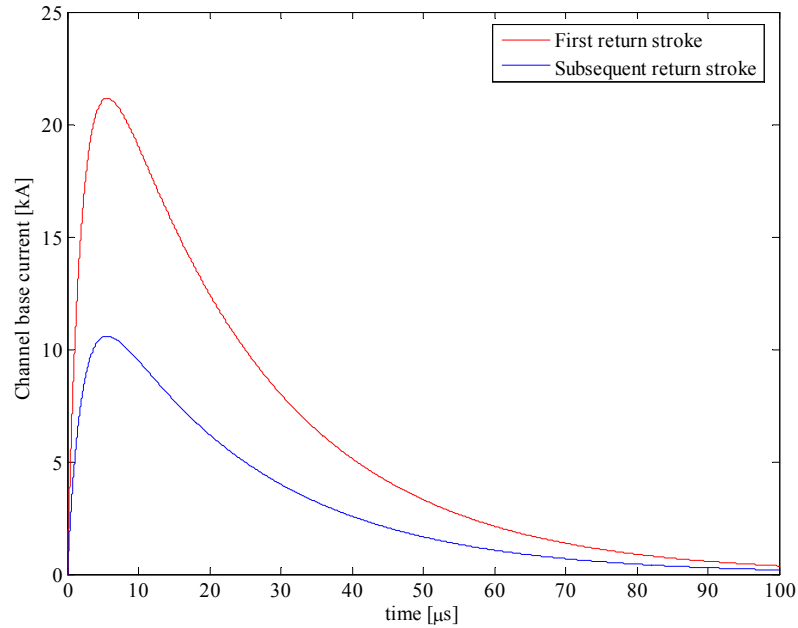


Figure 2.5: Bruce and Golde model for channel base current.

Typical channel base current waveshapes lead to several models adopted in literature for the return stroke models. In the following the most commonly adopted are presented.

1) *Bruce and Golde model*

The channel-base current proposed by Bruce and Golde in [13] have a double exponential form. In particular, Bruce and Golde proposed a channel base current expression for both the first and the subsequent return stroke, which reads:

$$i_{first}(0, t) = I_0(e^{-\alpha t} - e^{-\beta t}) \quad (2.14)$$

$$i_{subs}(0, t) = \frac{I_0}{2}(e^{-\alpha t} - e^{-\beta t}) \quad (2.15)$$

with  $I_0$  the peak value of the channel-base current. The value of the parameters in (2.14) and (2.15) assumed by Bruce and Golde are reported in table 2.3. Figure 2.5 shows the channel base current waveshape proposed by Bruce and Golde.

2) *Pierce and Cianos model*

Pierce, in [25], proposed a similar model to that of Bruce and Golde, but he considered different values for the current parameters  $I_0$ ,  $\alpha$  and  $\beta$ . The values he proposed are reported in table 2.3. Moreover, in [26], Pierce and Cianos proposed a new base channel current model in which a second current component added to the usual one (2.14) for the first return stroke. This second component have also a double exponential form, and leads to a more realistic waveshape, since it adjusts the longer time value of the current. The expression reads:

$$i_{first}(0,t) = I_0(e^{-\alpha t} - e^{-\beta t}) + I_{0i}(e^{-\gamma t} - e^{-\delta t}) \quad (2.16)$$

The values of the parameters  $I_{0i}$ ,  $\gamma$  and  $\delta$  are reported in table 2.3.

Parameters	First		Subsequent	
	Bruce and Golde	Pierce and Cianos	Bruce and Golde	Pierce and Cianos
$I_0$ [kA]	30	20	15	10
$I_{0i}$ [kA]	-	2	-	2
$\alpha$ [s <sup>-1</sup> ]	4.4 10 <sup>4</sup>	2 10 <sup>4</sup>	4.4 10 <sup>4</sup>	2 10 <sup>4</sup>
$\beta$ [s <sup>-1</sup> ]	4.6 10 <sup>5</sup>	2 10 <sup>6</sup>	4.6 10 <sup>5</sup>	2 10 <sup>6</sup>
$\gamma$ [s <sup>-1</sup> ]	-	10 <sup>3</sup>	-	10 <sup>3</sup>
$\delta$ [s <sup>-1</sup> ]	-	10 <sup>4</sup>	-	10 <sup>4</sup>

Table 2.3: Values of the parameters for the Bruce and Golde, and the Pierce and Cianos models proposed for the channel base current [13,25,26].

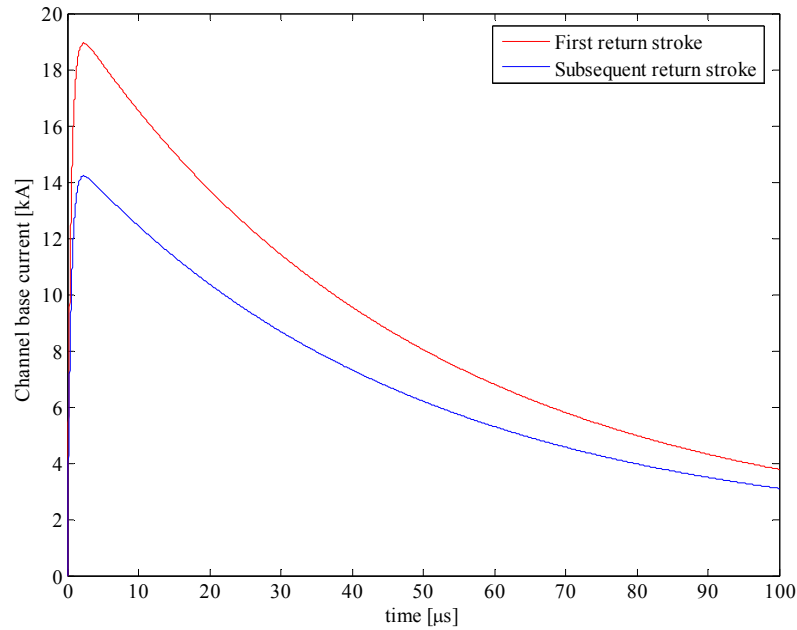


Figure 2.6: Pierce and Cianos model for channel base current.

Also for the subsequent return strokes, the same adjustments are applied, and the proposed values of the parameters are also given in table 2.3. Figure 2.6 shows the channel base current waveshape proposed by Pierce and Cianos, both for the first and the subsequent return strokes.

Eventually, one can note that both the Bruce and Golde model and the Pierce and Cianos one are characterized by an unrealistic convex channel-base current wavefront with a maximum current derivative at  $t = 0$ .

### 3) *Heidler model*

The Heidler model was presented in [14]. This model reproduces the observed concave rising portion of a typical channel base current waveform, i.e. it does not exhibit a discontinuity in its time derivative, unlike the double-exponential model above presented. The expression of this model reads:

$$i(0,t) = \frac{I_0}{\eta} \frac{(t/\tau_1)^n}{1+(t/\tau_1)^n} \exp(-t/\tau_2) u(t) \quad (2.17)$$

with  $\eta = \exp[-(\tau_1/\tau_2)(n\tau_2/\tau_1)^{1/n}]$ ,  $\tau_1$  the time constant of rising front current,  $\tau_2$  the decay constant of the wave form of the current,  $n$  a integer number in the range  $2 \div 10$ , and  $I_0$  is the amplitude of the channel base current. The expression (2.17) allows one to change conveniently the current peak, maximum current derivative, and associated electrical charge transfer nearly independently by changing  $I_0$ ,  $\tau_1$  and  $\tau_2$  respectively.

In table 2.4 typical values for the  $I_0$ ,  $\tau_1$  and  $\tau_2$  parameters are given [27]. The correspondent channel base current is plotted in figure 2.7. In figure 2.8 is also plotted a zoom of the channel base current. In this figure the concave rising portion of the current can be observed. Eventually, note that by changing  $I_0$ ,  $\tau_1$  and  $\tau_2$ , the subsequent return strokes could also be modelled.

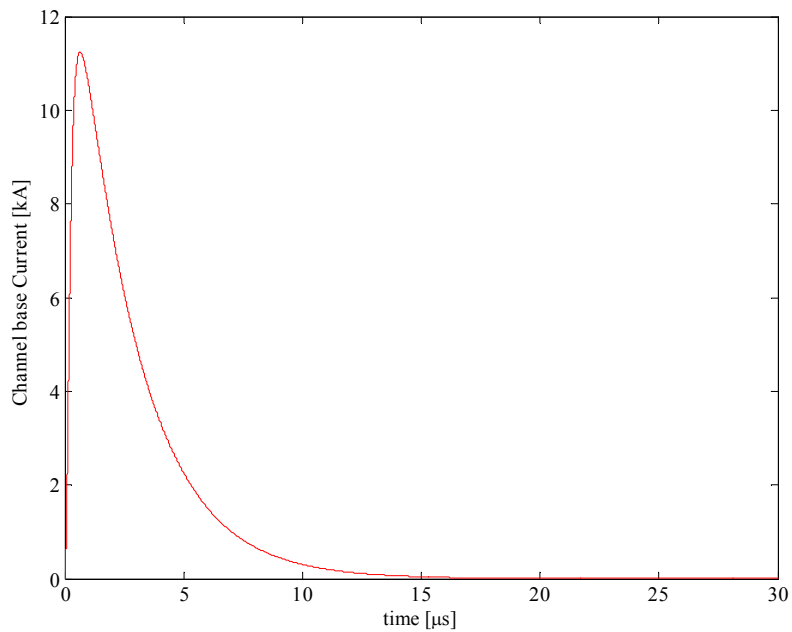


Figure 2.7: Heidler model for channel base current.

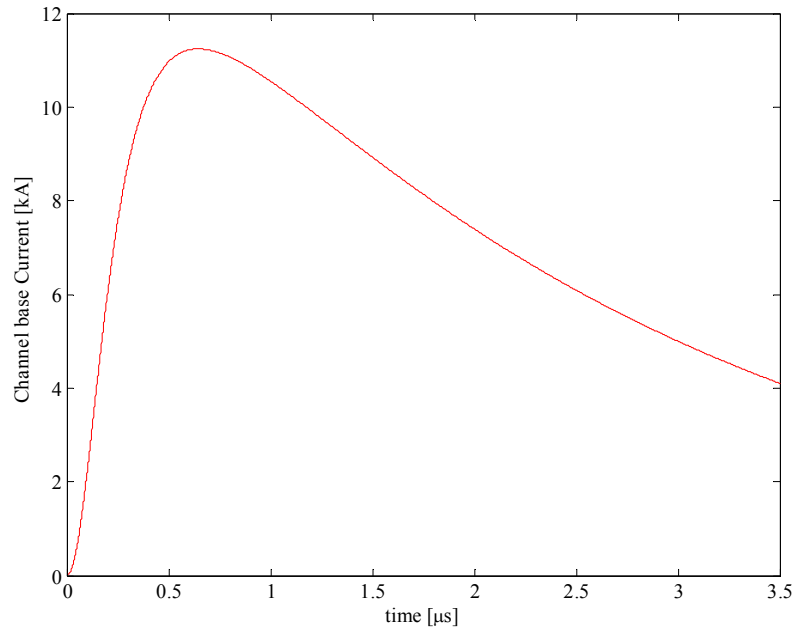


Figure 2.8: Heidler model for channel base current.

$I_0$ (kA)	$\tau_1$ ( $\mu$ s)	$\tau_2$ ( $\mu$ s)	$n$
10.7	0.25	2.5	2

Table 2.4: Typical values for Heidler channel base current [27].

Sometimes a sum of two Heidler functions with different parameters is used to approximate the desired current waveshape. Diendorfer and Uman [17], for example, described the subsequent-stroke current waveform at the channel base as the sum of two expressions given by (2.17), which reads:

$$i(0, t) = \left[ \frac{I_{01}}{\eta_1} \frac{(t/\tau_{11})^{n_1}}{1 + (t/\tau_{11})^{n_1}} \exp(-t/\tau_{12}) + \frac{I_{02}}{\eta_2} \frac{(t/\tau_{21})^{n_2}}{1 + (t/\tau_{21})^{n_2}} \exp(-t/\tau_{22}) \right] u(t) \quad (2.18)$$

with the parameters meaning already given for expression (2.17). In table 2.5 typical values for the parameters of expression (2.17) are reported [27].

$I_{01}$ (kA)	$\tau_{11}$ ( $\mu$ s)	$\tau_{21}$ ( $\mu$ s)	$n_1$	$I_{02}$ (kA)	$\tau_{12}$ ( $\mu$ s)	$\tau_{22}$ ( $\mu$ s)	$n_2$
10.7	0.25	2.5	2	6.5	2.1	230	2

Table 2.5: Typical values for Heidler channel base current [27].

The correspondent channel base current is plotted in figure 2.9. As shown in figure 2.9, the current waveshape estimates by expression (2.18) is, for longer time, more realistic than the current waveshape estimated by (2.17).

Eventually, Nucci et al. [19] proposed a channel base current as the sum of a Heidler expression and a double-exponential expression. This expression reads:

$$i(0,t) = \left[ \frac{I_{01}}{\eta} \frac{(t/\tau_1)^n}{1+(t/\tau_1)^n} \exp(-t/\tau_2) + I_{02}(\exp(-t/\tau_3) - \exp(-t/\tau_4)) \right] u(t) \quad (2.19)$$

In table 2.6 the typical value of the parameters in (2.19) are given [19]. In figure 2.10 the plot of the current expression (2.19) is shown.

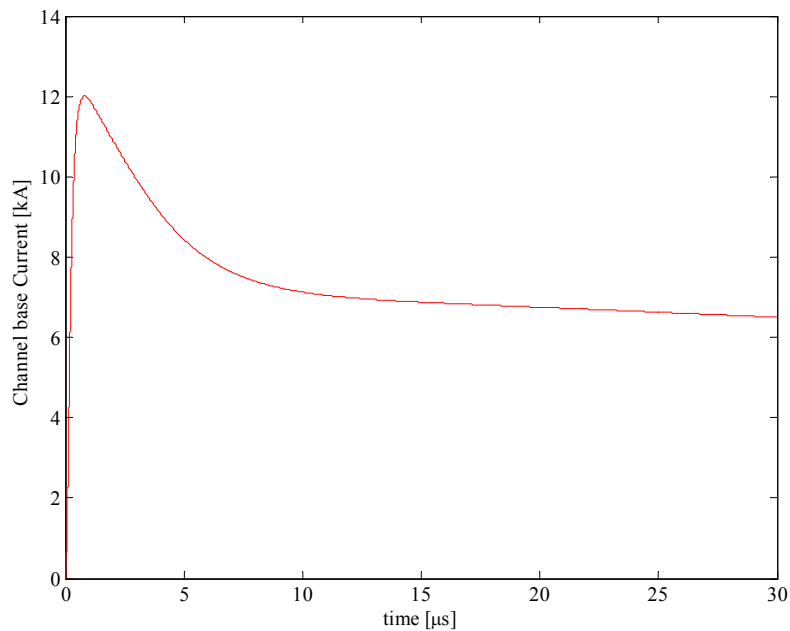


Figure 2.9: Channel base current given by summing two Heidler expressions.

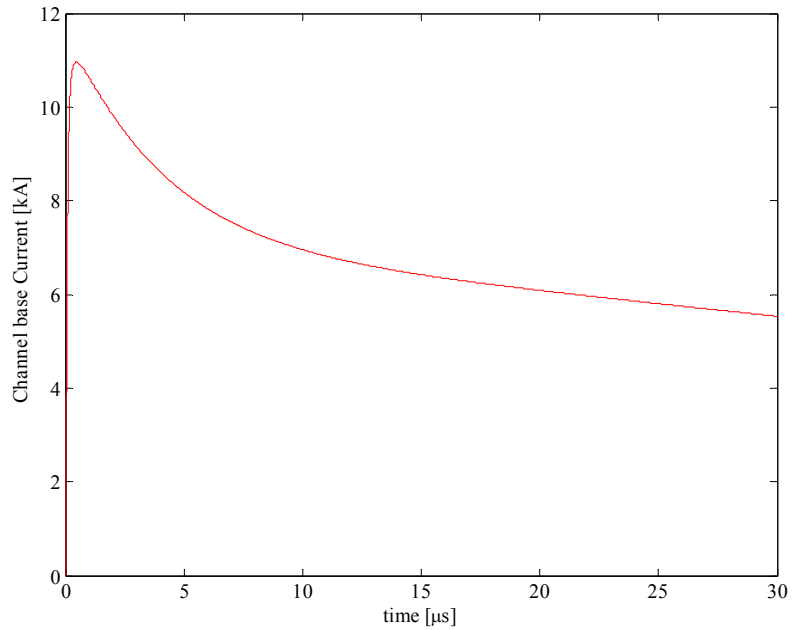


Figure 2.10: Channel base current proposed by Nucci et al. [20].

$I_{01}$ (kA)	$\tau_{11}$ (μs)	$\tau_{21}$ (μs)	$n$	$I_{02}$ (kA)	$\tau_{12}$ (μs)	$\tau_{22}$ (μs)
9.9	0.072	5	2	7.5	100	6

Table 2.6: Typical values for channel base current proposed by Nucci et al. [19].

#### 4) *Frequency Heidler model*

This model was proposed by Andreotti et al. in [28,29]. In [28] the authors presented the analytical evaluation of the Fourier transform of Heidler's lightning return stroke current expression (2.17) to evaluate lightning-induced overvoltages, when the frequency domain is considered. The expression of the Fourier transform of Heidler's lightning return stroke current is given in [29] and reads:

$$I(\omega) = \frac{I_0 \tau_1}{\eta p} \left[ 1 + \frac{1}{n} \sum_{k=0}^{n-1} (u_k p) \exp(-u_k p) E_1(-u_k p) \right] \quad (2.20)$$

with  $p = \frac{\tau_1}{\tau_2} + j\omega\tau_1$ , and

$$u_k = \cos\left[(2k+1)\frac{\pi}{n}\right] + j\sin\left[(2k+1)\frac{\pi}{n}\right] \quad (2.21)$$

for  $k = 0, 1, \dots, n-1$ , and with  $E_1$  the exponential integral function.

This model allows to use the Heidler model also in the frequency domain overcoming approximations previously made (e.g. [30-32]).

#### **2.2.4 Model validation**

The traditional approaches to validate the engineering models are based on *direct procedures*. For an assigned return stroke model, the electromagnetic fields are calculated at one or more distances and then compared to the observed ones. A return stroke model is then considered suitable if there is a relatively good coincidence between calculated and measured fields. In this view, two primary approaches to engineering model validation have been used: the *Typical Return Stroke* approach, and the *Specific Return-Stroke* approach [8].

##### **1) Typical Return Stroke approach**

This approach involves using a typical channel base current waveform and a typical return-stroke propagation speed as model inputs and then comparing the model predicted electromagnetic fields with typically observed fields. This approach has been adopted by Rakov and Dulzon [12], Nucci et al. [19], and Thottappillil et al. [18]. Nucci et al. [19] identified four characteristic features in the fields at 1–200 km measured by Lin et al. [33] and used those features as a

benchmark for their validation of the TL, MTLE, BG, TCS and MULS models. In figure 2.11 the lightning fields measured by Lin et al. [33] are showed. The characteristic features include:

- a) a sharp initial peak that varies approximately as the inverse distance beyond a kilometer or so in both electric and magnetic fields;
- b) a slow ramp following the initial peak and lasting in excess of  $100 \mu s$  for electric fields measured within a few tens of kilometers;
- c) a hump following the initial peak in magnetic fields within a few tens of kilometers, the maximum of which occurs between 10 and  $40 \mu s$  ;
- d) a zero crossing within tens of microseconds of the initial peak in both electric and magnetic fields at 50 to 200 *km* .

For the current and other model characteristics assumed by Nucci et al. [19], feature a) is reproduced by all the models examined, feature b) by all the models except for the TL model, feature c) by the BG, TL and TCS models but not by the MTLE model, and feature d) only by the MTLE model but not by the BG, TL, and TCS models. Diendorfer and Uman [17] showed that the DU model reproduces features a), b), and c), and Thottappillil et al. [34] demonstrated that a relatively insignificant change in the channel base current waveform (well within the range of typical waveforms) allows the reproduction of feature d), the zero crossing, by the TCS and DU models. Rakov and Dulzon [12] showed that the MTLL model reproduces features a), b) and d).

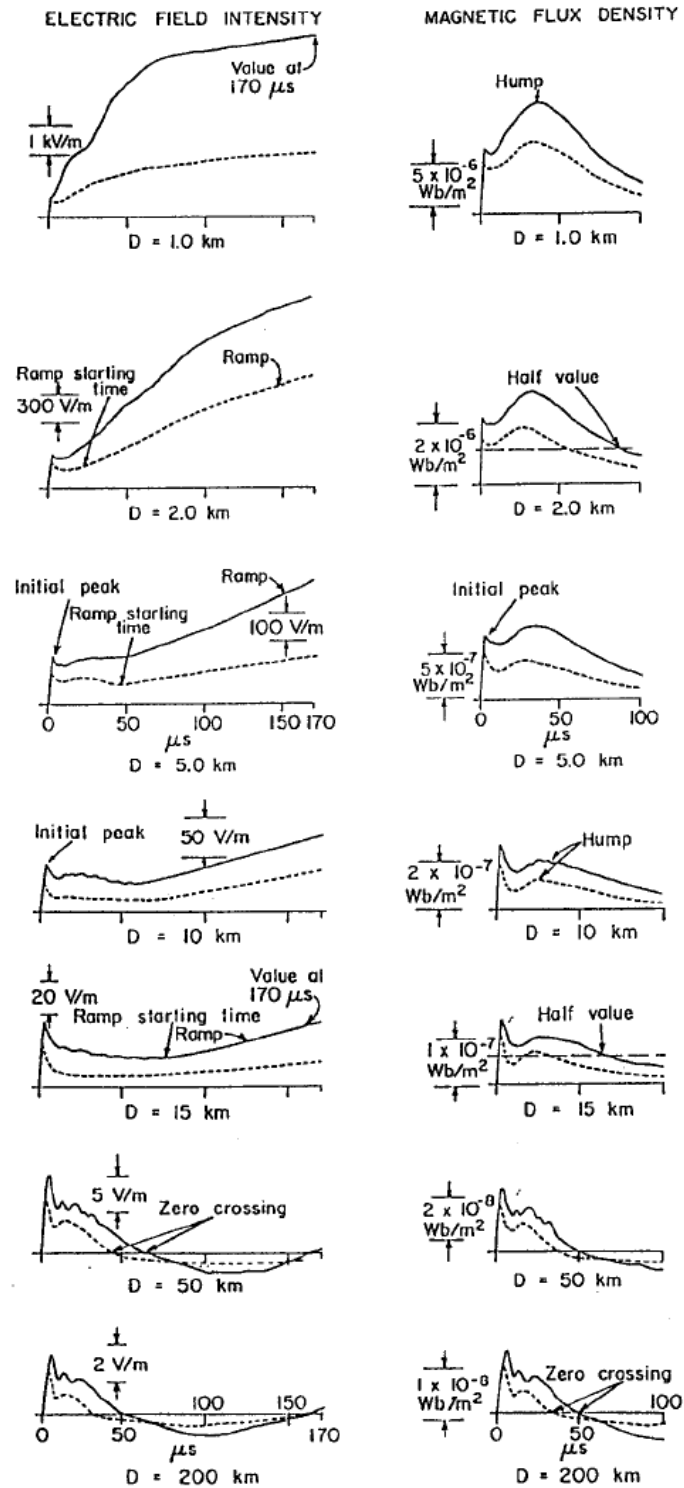


Figure 2.11: Typical vertical electric field intensity and horizontal magnetic flux density waveforms. The fields are plotted for first (solid line) and subsequent (dashed line) return strokes at distances of 1 - 200 km, adapted from [33].

2) *Specific Return-Stroke approach*

This approach involves using the channel base current waveform and the propagation speed measured for the same individual event and comparing computed fields with measured fields for that same specific event. This approach is able to provide a more definitive answer regarding model validity, but it is feasible only in the case of triggered-lightning return strokes or natural lightning strikes to tall towers where channel base current can be measured. In the field calculations, the channel is generally assumed to be straight and vertical with its origin at ground  $z'=0$ , conditions which are expected to be valid for subsequent strokes, but potentially not for first strokes.

This approach has been adopted by Thottappillil and Uman [21] who compared the TL, TCS, MTLE, DU, and MDU models. They used 18 sets of three simultaneously measured features of triggered lightning return strokes: channel-base current, return-stroke propagation speed, and electric field at about 5 km from the channel base, the data previously used by Willett et al. [35] for their analysis of the TL model. It has been found that the TL, MTLE, and DU models each predict the measured initial electric field peaks within an error whose mean absolute value is about 20%, while the TCS model has a mean absolute error about 40%.

The above presented approaches to validate return stroke models are based on *direct procedures*: a return stroke model is considered suitable if there is a relatively good coincidence between calculated and measured fields. In [36] Andreotti et al. describe the possibility of identifying exactly the attenuation function  $P(z')$ , by means of an *inverse procedure*, solving the equations relating the measured field to the channel base current. Two possible different procedures, one for different frequencies and one for different distances, to identify the lightning return stroke attenuation in the frequency domain were proposed. Both procedures are able to accurately identify  $P(z')$ .

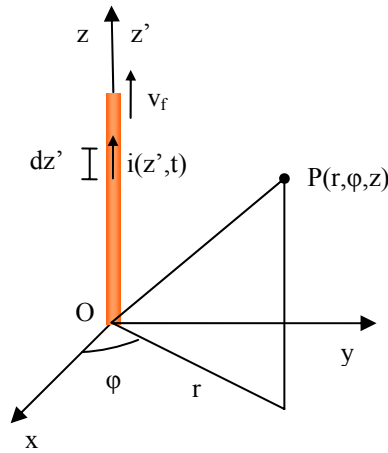


Figure 2.12: Geometry for return stroke field evaluation.

### 2.3. Calculation of lightning return stroke fields

Once the source is specified, fields can always be computed without approximation other than those involved in the computational process. In the problems concerning the lightning induced overvoltages calculations, the most commonly field equations adopted for the evaluation of return stroke fields have been proposed by Uman et al. in [37]. By assuming the ground as a perfect conductor, they have derived the equations for the electric and magnetic field originated by a vertical dipole of infinitesimal length, by solving Maxwell's equations in terms of retarded scalar and vector potentials. The geometry of the problem is shown in figure 2.12.

The field evaluated is originated by a vertical dipole of infinitesimal length  $dz'$  placed at height  $z'$ . In the cylindrical coordinate system shown in figure 2.12 the field generated by a vertical dipole is characterised, assuming ground as a perfect conductor, by the vertical and radial electric field component, and the azimuthal magnetic field component. The equations proposed in [37] are:

$$de_r(r, z, t) = \frac{dz'}{4\pi\epsilon_0} \left[ \frac{3r(z-z')-r^2}{R^5} \int_0^t i(z', \tau - R/c) d\tau + \frac{3r(z-z')-r^2}{cR^4} i(z', t - R/c) + \frac{r(z-z')}{c^2 R^3} \frac{\partial i(z', t - R/c)}{\partial t} \right] \quad (2.22)$$

$$de_z(r, z, t) = \frac{dz'}{4\pi\epsilon_0} \left[ \frac{2(z-z')-r^2}{R^5} \int_0^t i(z', t - R/c) d\tau + \frac{2(z-z')-r^2}{cR^4} i(z', t - R/c) + \frac{r^2}{c^2 R^3} \frac{\partial i(z', t - R/c)}{\partial t} \right] \quad (2.23)$$

$$dh_\phi(r, z, t) = \frac{1}{4\pi} \left[ \frac{r}{R^3} i(z', t - R/c) + \frac{r}{cR^2} \frac{\partial i(z', t - R/c)}{\partial t} \right] \quad (2.24)$$

with  $R = \sqrt{r^2 - (z - z')^2}$ . The equations refers to a return stroke current  $i(z', t)$ . In (2.22) and (2.23), the three terms are respectively called the electrostatic field, the induction field, and the radiation field. In (2.24) only the induction and radiation fields are present, respectively the first and second terms.

The total electric and magnetic fields are obtained by integrating (2.22)-(2.24) along the lightning channel and its image. The following expressions are obtained:

$$e_r(r, z, t) = \frac{1}{4\pi\epsilon_0} \left[ \int_{-H}^H \frac{3r(z-z')}{R^5} \int_0^t i(z', \tau - R/c) d\tau dz' + \int_{-H}^H \frac{3r(z-z')-r^2}{cR^4} i(z', t - R/c) dz' + \int_{-H}^H \frac{r(z-z')}{c^2 R^3} \frac{\partial i(z', t - R/c)}{\partial t} dz' \right] \quad (2.25)$$

$$e_z(r, z, t) = \frac{1}{4\pi\epsilon_0} \left[ \int_{-H}^H \frac{2(z-z')-r^2}{R^5} dz' \int_0^t i(z', \tau - R/c) d\tau + \int_{-H}^H \frac{2(z-z')-r^2}{cR^4} i(z', t - R/c) dz' - \int_{-H}^H \frac{r^2}{c^2 R^3} \frac{\partial i(z', t - R/c)}{\partial t} dz' \right] \quad (2.26)$$

$$h_\phi(r, z, t) = \frac{1}{4\pi} \left[ \int_{-H}^H \frac{r}{R^3} i(z', t - R/c) dz' + \int_{-H}^H \frac{r}{cR^2} \frac{\partial i(z', t - R/c)}{\partial t} dz' \right] \quad (2.27)$$

The expressions (2.25)-(2.27) have correspondent expressions in the frequency domain. By means of a Fourier transform, the expression obtained reads:

$$E_r(r, z, \omega) = \frac{1}{4\pi\epsilon_0} \left[ \int_{-H}^H \frac{3r(z-z')-r^2}{R^5} \frac{1}{j\omega} I(z', \omega) \exp(-j\omega R/c) dz' + \int_{-H}^H \frac{3r(z-z')-r^2}{cR^4} I(z', \omega) \exp(-j\omega R/c) dz' + \int_{-H}^H \frac{3r(z-z')-r^2}{c^2 R^3} j\omega I(z', \omega) \exp(-j\omega R/c) dz' \right] \quad (2.28)$$

$$E_z(r, z, \omega) = \frac{1}{4\pi\epsilon_0} \left[ \int_{-H}^H \frac{2(z-z')-r^2}{R^5} \frac{1}{j\omega} I(z', \omega) \exp(-j\omega R/c) dz' + \int_{-H}^H \frac{2(z-z')-r^2}{cR^4} I(z', \omega) \exp(-j\omega R/c) dz' - \int_{-H}^H \frac{r(z-z')-r^2}{c^2 R^3} j\omega I(z', \omega) \exp(-j\omega R/c) dz' \right] \quad (2.29)$$

$$H_{\varphi}(r, z, \omega) = \frac{1}{4\pi} \left[ \int_{-H}^H \frac{r}{R^3} I(z', \omega) \exp(-j\omega R/c) dz' + \int_{-H}^H \frac{r}{cR^2} j\omega I(z', \omega) \exp(-j\omega R/c) dz' \right] \quad (2.30)$$

where  $I(z', \omega)$  is obtained as

$$I(z', \omega) = \int_{-\infty}^{+\infty} i(z', t) \exp(-j\omega t) dt = \int_{z'/v}^{+\infty} i(0, t - z'/v) P(z') \exp(-j\omega t) dt \quad (2.31)$$

If  $u = t - z'/v$  is substituted in (2.31), the following expression is obtained:

$$\begin{aligned} I(z', \omega) &= P(z') \exp(-j\omega z'/v) \int_0^{\infty} i(0, u) \exp(-j\omega u) du = \\ &= I(0, \omega) P(z') \exp(-j\omega z'/v) \end{aligned} \quad (2.32)$$

where  $P(z')$  is the attenuation function of the return stroke current along the lightning channel. If (2.32) is substituted in (2.28)-(2.30), following expressions are obtained [36]:

$$E_r(r, z, \omega) = \frac{1}{4\pi\epsilon_0} \int_{-H}^H \left[ \frac{3r(z-z')}{R^5} \frac{1}{j\omega} + \frac{3r(z-z')}{cR^4} + \frac{r(z-z')}{c^2R^3} j\omega \right] I(0, \omega) \exp[-j\omega(R/c + |z'|/v)] P(z') dz' \quad (2.33)$$

$$E_z(r, z, \omega) = \frac{1}{4\pi\epsilon_0} \int_{-H}^H \left[ \frac{2(z-z')-r^2}{R^5} \frac{1}{j\omega} + \frac{2(z-z')-r^2}{cR^4} - j\omega \frac{r^2}{c^2R^3} \right] I(0, \omega) \exp[-j\omega(R/c + |z'|/v)] P(z') dz' \quad (2.34)$$

$$H_{\varphi}(r, z, \omega) = \frac{1}{4\pi} \int_{-H}^H \left( \frac{r}{R^3} + \frac{r}{cR^2} \right) I(0, \omega) \exp(-j\omega(R/c + z'/v)) P(z') dz', \quad (2.35)$$

## 2.4. Propagation effect

If the observation point  $P(r, \varphi, z)$  of the lightning fields is located on the ground surface, and the ground is assumed to be perfectly conducting, only two field components, the vertical electric field and the azimuthal magnetic field are present, as discussed in the previous paragraph. The horizontal electric field component is zero as required by the boundary condition on the surface of a perfect conductor. At an observation point above a perfectly conducting ground, a nonzero horizontal electric field component exists. A horizontal electric field exists above ground and also both on and below its surface in the case of a finite ground conductivity. Propagation effects include the preferential attenuation of the higher frequency components in the vertical electric field and azimuthal magnetic field waveforms and the appearance of a horizontal radial electric field which can be viewed as producing the radial current flow and resultant ohmic losses in the earth. A good review of the literature on the effects of finite ground conductivity on lightning electric and magnetic fields is given by Rachidi et al. [38].

Two approximate equations, both in the frequency domain, are commonly used for the computation of the horizontal electric field in air within 10 m or so of a finitely conducting earth. The first is namely the wavetilt formula and was proposed by Zenneck [39], while the second, namely Cooray–Rubinstein formula, was presented by Cooray [40] and by Rubinstein [41].

### 1) *Wavetilt formula*

The term “wavetilt” originates from the fact that when a plane electromagnetic wave propagates over a finitely conducting ground, the total electric field vector at the surface is tilted from the vertical because of the

presence of a nonzero horizontal (radial) electric field component. The tilt is in the direction of propagation if the vertical electric field component is directed upward and in the direction opposite to the propagation direction if the vertical electric field component is directed downward with the vertical component of the Poynting vector being directed into the ground in both cases.

The wavetilt formula states that for a plane wave the ratio of the Fourier transform of the horizontal electric field  $E_r(P, \omega)$  to that of the vertical electric field  $E_z(P, \omega)$  is equal to the ratio of the propagation constants in the air and in the ground [39]:

$$E_r(r, z, \omega) = E_z(r, z, \omega) \frac{1}{\sqrt{\epsilon_{rg} + \sigma_g / (j\omega\epsilon_0)}} \quad (2.40)$$

where  $\sigma_g$  and  $\epsilon_{rg}$  are the conductivity and relative permittivity of the ground, respectively, and  $\omega$  is the angular frequency. The formula is a special case (valid for grazing incidence) of the theory of the reflection of electromagnetic waves off a conducting surface and, hence, is a reasonable approximation only for relatively distant lightning or for the early microseconds of close lightning when the return stroke is near ground.  $E_z(r, z, \omega)$  is typically computed assuming a perfectly conducting ground or is measured.

In 1988 Thomson et al. [42] presented the horizontal field magnitude from the vertical electric field by using the time domain approach described by Master in 1982 [43]. In Master's technique the vertical electric field is approximated as a sequence of superposed delayed ramps, since a ramp has an analytical inverse transform of the wavetilt expression (2.40). The horizontal electric field is then determined in the time domain as the superposition of the ramp responses. For example, for the ramp, given by

$$e_z(t) = m t u(t - t_1) \quad (2.41)$$

the wavetilt response is

$$e_r(t) = \frac{m}{\sqrt{\varepsilon_r}} (t - t_1) [I_0(pt) + I_1(pt)] \exp[-p(t - t_1)] u(t - t_1) \quad (2.42)$$

with  $p = \sigma / (2\varepsilon_{rg}\varepsilon_0)$ ,  $I_0$  and  $I_1$  are the modified Bessel's functions of the first kind of the zeroth and first order, respectively.

## 2) Cooray–Rubinstein equation

The Cooray–Rubinstein equation is expressed as follows [40], [41]:

$$E_r(r, z, \omega) = E_{rp}(r, z, \omega) - H_{\varphi p}(r, 0, \omega) \frac{c\mu_0}{\sqrt{\varepsilon_{rg} + \sigma_g / (j\omega\varepsilon_0)}} \quad (2.43)$$

where  $\varepsilon_0$  is the free space permeability and  $E_{rp}(r, z, \omega)$  is the Fourier transforms of the horizontal electric field at height  $z$  above ground and  $H_{\varphi p}(r, 0, \omega)$  is the azimuthal magnetic field at ground level, respectively, both computed for the case of a perfectly conducting ground. The second term is equal to zero for  $\sigma_g \rightarrow \infty$  and becomes increasingly important as  $\sigma_g$  decreases.

## 2.5. Field to Line Coupling

Once the electromagnetic field is calculated making use of a return stroke current model, it is used to calculate the induced overvoltages, by means of a coupling model which describes the interaction between the field and the line conductors. As far as the calculation of the electromagnetic field it has already been the object of the previous paragraphs. As far as the coupling models they are the object of this paragraph. In particular, the most used coupling models will be summarised and discussed.

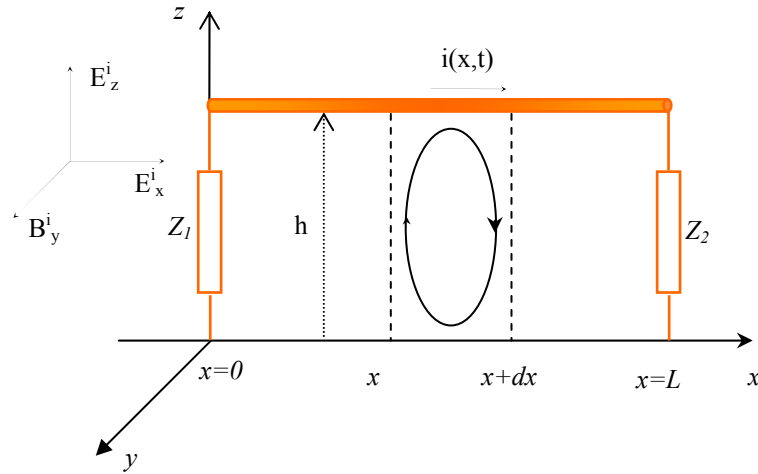


Figure 2.13: Geometry used for the field to line coupling problem.

In literature different formulations have been proposed for field to line interaction. The most popular coupling models, for calculations concerning lightning, are:

- o Taylor, Satterwhite and Harrison model, proposed in [44];
- o Agrawal, Price, Gurbaxani model, proposed in [45];
- o Rachidi model, proposed in [46];
- o Rusck model, proposed in [47];
- o Chowdhuri and Gross model, proposed in [48].

All these models are based on the *Transmission Line* approximation, which means that the transverse dimension of the line is considered much smaller than the minimum significant wavelength, and that the response of the line to the lightning electromagnetic field is quasi-transverse electromagnetic. In figure 2.13 the geometry used for the calculation of overvoltages induced on an overhead power line by an indirect lightning return stroke is reported. The line have height  $h$ , length  $L$ , is parallel to  $x$ -axis and is contained in the  $xz$ -plane.

In what follows the Taylor et al., Agrawal et al. and Rachidi coupling models and their formulations will be summarised. The last two models, the

Rusck and the Chowdhuri-Gross ones, are very popular for analytical approaches. For this reason these two models will be discussed in the next chapter, since it is focused on the methods based on analytical tools.

Each of these coupling model formulations is expressed by means of a pair of equations involving time and space-derivatives of induced voltages and currents along the line plus some forcing function, or source terms, that are a function of the incident electromagnetic field component.

1) *Taylor, Satterwhite and Harrison model*

This coupling model refers to a two-wire transmission line and the source of line excitation is an external electromagnetic field. With respect to the figure 2.13, the first wire is located at  $z = 0$  and the second one at  $z = h$ . The incident magnetic field  $B^i$  is taken in the  $y$  direction and the incident electric field  $E^i$  in  $xz$  plane. This model is described by two coupling equation in the frequency domain, which reads:

$$\begin{cases} \frac{dV(x)}{dx} + Z'I(x) = j\omega \int_0^h B_y^i(x, z) dz \\ \frac{dI(x)}{dx} + Y'V(x) = -Y' \int_0^h E_x^i(x, z) dz \end{cases} \quad (2.44)$$

where  $V(x)$  and  $I(x)$  are the voltage and current along the line, respectively,  $Z'$  and  $Y'$  are the line conductor distributed series impedance and shunt admittance respectively, given by [44]:

$$Z' = Z^i + j\omega L^e \quad (2.45)$$

$$Y' = j \left( \frac{k^2}{\omega L^e} \right) \quad (2.46)$$

where  $Z^i$  is the internal impedance of the line conductor,  $L^e = (\mu/\pi)\ln(h/a)$ ,  $a$  is the conductor radius and  $k = \omega\sqrt{\mu(\varepsilon - j\sigma/\omega)}$ .

The boundary condition are:

$$\begin{aligned} V(0) &= -I(0)Z_1 \\ V(L) &= I(L)Z_2 \end{aligned} \tag{2.47}$$

The second members of (2.44) are the source terms, which are expressed in terms of transverse magnetic induction and vertical electric components of inducing field. In figure 2.14 the equivalent circuits of this coupling model is showed for a lossy single wire overhead line.

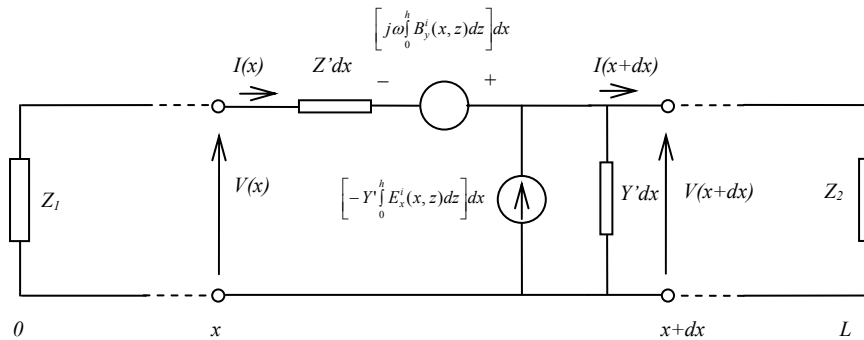


Figure 2.14: Equivalent coupled circuit according to the Taylor et al. model for a lossy single wire line.

## 2) Agrawal, Price, Gurbaxani model

This coupling model refers to the general case of a multiconductor line plus a reference conductor and the source of line excitation is a nonuniform electromagnetic field. With respect to the figure 2.13, the conductor is located at  $z = h$  and the reference one is located at  $z = 0$ . The incident magnetic field  $B^i$  is taken in the  $y$  direction and the incident electric field  $E^i$  in  $xz$  plane. This model is described by two coupling equation in the frequency domain, which reads:

$$\begin{cases} \frac{dV^s(x)}{dx} + Z'I(x) = E_x^i(x, h) \\ \frac{dI(x)}{dx} + Y'V^s(x) = 0 \end{cases} \quad (2.48)$$

where  $E_x^i(x, h)$  the horizontal component along the wire of the incident electric field,  $Z'$  and  $Y'$  are the longitudinal and transverse per-unit-length impedance and admittance respectively, and  $V^s(x)$  is the scattered voltage, related to the total voltage by the following equation

$$V^s(x) = V(x) - V^i(x) = V(x) - \int_0^h E_z^i(x, z) dz \quad (2.49)$$

with  $V^i(x)$  the called incident voltage. The expression of  $Z'$  and  $Y'$  have already been discussed. In particular, when the lossy ground is considered they read [38]

$$Z' = j\omega L' + Z'_w + Z'_g \quad (2.50)$$

$$Y' = \frac{(G' + j\omega C')Y'_g}{G' + j\omega C' + Y'_g} \quad (2.51)$$

with  $Z'_w$  and  $Z'_g$  the wire and the ground impedances  $L'$  and  $C'$  the external per-unit-length inductance and capacitance, respectively, calculated for a lossless wire above a perfectly conducting ground,  $Y'_g$  is the ground admittance and  $G'$  is the per-unit-length transverse conductance.

The boundary conditions are

$$V^s(0) = -Z_1 I(0) + \int_0^h E_z^i(0, z) dz \tag{2.52}$$

$$V^s(L) = -Z_2 I(L) + \int_0^h E_z^i(L, z) dz$$

In figure 2.15 the equivalent circuits of this coupling model is showed for a lossy single wire overhead line.

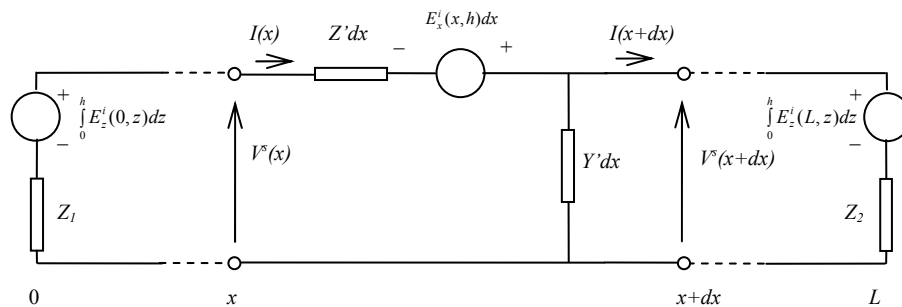


Figure 2.14: Equivalent coupled circuit according to the Agrawal et al. model for a lossy single wire line.

The difference between the formulation (2.48) proposed by Agrawal et al. and the formulation (2.44) are lies essentially in the representation of the source terms. In the formulation of Taylor et al., source terms are functions of both electric and magnetic incident fields. In the formulation of Agrawal et al., the source terms involve only the electric incident field components.

### 3) Rachidi model

This coupling model refers to the general case of a multiconductor line plus a reference conductor and the source of line excitation is a nonuniform electromagnetic field. With respect to the figure 2.13, the conductor is located at  $z = h$  and the reference one is located at  $z = 0$ . The incident magnetic field  $B^i$  is taken in the  $y$  direction and the incident electric field  $E^i$  in  $xz$  plane. This model is described by two coupling equation in the frequency domain, which reads:

$$\begin{cases} \frac{dV(x)}{dx} + Z' I^s(x) = 0 \\ \frac{dI^s(x)}{dx} + Y' V(x) = -\frac{1}{Z'_0} \int_0^h \frac{\partial B_x^i(x, z)}{\partial y} dz \end{cases} \quad (2.53)$$

with  $B_x^i(x, z)$  the horizontal component along the conductor of the incident magnetic field, and  $I^s(x)$  the scattered current, related to the total current by the following equation

$$I^s(x) = I(x) - I^i(x) = I(x) + \frac{1}{Z'_0} \int_0^h B_y^i(x, z) dz \quad (2.54)$$

with  $I^i(x)$  the called incident current, and with  $Z'$  and  $Y'$  meaning already given for the Agrawal et al. model. The boundary conditions are

$$\begin{aligned} I^s(0) &= -\frac{I(0)}{Z_1} - \frac{1}{Z'_0} \int_0^h B_y^i(0, z) dz \\ I^s(L) &= -\frac{I(L)}{Z_2} - \frac{1}{Z'_0} \int_0^h B_y^i(L, z) dz \end{aligned} \quad (2.55)$$

In this formulation, the source terms are expressed in terms of magnetic incident field components. The use of this formulation is particularly interesting when the exciting field is determined experimentally, since only the measurement of magnetic field-generally much easier than that of electric field is needed. In figure 2.16 the equivalent circuits of this coupling model is showed for a lossy single wire overhead line.

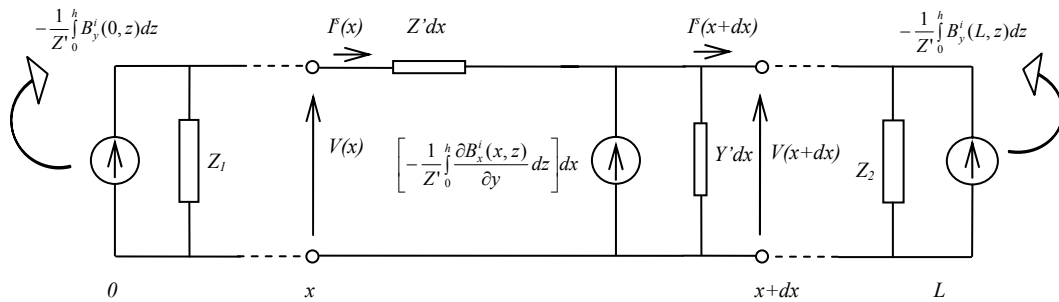


Figure 2.16: Equivalent coupled circuit according to the Rachidi model for a lossy single wire line.

The summarised models have been presented by means three different, but equivalent, formulations (2.44), (2.48) and (2.53) and the total induced voltages predicted by these three formulations are identical, as shown by Nucci and Rachidi [49].

## 2.6. Indirect Lightning Induced Voltages Calculation

Most numerical methods on lightning induced voltages on overhead power lines use a direct time domain analysis to solve the field to transmission line coupling equations. The use of a direct time domain analysis is useful because of its straightforwardness in dealing with insulation coordination problems, and its ability to handle non-linearities, which arise in presence of protective devices such as surge arresters or corona phenomenon. One of the most popular approaches to solve the transmission line coupling equations in time domain is the finite difference time domain (FDTD) technique. Such a technique was used, for example, by Agrawal et al. in [45]. A comprehensive review of the procedure involving numerical solutions of coupling equation is reported in [38].

The field to transmission line coupling equations (2.44), (2.48) and (2.53), presented in the frequency domain, can be converted in the time domain. The frequency dependent parameters, such as the wire and ground impedances, can be represented using a convolution integral. As a consequence a considerable time and computer memory storage requirements could be needed to carry out a time

domain solution. Hence, any numerical methods need to involve approximated procedure to solve the coupling equations, e.g. [49,50].

In the following the induced voltages evaluated by means of a finite difference time domain computer code proposed in [37] are reported. The geometry of the case studio is reported in figure 2.17.

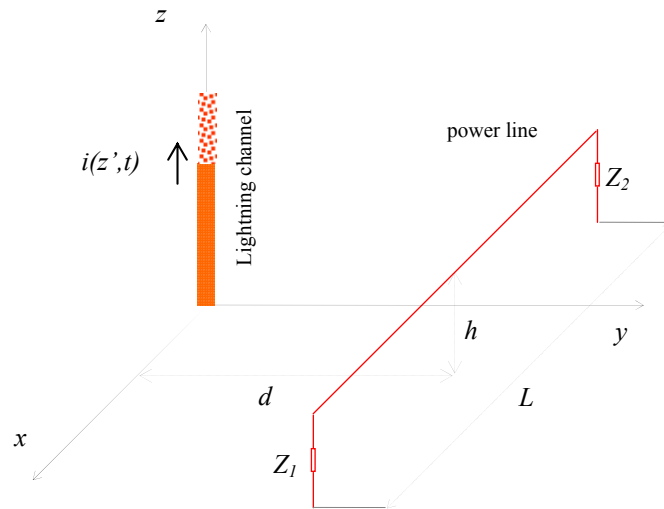


Figure 2.17: Geometry of the problem for induced voltages calculation.

The case studio considered is the one of a single conductor lossless line above a lossy ground. The line is matched at both ends,  $1\text{ km}$  long and  $10\text{ m}$  height. The lightning impact point is  $50\text{ m}$  far from the line, equidistant between the two line ends. The induced voltage at the abscissa  $x = 0$  is showed in figure 2.18. This figure is adapted from [38] and refers to a typical return stroke.

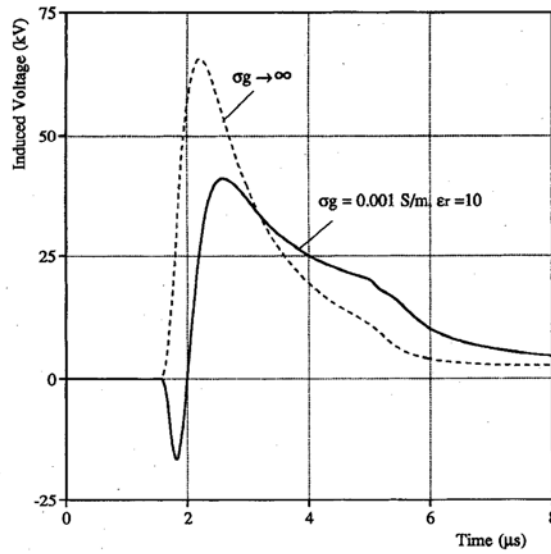


Figure 2.18. Induced Voltages on an overhead line 1 km long and 10 m height. A typical return stroke is considered. Adapted from [38].

In figure 2.18 the induced voltage is plotted both for the cases of finite and infinite ground conductivity. As shown, the ground conductivity affects the induced voltages both for the magnitude and the polarity.

## References

- [1] K.W. Wagner, "Elektromagnetische ausgleichsvorgange in freileitungen und kabeln", (in German), par. 5, Leipzig, 1908.
- [2] L.V. Bewley, "Traveling waves due to lightning", Transactions A.I.E.E., Vol. 48, pp. 1050-1064, July 1929.
- [3] H. Norinder, "Some recent tests on the investigation of induced surges", CIGRE, paper 303, Paris, 1936.
- [4] C.F. Wagner, G.D. Mc Cann, "Induced Voltages on Transmission Lines", AIEE Transactions, Vol. 61, pp. 916- 930, 1942.
- [5] B.F.J. Schonland, "Progressive lightning", part II, Proc. Roy. Soc. London, Ser. A, 143, pp. 654-674, 1934.
- [6] M.A. Uman, "Natural Lightning", IEEE Transactions on Industry Application, vol. 30, No. 3, May/June, 1994.
- [7] C. Gomez, V. Cooray, "Concepts of lightning return stroke", IEEE Transactions on Electromagnetic Compatibility, vol. 42, No. 1, February 2000.
- [8] V. Rakov, M. Uman, "Review and Evaluation of Lightning Return Stroke Models Including Some Aspects of Their Application", IEEE Transactions on Electromagnetic Compatibility, vol. 40. No. 4, November 1998.
- [9] M.A. Uman, D.K. McLain, "Magnetic field of lightning return stroke", Journal of Geophysical Research, Vol. 74, 1969.
- [10] C.A. Nucci, F. Rachidi, "Experimental validation of a modification to the Transmission Line model for LEMP calculations", Proc. of the 8th International Symposium and Technical Exhibition on Electromagnetic Compatibilty, pp. 389-394, Zurich, 7-9 March, 1989.
- [11] V.A. Rakov, "Lightning electromagnetic fields: Modeling and measurements", in Proc. 12th Int. Zurich Symp. Electromagnetic Compatibility, Zurich, Switzerland, pp.59-64, Feb.1997.
- [12] V.A. Rakov and A.A. Dulzon, "A modified transmission line model for lightning return stroke field calculations", in Proc. 9th Int. Zurich Symp. Electromagnetic Compatibility, Zurich, Switzerland. Mar.1991.
- [13] C.E.R. Bruce and R.H. Golde, "The lightning discharge", J. Inst. Elect. Eng. Pt.2, vol.88, pp.487-520, 1941.
- [14] F. Heidler, "Travelling current source model for LEMP calculation", Proc of the 6th Symposium and Technical Exhibition on Electromagnetic Compatibility, Zurich, March 5-7, 1985.

- [15] C.A. Nucci, C. Mazzetti, F. Rachidi, and M. Ianoz, "On lightning return stroke models for LEMP calculations", in Proc.19th Int. Conf. Lightning Protection, Graz, Austria, Apr.1988.
- [16] M.J. Master, M.A. Uman, Y.T. Lin, R.B. Standler, "Calculations of lightning return stroke electric and magnetic fields above ground", J. Geophys. Res., vol. 86, pp. 2,127-12,132, 1981.
- [17] G. Diendorfer, M. A. Uman, "An improved return stroke model with specified channel-base current", Journal of Geophysical Research, v. 95, p. 13621-13644, 1990.
- [18] R. Thottappillil, V. A. Rakov, and M. A. Uman, "Distribution of charge along the lightning channel: Relation to remote electric and magnetic fields and to return stroke models", J. Geophys. Res., vol. 102, pp. 6887–7006, 1997.
- [19] C.A. Nucci, G. Diendorfer, M.A. Uman, F. Rachidi, C. Mazzetti, "Lightning return-stroke models with channel-base specified current: a review and comparison", Journal of Geophysical Research, Vol. 95, No. D12, November 1990.
- [20] M.A. Uman, "The lightning discharge", Academic Press, Orlando FL, 1987.
- [21] R. Thottappillil and M. A. Uman, "Comparison of lightning return stroke models," J. Geophys. Res., vol. 98, no. D12, pp. 22 903–22 914, 1993.
- [22] C.A. Nucci, F. Rachidi, M. Ianoz, C. Mazzetti, "Lightning-induced overvoltages on overhead lines", IEEE Trans. on EMC, Vol. 35, No. 1, February 1993.
- [23] K. Berger, R.B. Anderson, H. Kroninger, "Parameters of lightning flashes", Electra, No. 41, 1975.
- [24] R.B. Anderson, A.J. Eriksson, "Lightning parameters for engineering application", Electra, No. 69, 1980.
- [25] E. T. Pierce, "Triggered lightning and some unsuspected lightning hazards", Naval Res. Rev. vol. 25: pp.14-28, 1972.
- [26] E.T. Pierce, N. A. Cianos, "Ground-lightning environment for engineering usage", Stanford: Research Institute, 1972, Report, Technical Report 1.
- [27] C.A. Nucci, "Tensions induites par la foudre sur les lignes aériennes de transport d'énergie; Partie I: Modèles de courant d'arc en retour avec un courant spécifié à la base du canal pour l'évaluation des champs électromagnétiques correspondants", .Electra 161, pp 74–102, Août, 1995.
- [28] A. Andreotti, U. De Martinis, A. Maffucci, G. Miano, L. Verolino, "Lightning Induced Overvoltages: a different approach", Speedam, Sorrento, 1998.
- [29] A. Andreotti, S. Falco, L. Verolino, "Some integrals involving Heidler's lightning return stroke current expression," Electrical Engineering, Vol 87, No. 3, pp. 121-128, 2005.

- [30] Z. Flisowski, C. Mazzetti, A. Orlandi, M. Yarmarkin, “Systematic approach for the analysis of the electromagnetic environment inside a building during lightning strike”, *IEEE Transaction on Electromagnetic Compatibility*, vol. 40, no. 4, pp. 521–535, 1998.
- [31] F. Heidler, J. Cvetić, “A class of analytical functions to study the lightning effects associated with the current front”, *European Transaction on Electrical Power*, vol. 12(2), pp. 141–150, 2002.
- [32] Z. Feizhou, L. Shanghe, “A new function to represent the lightning return-stroke currents”, *IEEE Transaction on Electromagnetic Compatibility*, vol. 44(4), pp. 595–597, 2003.
- [33] Y. T. Lin, M. A. Uman, J. A. Tiller, R. D. Brantley, W. H. Beasley, E. P. Krider, and C. D. Weidman, “Characterization of lightning return stroke electric and magnetic fields from simultaneous two-station measurements”, *J. Geophys. Res.*, vol. 84, pp. 6307–6314, 1979.
- [34] R. Thottappillil, M. A. Uman, and G. Diendorfer, “Influence of channel base current and varying return stroke speed on the calculated fields of three important return stroke models”, in *Proc. 1991 Int. Conf. Lightning Static Electricity*, Cocoa Beach, FL, pp. 118.1–118.9, Apr. 1991.
- [35] J. C. Willett, J. C. Bailey, V. P. Idone, A. Eybert-Berard, and L. Barret, “Submicrosecond intercomparison of radiation fields and currents in triggered lightning return strokes based on the transmission-line model”, *J. Geophys. Res.*, vol. 94, pp. 13,275–13,286, 1989.
- [36] A. Andreotti, U. De Martinis, L. Verolino, “An Inverse Procedure for the Return Stroke Current Identification”, *Transaction on Electromagnetic Compatibility*, vol. 43, no. 2, pp. 155-160, May 2001.
- [37] M.A. Uman, D.K.McLain, E.P.Krider, “The electromagnetic radiation from a finite antenna”, *American Journal of Physics*, vol.43, pp.33-38, 1975.
- [38] F. Rachidi, C. A. Nucci, M. Ianoz, and C. Mazzetti, “Influence of a lossy ground on lightning-induced voltages on overhead lines”, *IEEE Trans. Electromagnetic Compatibility*, vol. 38, pp. 250–264, Aug. 1996.
- [39] J. Zenneck, *Wireless Telegraphy*. New York: McGraw-Hill, 1915 (Engl. transl., A.E. Seelig).
- [40] V. Cooray, “Horizontal fields generated by return stroke strokes,” *Radio Sci.*, vol. 27, pp. 529–537, 1992.
- [41] M. Rubinstein, “An approximate formula for the calculation of the horizontal electric field from lightning at close, intermediate, and long range”, *IEEE Trans. Electromagnetic Compatibility*, vol. 38, pp. 531–535, 1996.
- [42] E. M. Thomson, P.J. Medelius, M. Rubinstein, M.A. Uman, J. Johnson, J.W. Stone, “Horizontal Electric Fields from Lightning Strokes”, *J. of Geophysical Research*, Vol. 93, no. D3, pp. 2429-2441, March 20, 1988.

- [43] M.J. Master, "Lightning induced voltages on power lines: Theory and experiments", Ph.D. dissertation University of Florida, Gainesville, 1982.
- [44] C. Taylor, R. Satterwhite, C. Jr. Harrison, "The response of a terminated two-wire transmission line excited by a nonuniform electromagnetic field", IEEE Trans. on Antennas and Propagation, vol.13, no.6, pp. 987-989, Nov 1965.
- [45] A. Agrawal, A. H. Price, S. Gurbaxani, "Transient response of multiconductor transmission lines excited by a nonuniform electromagnetic field", Antennas and Propagation Society International Symposium, vol.18, pp. 432-435, June 1980.
- [46] F. Rachidi, "Formulation of the field-to-transmission line coupling equations in terms of magnetic excitation field", IEEE Transaction of Electromagnetic Compatibility, Vol. 35., No.3, pp. 404-407, 1993.
- [47] S. Rusck, "Induced Lightning over-voltages on power transmission lines with special reference to the overvoltage protection of low-voltage networks", Trans. Royal Inst. of Tech., no. 120, pp.1-118, 1958.
- [48] P. Chowduri and E.T.B. Gross, "Voltage surges induced on overhead lines by lightning strokes", Proc. IEE, Vol. 114, no.12, pp. 1899-1907, Dec. 1967.
- [49] C. A. Nucci, F. Rachidi, "On the Contribution of the Electromagnetic Field Components in Field-to-Transmission Line Interaction", IEEE Transaction on Electromagnetic Compatibility, Vol. 37, no. 4, November 1995.
- [50] M. J. Master and M.A. Uman, "Lightning induced voltages on power lines: Theory", IEEE Transaction on Power Apparatus System, Vol. 103, pp. 2502-2518, September 1984.
- [51] M. Rubinstein, A. Y. Tzeng, M.A. Uman, P.J. Medelius and E.M. Thomson, "Lightning induced voltages on an overhead wire", IEEE Transaction on Electromagnetic Compatibility, Vol. 31, November 1989.

## **CHAPTER 3**

# **ANALYTICAL FORMULATIONS FOR LIGHTNING INDUCED OVERVOLTAGES CALCULATIONS**

In literature many efforts have been directed to improve the knowledge of the lightning phenomenon and its effects on power circuits. In particular, many numerical approaches have been proposed for the evaluation of the overvoltages induced on an overhead line by indirect lightning, as discussed in the chapter 2. However, closed form solutions provide considerable insight into the phenomenon, which is often obscured in numerical approaches. For this reason closed form solutions are very important in the design phase (e.g. [1]), in parametric evaluation and sensitivity analysis (e.g. [2]), and in economic analysis (e.g. [3]).

In literature, two main analytical formulations are very popular: the formulae proposed by Rusck [4], and the formulae proposed by Chowdhuri and Gross [5]. Moreover, Hoidalén, in [6], and Liew and Mar in [7] have presented other two analytical formulations. The closed form solutions proposed by Rusck [4], in particular, are very relevant since they are used in the Standard IEEE 1410 [1]. All these closed form solutions have been investigated by many authors; in particular, both the validity of the models underlying the solutions and the approximations used in those models were analysed (e.g. [8-11]). However, those

closed form solutions have never been compared with a rigorous analytical formulation, which is not available in literature and will be one of the contributions of the present work. We will, therefore, in this chapter, obtain the *exact closed form solution* in the hypothesis of lightning event model adopted in [4-7]. This solution will be then used to compare the other closed form solutions with the exact one in order to highlight their accuracy.

This chapter is organised as follows: in paragraphs 3.1, 3.2, 3.3 and 3.4, the Rusck's, Chowdhuri and Gross', Liew and Mar's and Hoidalén's formulations, respectively, will be presented. In paragraph 3.5 the exact closed form solutions will be derived and the results discussed. In paragraph 3.6, the four closed forms presented in literature will be then compared with the exact one.

### **3.1. The Rusk Formulae**

In this paragraph the Rusck formulation will be summarised. This formulation was proposed in the 1958 [4]. The Rusck lightning event model applies to the case of a vertical and straight lightning channel (see figure 3.1). To take into account the leader effect, a negative charge is uniformly distributed along the lightning path before the return stroke starts. The return stroke is a current surge with the shape of a step-function which propagates upwards along the lightning channel with the constant velocity  $v$ , neutralizing the charge. This type of propagation along the lightning channel is known as TL model (detailed in chapter 2). The power line is assumed to be an infinitely long lossless single conductor line above a perfectly conducting ground.

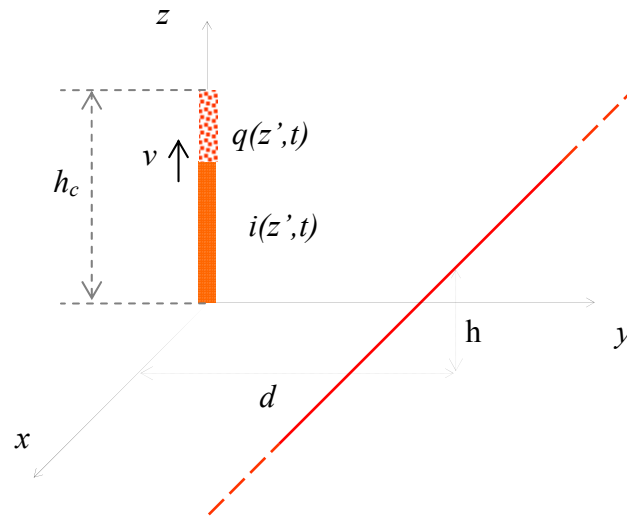


Figure 3.1: Lightning event model of the Rusck formulation.

As in any other method for the evaluation of induced voltages in power lines, Rusck first evaluates the electromagnetic field, and then calculates the field to line coupling. In the next section the electromagnetic field as evaluated by Rusck will be presented, and then in 3.1.2 the Rusck coupling model will be then introduced. In 3.1.3 the induced voltages predicted by Rusck formulae will be shown and discussed.

### 3.1.1 The Lightning Electromagnetic Field

The Rusck return stroke model applies to the case of a vertical and straight lightning channel initially charged by a uniform distribution charge, as shown in figure 3.1. The geometry of the problem, for the evaluation of the field, is shown in figure 3.2. The return stroke current is a step-current (figure 3.3) which propagates along the channel undistorted and unattenuated. The expression describing the current distribution for the model under study is given by

$$i(z', t) = I_0 u(t - z'/v) \quad (3.1)$$

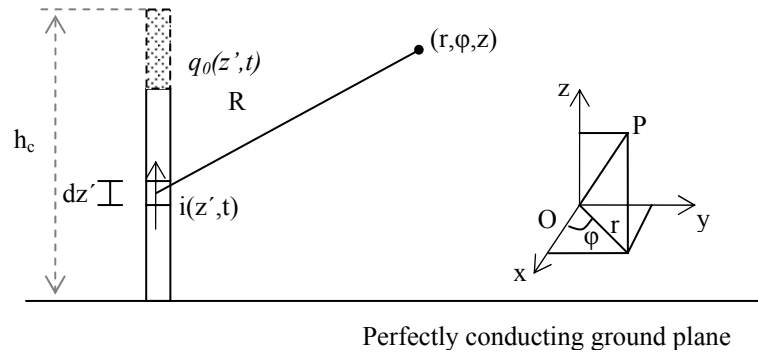


Figure 3.2: Geometry of the problem for the evaluation of the field according to Rusck formulation.

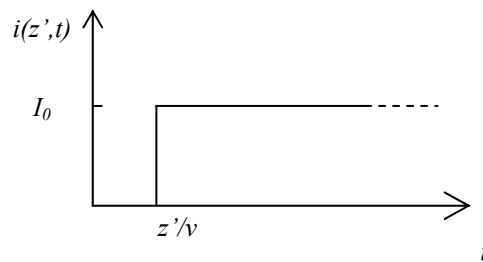


Figure 3.3: Return stroke current adopted in the Rusck formulation.

This return stroke current, as it moves along the channel, leaves a positive charge distribution  $q_0$  which neutralise the initial negative charge distribution. The initially charged channel is assumed of finite length  $h_c$ , as shown in figure 3.2. The relation between the current and charge distributions  $q_0$  is given by  $I_0 = q_0 v$ .

Rusck calculates the scalar potential  $\phi$  and the vector potential  $\vec{A}$  which can be written as

$$\phi(r, z, t) = \frac{1}{4\pi\epsilon_0} \int_{s_1}^{h_c} \frac{q\left(z', t - \frac{R}{c}\right)}{R} dz' \quad (3.2)$$

$$\vec{A}(r, z, t) = \frac{\mu_0}{4\pi} \int_0^{s_1} \frac{\vec{i}\left(z', t - \frac{R}{c}\right)}{R} dz' \quad (3.3)$$

As far as the scalar potential  $\phi$ , disregarding the influence of the mirror image for the while, the equation (3.2) will be simply

$$\phi(r, z, t) = -\frac{q_0}{4\pi\epsilon_0} \int_{s_1}^{h_c} \frac{dz'}{\sqrt{(z_s - z)^2 + r^2}} \quad (3.4)$$

with the lower limit of integration  $s_1$  obtained from the condition that the travelling time of the return stroke from the ground to the point  $z = s_1$  plus the travelling time from this point to the place where the potential is desired, i.e. the point  $(r, \phi, z)$ , must be equivalent to the time  $t$ . The following equation is obtained

$$t = \frac{s_1}{v} + \frac{\sqrt{(s_1 - z)^2 + r^2}}{c}. \quad (3.5)$$

Solving for  $s_1$

$$s_1 = \beta\gamma^2 \left[ ct - \beta z - \sqrt{(vt - z)^2 + \left(\frac{r}{\gamma}\right)^2} \right] \quad (3.6)$$

By integrating (3.4) and substituting (3.6), the scalar potential reads:

$$\phi(r, z, t) = \frac{q_0}{4\pi\epsilon_0} \cdot \left[ \ln \left( vt - z + \sqrt{(vt - z)^2 + \left(\frac{r}{\gamma}\right)^2} \right) - \ln(1 + \beta) - \ln \left( h_c - z + \sqrt{(h_c - z)^2 + r^2} \right) \right] \quad (3.7)$$

Eventually, the potential of the mirror image is obtained from (3.7) by changing the sign of  $z$ .

As far as the vector potential  $\vec{A}$ , disregarding the field of the mirror image, the equation of the vector potential (3.3) can be written as

$$\vec{A}(r, z, t) = \frac{\mu_0 I_0}{4\pi} \hat{z} \int_0^{s_1} \frac{dz'}{\sqrt{(z' - z)^2 + r^2}} \quad (3.8)$$

By integrating (3.8) and substituting  $s_1$  from (3.6), the vertical component of the vector potential can be calculated as:

$$A_z(r, z, t) = \frac{\mu_0 I_0}{4\pi} \cdot \left[ \ln \left( vt - z + \sqrt{(vt - z)^2 + \left(\frac{r}{\gamma}\right)^2} \right) - \ln(1 + \beta) - \ln \left( -z + \sqrt{z^2 + r^2} \right) \right] \quad (3.9)$$

Eventually, the vector potential of the mirror image is obtained from (3.9) by changing the sign of  $z$ .

Now, the electric field  $\vec{E}$  and the magnetic field  $\vec{B}$  can be evaluated through the following equations:

$$\vec{e}(r, z, t) = -\vec{\nabla} \phi(r, z, t) - \frac{\partial}{\partial t} \vec{A}(r, z, t) \quad (3.10)$$

$$\vec{b}(r, z, t) = \vec{\nabla} \times \vec{A}(r, z, t) \quad (3.11)$$

In [4] Rusck gives the expression of the vertical component of the electric field. More in details, he split the vertical component of the electric field in two terms: the first due to the scalar potential  $e_\phi$  and the second due to the vector potential  $e_A$ . The terms  $e_\phi$  and  $e_A$  can be obtained by the vertical component of the first and second term in the R.H.S. of (3.10), respectively, and read:

$$e_\phi(r, z, t) = \frac{\zeta_0 I_0}{4\pi\beta} \left( \frac{1}{\sqrt{(vt-z)^2 + \left(\frac{r}{\gamma}\right)^2}} + \frac{1}{\sqrt{(vt+z)^2 + \left(\frac{r}{\gamma}\right)^2}} - \frac{1}{\sqrt{(h_c-z)^2 + r^2}} - \frac{1}{\sqrt{(h_c+z)^2 + r^2}} \right) \quad (3.12)$$

$$e_A(r, z, t) = -\frac{\zeta_0 I_0}{4\pi} \beta \left( \frac{1}{\sqrt{(vt-z)^2 + \left(\frac{r}{\gamma}\right)^2}} + \frac{1}{\sqrt{(vt+z)^2 + \left(\frac{r}{\gamma}\right)^2}} \right) \quad (3.13)$$

The two components of the electric field strength at the ground, are obtained by (3.12) and (3.13) by substituting  $z = 0$ .

$$e_\phi(r, z=0, t) = \frac{\zeta_0 I_0}{2\pi\beta} \left[ \frac{1}{\sqrt{(vt)^2 + (r/\gamma)^2}} - \frac{1}{\sqrt{h_c^2 + r^2}} \right] \quad (3.14)$$

$$e_A(r, z = 0, t) = -\frac{\zeta_0 I_0}{4\pi} \beta \frac{1}{\sqrt{(vt)^2 + (r/\gamma)^2}} \quad (3.15)$$

Rusck gives also the magnetic field strength at the ground level, which reads:

$$b_\phi(r, z = 0, t) = 2 \frac{\zeta_0 I_0}{r^2} \frac{\beta t}{\sqrt{1 + \beta^2 \left[ \left( \frac{ct}{r} \right)^2 - 1 \right]}} \quad (3.16)$$

These expression are not, of course, valid until the field of the return stroke have not reached the observation point, i.e. not until the time  $t = r/c$ . Before this time, the field is determined by the stepped leader process which, in comparison with the field of the turn stroke, may be considered stationary and consequently cannot induce voltages. At the moment when the tip of the stepped leader reaches the ground, the electric field is determined by the uniformly distributed charge in the lightning channel. The study in [4] shows that the field strength is then given by

$$e_{\phi 0}(r, z = 0, t) = \frac{\zeta_0 I_0}{2\pi\beta} \left[ \frac{1}{r} - \frac{1}{\sqrt{h_c^2 + r^2}} \right] \quad (3.17)$$

i.e. the same value which is obtained by substituting  $t = r/c$  in equation (3.14). The time derivative of  $e_\phi$  is consequently limited at  $t = r/c$  even if the front time of lightning current is zero (as in the case of a step current), which is of importance when computing the induced voltage. The component of  $e_\phi$ , dependent on the charge, starts at a positive value  $e_{\phi 0}$  and decreases to zero when

the return stroke approaches to cloud. The component  $e_A$ , dependent on the lightning current, increases from zero at  $t = r/c$  to the value

$$e_A = -\frac{\zeta_0}{2\pi} I_0 \frac{\beta}{r} \quad (3.18)$$

and will then monotonously die out.

In figures (3.4), (3.5) and (3.6)  $e_\phi - e_{\phi 0}$ ,  $e_A$  and  $b_\phi$  have been plotted, respectively, as functions of the time for a number of different values of the lightning current.

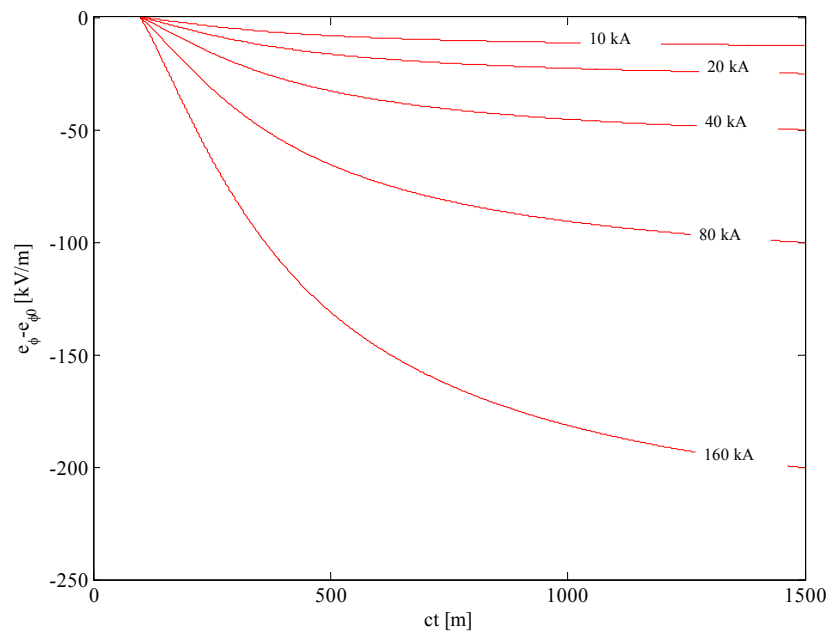


Figure 3.4: The vertical electric field component dependent on the charge distributed along the lightning channel a function of the time and for different lightning current, for  $r = 100$  m ad  $z = 0$ .

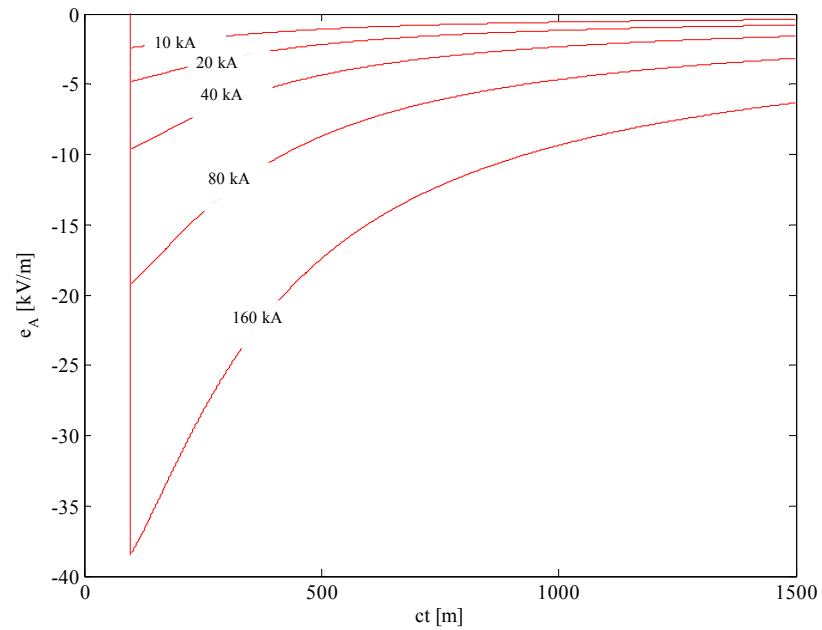


Figure 3.5: The vertical electric field component dependent on the lightning current as a function of the time and for different lightning current, for  $r = 100$  m and  $z = 0$ .

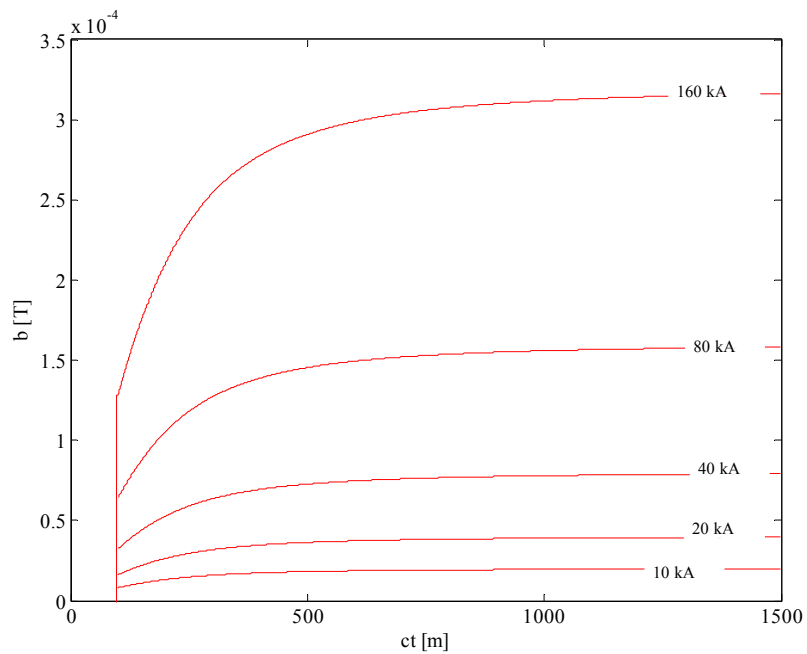


Figure 3.6: The magnetic field as a function of the time and for different lightning current, for  $r = 100$  m and  $z = 0$ .

### 3.1.2 Field to Line coupling

Rusck in [4] presented a field to wire coupling model derived in terms of the distributed currents and voltages along the line. The proposed transmission lines equations associated with the model were derived relating the total electric field on the conductor surface to the scalar and vector potentials. Considering the geometry presented in figure 3.1, the transmission line equations derived by Rusck [4,9] are:

$$\frac{\partial v^\phi(x,t)}{\partial x} + l' \frac{\partial i(x,t)}{\partial t} = 0 \quad (3.19)$$

$$\frac{\partial i(x,t)}{\partial x} + c' \frac{\partial v^\phi(x,t)}{\partial t} = c' \frac{\partial \phi^i(x,h,t)}{\partial t} \quad (3.20)$$

In equations (3.19) and (3.20)  $v^\phi(x,t)$  is the voltage induced on the line due to the scalar potential  $\phi^i$  of the incident field,  $l'$  and  $c'$  are the corresponding line inductance and capacitance per unit length, respectively,  $i(x,t)$  is the current along the line. The total voltage  $v(x,t)$  along the line is given by

$$v(x,t) = v^\phi(x,t) + \int_0^h \frac{\partial A_z^i(x,z,t)}{\partial t} dz \quad (3.21)$$

Figure 3.7 depicts the transmission line representation of the Rusck model.

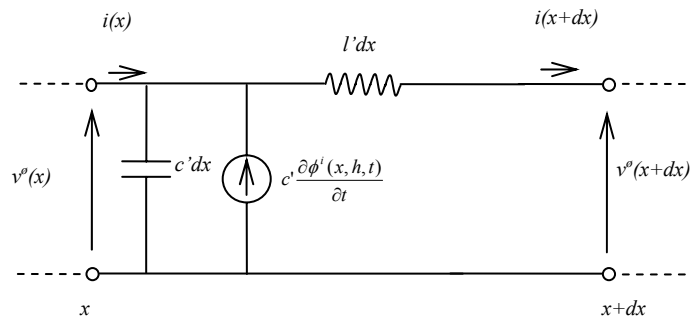


Figure 3.7: Transmission line segment representing Rusck coupling model.

To simplify the process of getting the final solution, Rusck assumes the electric field, the scalar and vector potentials between the ground and the line height to be constant and equal to those on the ground surface. With these approximations the final solution found by Rusck, after integration of (3.19) and (3.20) reads:

$$v(x,t) = \frac{\zeta_0 I_0 h}{4\pi} \beta \cdot \left[ \frac{ct-x}{d^2 + \beta^2(ct-x)^2} \left( 1 + \frac{x + \beta^2(ct-x)}{\sqrt{(\beta ct)^2 + (x^2 + d^2)/\gamma^2}} \right) + \frac{ct+x}{d^2 + \beta^2(ct+x)^2} \left( 1 + \frac{x + \beta^2(ct+x)}{\sqrt{(\beta ct)^2 + (x^2 + d^2)/\gamma^2}} \right) \right] \quad (3.22)$$

The voltage at the point nearest to the lightning stroke ( $x = 0$ ) is given by

$$v(0,t) = \frac{\zeta_0 I_0 h}{4\pi d^2} \frac{2\beta ct}{1 + (\beta ct/d)^2} \left( 1 + \beta^2 \frac{ct/d}{\sqrt{1 + \beta^2 \left[ \left( \frac{ct}{d} \right)^2 - 1 \right]}} \right) \quad (3.23)$$

In figure 3.8 the voltage induced on a line 10 m height and 50 m far from the lightning stroke is plotted. The voltage is shown for a lightning current of 10 kA and for different values of  $\beta$ .

As  $\beta$  is generally much smaller than unity the last term in the bracket in equation (3.23) may be neglected when determining the maximum value of  $v(0,t)$ . With this approximation it is found that equation (3.23), is at its maximum when

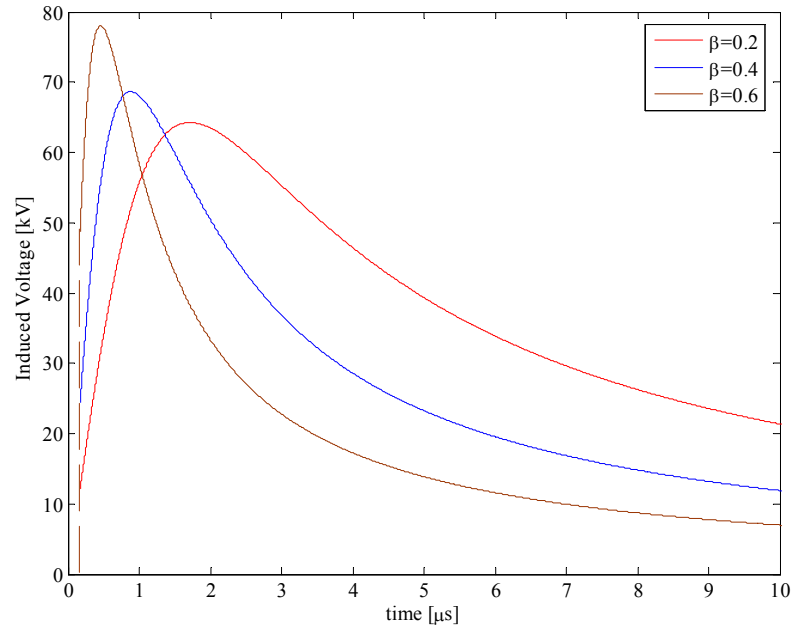


Figure 3.8: The induced voltage at  $x = 0$  according to the Rusck formula. The voltage is calculated on a line 10 m height, 50 m far from the lightning stroke, for a lightning current  $I_0=10$  kA, and is plotted for different values of  $\beta$ .

$$\beta \frac{ct}{d} = 1 \quad (3.24)$$

which gives

$$v_{peak} = \frac{\zeta_0 I_0 h}{4\pi d} \left[ 1 + \beta \frac{1}{\sqrt{2 - \beta^2}} \right] \quad (3.25)$$

Expression (3.25) is fundamental since the IEEE standard 1410 [1] proposes this formula for the peak evaluation of the induced voltage.

The Rusck formulation has been investigated by many authors; in particular, both the validity of the model underlying the solutions, and the approximations

used in this model were analysed. The validity of the underlying model was considered questionable by Parker et al. [7], since it could be responsible for the significant differences between experimental data and theoretical results. Cooray in [9] actually found a missing term in the coupling model, which however was not relevant to geometries where the lightning channel was perpendicular to the power line. In [10] Nucci et al. found that the approach may defects for situation where the overvoltage is calculated not in front of the lightning channel but in offset positions. However, the closed form solutions proposed by Rusck have never been compared with the only legitimate term of reference which is its corresponding exact analytical formulation, which, we repeat, will be derived in what follows.

### **3.2. Chowdhuri and Gross Formulae**

In this paragraph the Chowdhuri and Gross formulation will be summarised. This formulation was originally proposed in the 1967 [5]. In Cornfield [12] some errors were found in the original formulation and Chowdhuri himself proposed a corrected formulation in [13]. The basic assumptions are exactly the same as those used by Rusck, here recalled for sake of clarity:

- o vertical stroke channel with a single return stroke originating from the ground plane at time  $t = 0$ ;
- o velocity of the return stroke is constant  $v$ ;
- o uniform charge distribution along the leader stroke;
- o the line conductor is lossless and doubly infinite and the earth is perfectly conducting.

The lightning event model adopted by Chowdhuri and Gross is that in figure 3.1. The type of propagation along the lightning channel is the TL model (detailed in chapter 2).

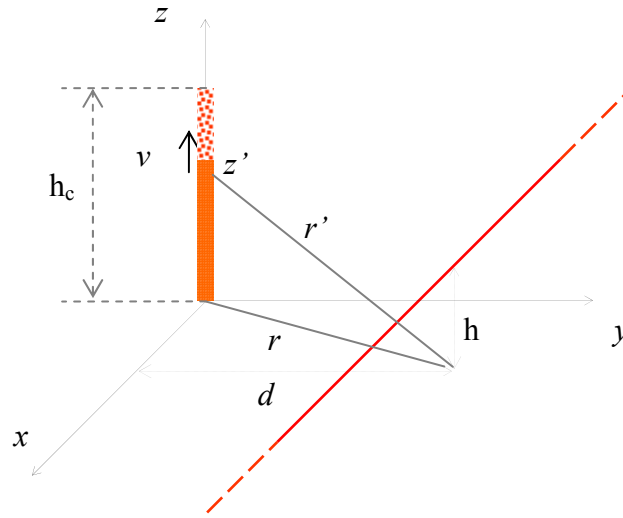


Figure 3.9: Geometry of the problem of the lightning event model of the Chowdhuri and Gross formulation.

### 3.2.1 Electromagnetic field

In this formulation a rectangular system coordinates in space of figure 3.9 was chosen. The electromagnetic field associated with the charge and the current in the lightning stroke at any point in space is

$$\vec{e}(x, y, z, t) = -\vec{\nabla} \phi(x, y, z, t) - \frac{\partial}{\partial t} \vec{A}(x, y, z, t) \quad (3.26)$$

with  $\phi$  the inducing scalar potential created by the charge of the lightning stroke and  $\vec{A}$  the inducing vector potential created by the current of the lightning stroke. These two electromagnetic inducing potentials are deduced from Maxwell's field equations

$$\phi(r, t) = \frac{1}{4\pi\epsilon_0} \int_{vol} \frac{\rho\left\{r', t - \sqrt{(\epsilon_0\mu_0)}|r - r'|\right\}}{|r - r'|} dv' \quad (3.27)$$

$$\vec{A}(r, t) = \frac{\mu_0}{4\pi} \int_{vol} \frac{\vec{J}\left\{r', t - \sqrt{(\epsilon_0 \mu_0)}|r - r'|\right\}}{|r - r'|} dv' \quad (3.28)$$

where  $r$ ,  $r'$  are the field and source points, respectively,  $\rho$  is the charge density,  $\vec{J}$  is the current density and the integration is taken over a volume enclosing the source.

For the problem of lightning induced voltage calculations, the source is the lightning stroke, and the field point is any point along the power line. The line integral of  $\vec{e}$  will then provide the *inducing voltage* at the power line

$$v_i(x, t) = -\int_0^h e_z^i dz \quad (3.29)$$

The inducing voltage (3.29) will act on each point along the length of the power line.

Because of the retardation effect, the electromagnetic potentials  $\phi$  and  $\vec{A}$  at the field point  $r$  and at time  $t$  must be originated at the source point  $r'$  at an earlier time  $t' = t - |r - r'|/c$ . It is convenient to choose the instant at which the return stroke starts from the ground as the origin of time, i.e.  $t = 0$ . The disturbance of an element of charge or current at a height  $z'$  above the ground and along the return stroke will be felt at a field point  $r$  on the ground at time

$$t = \frac{z'}{v} + \frac{\sqrt{z'^2 + x^2 + d^2}}{c} \quad (3.30)$$

Therefore, the earliest time at which the disturbance from the return stroke will reach a field point would be

$$t_0 = \frac{\sqrt{x^2 + d^2}}{c} \quad (3.31)$$

In other words, the inducing voltage at a field point remains zero till  $t = t_0$ . Hence, the inducing voltage is a sectioned function

$$v_i(x, t) = \psi(x, t)u(t - t_0) \quad (3.32)$$

with  $u(t - t_0)$  the shifted Heaviside function. The continuous function  $\psi(x, t)$  is evaluated from the assumed structure of the lightning stroke. When the channel base current is a step function (figure 3.3) with magnitude  $I_0$ ,  $\psi(x, t)$  reads

$$\psi(x, t) = \frac{-60I_0h}{\beta} \left[ \frac{1}{\gamma^2 \sqrt{(\beta ct)^2 + (r/\gamma)^2}} - \frac{1}{\sqrt{h_c^2 + r^2}} \right] \quad (3.33)$$

Note that  $2\zeta_0/(4\pi) = 60\Omega$ .

### 3.2.2 Field to Line coupling

In the Chowdhuri and Gross model a power line is represented as consisting of distributed series inductance and distributed shunt capacitance. The transmission line equations based on the Chowdhuri and Gross coupling model are

$$-\frac{\partial v(x, t)}{\partial x} = l' \frac{\partial i(x, t)}{\partial t} \quad (3.34)$$

$$-\frac{\partial i(x, t)}{\partial x} = c' \frac{\partial}{\partial t} [v(x, t) - v_i(x, t)] \quad (3.35)$$

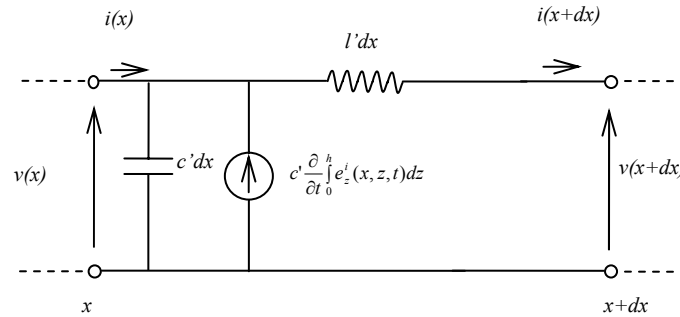


Figure 3.10: Transmission line segment representing Chowdhuri and Gross coupling model.

with  $l'$  and  $c'$  the corresponding line inductance and capacitance per unit length, respectively,  $v(x,t)$  and  $i(x,t)$  the voltage and current along the line, respectively. The equivalent transmission line representation based on Chowdhuri and Gross coupling model is shown in figure 3.10.

It should be mentioned here that the transmission line equations presented by Chowdhuri and Gross [5] are similar to those of Rusck [4], but they are expressed in terms of total line voltage. The source term along each point of the line counts of the *inducing voltage*  $v_i(x,t)$ . Chowdhuri and Gross state that since the height of the line conductor is small compared with the height of the cloud (i. e. the length of the lightning channel), the inducing electric field below the line conductor can be assumed constant and equal to that on the ground surface. Then, the inducing voltage  $v_i(x,t)$  can be written as:

$$v_i(x,t) = -\int_0^h e_z^i dz \cong -he_z^i \quad (3.36)$$

Chowdhuri and Gross proposed two closed form solutions: in the first a step current along the lightning channel was assumed, while in the second a linearly rising current. In the following both these two formulae will be summarised.

### 3.2.3 Induced Voltage: Step Current along the lightning channel

The first closed form solution presented by Chowdhuri and Gross applies to the case of a step current propagating along the lightning channel, plotted in figure 3.3. The channel base current is then a step function, as in the Rusck formulae. The expression describing the current distribution for the model under study is given by (3.1).

The inducing voltage  $v_i(x,t)$ , is (3.32). By solving the coupling equations (3.34) and (3.35) the induced voltage is evaluated. According to the Chowdhuri and Gross model, the total voltage is given by

$$v(x,t) = \begin{cases} 0 & t < t_0 \\ v_{11} + v_{12} + v_{21} + v_{22} & t \geq t_0 \end{cases} \quad (3.37)$$

with

$$v_{11} = \frac{30I_0h}{\beta^2\gamma^2(ct-x)^2 + d^2} \left[ \beta(ct-x) + \frac{(ct-x)x - d^2}{\sqrt{(ct)^2 + \frac{x^2 + d^2}{\beta^2\gamma^2}}} \right] \quad (3.38)$$

$$v_{12} = \frac{-30I_0h}{\beta} \left( \frac{1}{\gamma^2} - \frac{1}{\sqrt{k_1^2 + 1}} \right) \frac{1}{ct-x} \quad (3.39)$$

$$v_{21} = \frac{30I_0h}{\beta^2\gamma^2(ct+x)^2 + d^2} \left[ \beta(ct+x) - \frac{(ct+x)x + d^2}{\sqrt{(ct)^2 + \frac{x^2 + d^2}{\beta^2\gamma^2}}} \right] \quad (3.40)$$

$$v_{22} = \frac{-30I_0h}{\beta} \left( \frac{1}{\gamma^2} - \frac{1}{\sqrt{k_2^2 + 1}} \right) \frac{1}{ct + x} \quad (3.41)$$

where

$$k_1 = k_2 = \frac{h_c}{\sqrt{x^2 + d^2}} \quad (3.42)$$

In [13,14] Chowdhuri introduced a correction to this formula, considering the suggestion given by Cornfield [12]. In particular, the correction regards the coefficients  $k_1$  and  $k_2$  which take the form

$$\begin{aligned} k_1 &= \frac{2h_c(ct - x)}{d^2 + (ct - x)^2} \\ k_2 &= \frac{2h_c(ct + x)}{d^2 + (ct + x)^2} \end{aligned} \quad (3.43)$$

In figure 3.11 the voltage induced on a line 10 m height and 50 m far from the lightning stroke is plotted. The voltage is shown for a lightning current of 10 kA, for  $\beta = 0.4$  and the lightning channel is assumed 5 km long.

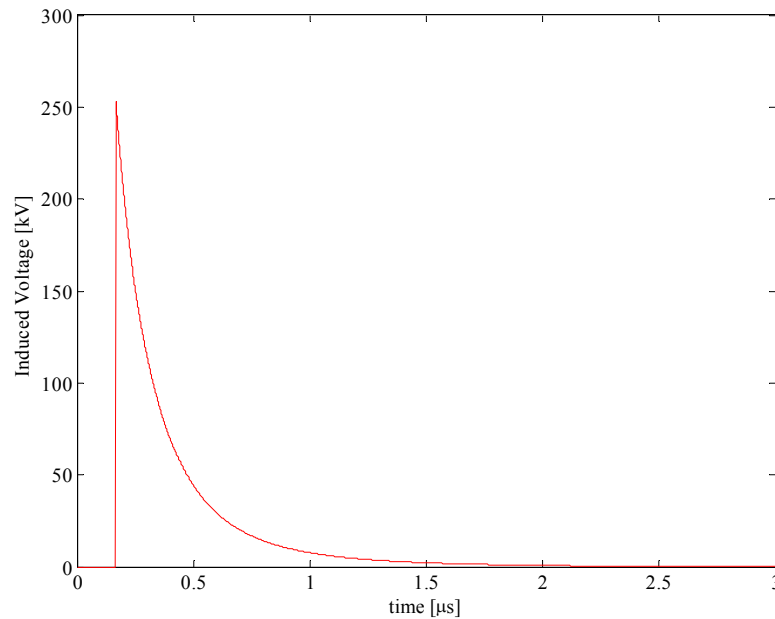


Figure 3.11: The induced voltage at  $x = 0$  according to the Chowdhuri and Gross formula for a lightning step current. The voltage is calculated on a line 10 m height, 50 m far from the lightning stroke, for a lightning current  $I_0=10$  kA,  $\beta=0.4$  and for a lightning channel 5 km long.

### 3.2.4 Induced Voltage: Linearly rising front current along the lightning channel

Once the induced voltage on an overhead line caused by a rectangular current wave in the return stroke is known, the corresponding induced voltage caused by any other form of current in the return stroke can be computed by the application of Duhamel's theorem [15,16], so explained by Chowdhuri and Gross:

*“if the current in the return stroke  $i'(t)$  is of exponential order and is a continuous function of  $t$ , and if its first derivative with respect to  $t$  is sectionally continuous, the induced voltage caused by this current is*

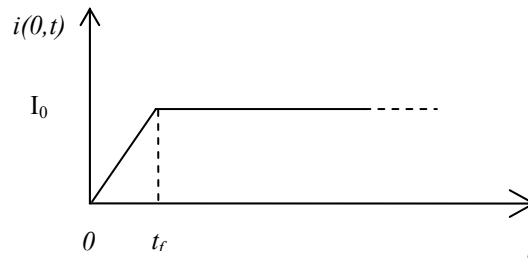


Figure 3.12: Channel base current linearly rising front time.

$$v(x,t) = i'(t=0)v_0(x,t) + \int_0^t \frac{d}{dt} i(t-\tau)v_0(x,\tau)d\tau \quad (3.44)$$

where  $v_0(x,t)$  is the induced voltage caused by the unit-step-function return stroke current”.

By means of the Duhamel’s theorem Chowdhuri and Gross presented the closed form solution for the case of a linearly rising front channel base current propagating along the lightning channel. In figure 3.12 the current waveshape is plotted. The expression describing the channel base current waveshape is

$$i(0,t) = I_0 \cdot \begin{cases} \alpha t & t \leq t_f \\ 1 & t > t_f \end{cases} \quad (3.45)$$

with  $\alpha = t_f/t$ . The expression for induced voltage due to this lightning current waveshape was given by Chowdhuri and Gross as:

$$v(x,t) = \begin{cases} 0 & t \leq t_0 \\ v^1(x,t) & t_0 < t \leq t_0 + t_f \\ v^1(x,t) - v^1(x,t-t_f) & t > t_0 + t_f \end{cases} \quad (3.46)$$

with

$$v^1(x,t) = \frac{30I_0h}{t_f\beta c} \cdot \left[ \frac{1}{\gamma^2} \ln \left( \frac{(1-\beta^2)(\beta^2x^2 + d^2) + (\beta ct)^2(1+\beta^2)}{(1-\beta^2)^2 d^2} - \frac{2\gamma^4\beta^2 ct \sqrt{(\beta ct)^2 + \frac{x^2 + d^2}{\gamma^2}}}{d^2} \right) + \left. - \left\{ 1 - \frac{1}{\sqrt{k^2 + 1}} - \beta^2 \right\} \ln \left( \frac{(ct)^2 - x^2}{d^2} \right) \right] \quad (3.47)$$

In [11] Chowdhuri introduced the correction to the original formula (3.47), considering the suggestion given by Cornfield [12], reported in (3.43).

Both the two closed form solutions (3.36) and (3.46) proposed by Chowdhuri and Gross have been investigated by many authors, e.g. [11,16,17]; in particular, both the validity of the model underlying the solutions, and the approximations used in those models were analysed. In particular Nucci et al. in [11] found the Chowdhuri and Gross coupling model incomplete, since it is missing one term which is very relevant to overvoltages calculations.

### 3.3 Liew and Mar Formulae

Liew and Mar in [7] proposed, following a similar procedure to that of Chowdhuri and Gross, a new closed form solution for both the step current and the linearly rising current. The basic assumptions are exactly the same as those used by Chowdhuri and Gross and also by Rusck. The geometry of the problem is shown in figure 3.9.

Liew and Mar consider the inducing voltage as

$$v_i(x,t) = -\int_0^h \frac{\partial A_z}{\partial t} dz \cong -h \frac{\partial A_z}{\partial t} \quad (3.48)$$

instead of (3.36). In the following we summarise the two formulae presented by Liew and Mar.

### 3.3.1 Induced Voltage: Lightning Step Current along the lightning channel

In this case of step current along the lightning channel (figure 3.3), Liew and Mar proposed the following formula for induced voltage evaluation reads

$$v(x,t) = \begin{cases} 0 & t < t_0 \\ v_1 + v_2 & t \geq t_0 \end{cases} \quad (3.49)$$

with

$$\begin{aligned} v_1 = & \frac{30I_0h}{\beta^2(ct-x)^2 + d^2} \left[ \beta(ct-x) + \frac{(ct-x)x - d^2}{\sqrt{(ct)^2 + \frac{x^2 + d^2}{\beta^2\gamma^2}}} \right] + \\ & - \frac{30I_0h}{\beta} \left[ \left( 1 - \frac{1}{\sqrt{k_1^2 + 1}} \right) \frac{1}{ct-x} + \left( 1 - \frac{1}{\sqrt{k_2^2 + 1}} \right) \frac{1}{ct+x} \right] \\ & + \frac{30I_0h}{\beta^2(ct+x)^2 + d^2} \left[ \beta(ct+x) - \frac{(ct+x)x + d^2}{\sqrt{(ct)^2 + \frac{x^2 + d^2}{\beta^2\gamma^2}}} \right] \end{aligned} \quad (3.50)$$

and

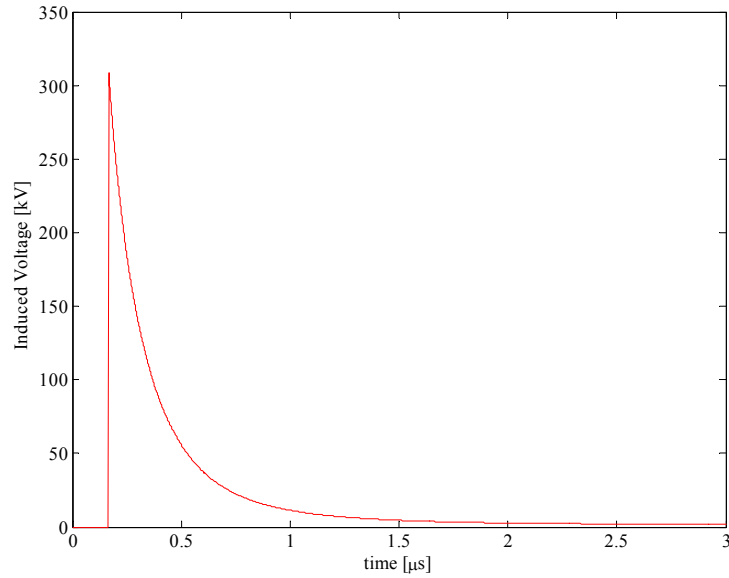


Figure 3.13: The induced voltage at  $x = 0$  according to the Liew and Mar formula for a lightning step current. The voltage is calculated on a line 10 m height, 50 m far from the lightning stroke, for a lightning current  $I_0=10$  kA,  $\beta=0.4$  and for a lightning channel 5 km long.

$$v_2 = \frac{60I_0h}{\beta} \left[ \frac{\beta^2}{\sqrt{(\beta ct)^2 - (x^2 + d^2)/\gamma^2}} \right] \quad (3.51)$$

with  $k_1$  and  $k_2$  already given in (3.43).

In figure 3.13 the voltage induced on a line 10 m height and 50 m far from the lightning stroke is plotted. The voltage is shown for a lightning current of 10 kA, for  $\beta = 0.4$  and the lightning channel is assumed 5 km long.

### 3.3.2 Induced Voltage: Linearly Rising Current along the lightning channel

The expression for induced voltage due to this lightning current waveshape (figure 3.12) was given by Liew and Mar as:

$$v(x,t) = \begin{cases} 0 & t \leq t_0 \\ v^1(x,t) & t_0 < t \leq t_0 + t_f \\ v^1(x,t) - v^1(x,t-t_f) & t > t_0 + t_f \end{cases} \quad (3.52)$$

$$v^1(x,t) = \frac{30I_0h}{t_f\beta c} \cdot \left[ \ln \left( \frac{(1-\beta^2)(\beta^2x^2 + d^2) + (\beta ct)^2(1+\beta^2)}{(1-\beta^2)^2d^2} - \frac{2\gamma^4\beta^2ct\sqrt{(\beta ct)^2 + \frac{x^2+d^2}{\gamma^2}}}{d^2} \right) + 2\beta \left( \sinh^{-1} \frac{\beta ct}{\sqrt{1-\beta^2}} - \sinh^{-1} \frac{\beta ct_0}{\sqrt{1-\beta^2}} \right) \right] + G(x,t) \quad (3.53)$$

with

$$G(x,t) = \frac{30I_0h}{t_f\beta c} \left[ -\ln \frac{(ct)^2 - x^2}{d^2} + \frac{1}{2} \left( \cosh^{-1} \frac{u+p}{\sqrt{p^2-q^2}} - \cosh^{-1} \frac{u_0+p}{\sqrt{p^2-q^2}} + \cosh^{-1} \frac{z+p/q}{\sqrt{p^2/q^4-1/q^2}} - \cosh^{-1} \frac{z_0+p/q}{\sqrt{p^2/q^4-1/q^2}} + \cosh^{-1} \frac{w+p}{\sqrt{p^2-q^2}} - \cosh^{-1} \frac{w_0+p}{\sqrt{p^2-q^2}} + \cosh^{-1} \frac{v+p/q}{\sqrt{p^2/q^4-1/q^2}} - \cosh^{-1} \frac{v_0+p/q}{\sqrt{p^2/q^4-1/q^2}} \right) \right] \quad (3.54)$$

where

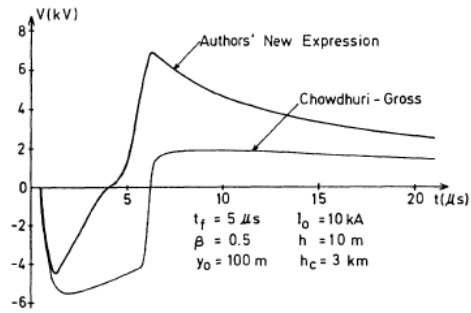


Figure 3.14: Induced voltage for a linearly rising front time lightning current at  $x = 0$ , adapted from [7]. In the plot  $y_0 = d$  and the *Authors' New Expression* is the Liew and Mar expression.

$$\begin{aligned}
 w &= (ct + x)^{-2} & w_0 &= (ct_0 + x)^{-2} \\
 v &= (ct + x)^2 & v_0 &= (ct_0 + x)^2 \\
 u &= (ct - x)^{-2} & u_0 &= (ct_0 - x)^{-2} \\
 z &= (ct - x)^2 & z_0 &= (ct_0 - x)^2 \\
 p &= \frac{d^2 + 2h_c^2}{d^4} & q &= 1/d^2
 \end{aligned}$$

In figure 3.14 both the Chowdhuri and Gross and the Liew and Mar formulae are reported, adapted from [7].

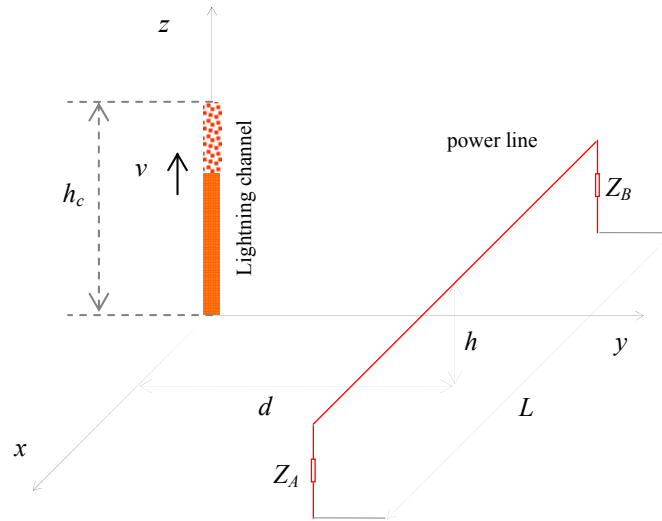


Figure 3.15: The lightning event model used by Hoidalén.

### 3.4. Hoidalén Formulae

The configuration of the system is shown in Fig. 3.15. The lightning channel is assumed to be straight and vertical and the lightning return stroke model of the type TL, detailed in chapter 2. The line is considered lossless. The formulation of Hoidalén aims to consider the lossy behaviour of the ground in order to evaluate the induced overvoltages.

#### 3.4.1 Electromagnetic Field over a lossless ground

The hypothesis of the Hoidalén formulation are identical to the previous discussed formulation except for the situation of the lightning channel, which is now assumed initially free of charges, so disregarding the effects of the initial stepped leader. A step current with amplitude  $I_0$  and velocity  $v$  is assumed for the return stroke. The field expressions calculated by Hoidalén read:

$$e_{x0}(x, y, z, t) \cong \frac{\partial e_{x0}(x, y, z, t)}{\partial z} \Big|_{z=0} \cdot z = \frac{\mu_0 c I_0}{2\pi\beta} \cdot x \cdot z \cdot \left( -\frac{1-\beta^2}{\xi^3} + \frac{1}{r^3} \right) \quad (3.55)$$

$$e_{z0}(x, y, z = 0, t) = \frac{\mu_0 c I_0}{2\pi\beta} \left( \frac{1 - \beta^2}{\xi} - \frac{1}{r} \right) \quad (3.56)$$

$$b_{y0}(x, y, z = 0, t) = \frac{\mu_0 I_0}{2\pi r^2} \frac{\beta c t x}{\xi} \quad (3.57)$$

with

$$\xi = \xi(x, y, t) = \sqrt{(\beta c t)^2 + \frac{x^2 + y^2}{\gamma^2}} \quad (3.58)$$

The horizontal electric field is approximated by the first term of a series expansion around  $z = 0$ , (note that  $e_{x0}(x, y, z = 0, t) = 0$ ). The vertical component of the electric field and the magnetic field are equal to Rusck's expressions, when the static field from the charged leader is ignored [6].

### 3.4.2 Effect of lossy ground

According to the Cooray Rubinstein approximation [19,20], as discussed in chapter 2, the horizontal electric field over a lossy ground is the sum of the lossless field and a surface impedance contribution depending on the horizontal magnetic field. In the time domain it reads:

$$e_x^\sigma(x, y, z, t) = e_x^0 + e_x^A = e_x^0(x, y, z, t) - g_0(t) * b_{y0}(x, y, z = 0, t) \quad (3.59)$$

where  $e_x^A$  is the lossy ground contribution,  $e_x^\sigma$  is the horizontal electric field over a lossy ground, the sign \* denotes a convolution and  $g_0(t)$  is the surface function in the time domain. The surface function is in the laplace domain [18]

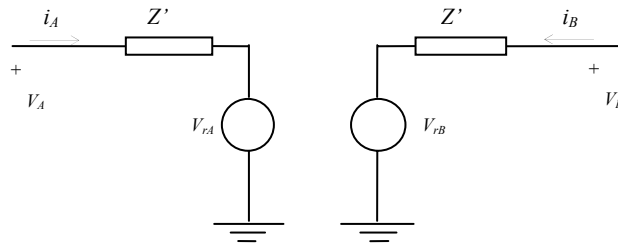


Figure 3.16: Electric model of an overhead line adopted by Hoidalen.

$$g_0(s) = \sqrt{\frac{\epsilon_0 s}{\sigma + \epsilon_r \epsilon_0 s}} = \frac{1}{\sqrt{\epsilon_r}} \sqrt{\frac{s}{s + 2a}} \quad (3.60)$$

with the ground factor  $a = \sigma / (2\epsilon_r \epsilon_0)$ ,  $\sigma$  the ground conductivity and  $\epsilon_r$  relative ground permittivity.

The lossy ground effect on the vertical electrical field and the magnetic field can be ignored since they do not give significant contributions [6].

### 3.4.3 Induced Voltage

Hoidalen uses the Agrawal et al. coupling model [20] to calculate the lightning induced voltages. This coupling model was detailed in chapter 2. The calculation of the induced voltages is formulated using a procedure proposed by Hoidalen himself in [21]. According to that, the overhead line can be electrically modelled by the classical Bergeron model as shown in figure 3.15, where the voltage sources are constructed as

$$\begin{aligned} v_{rA}(t) &= v_{ind}^\sigma(x_A, t) + v_B(t - \tau) + Z' i_B(t - \tau) \\ v_{rB}(t) &= v_{ind}^\sigma(-x_B, t) + v_A(t - \tau) + Z' i_A(t - \tau) \end{aligned} \quad (3.61)$$

with  $v_{rA}$  and  $v_{rB}$  the sources at terminal  $A$  and  $B$ . The source at terminal  $A$  consists of a resultant inducing voltage term called  $v_{ind}^\sigma$  and the reflection from terminal  $B$  delayed a time  $\tau$ . Based on the sum in (3.38) the inducing voltage  $v_{ind}^\sigma$  is split in a lossless contribution  $v_{ind}^0$  and an additional lossy ground contribution  $v_{ind}^A$  as

$$v_{ind}^\sigma(x, t) = v_{ind}^0(x, t) + v_{ind}^A(x, t) \quad (3.62)$$

The lossless contribution to the induced voltage at a terminal can be written as

$$v_{ind}^0(x, t) = g_1(t) * v_0(x, t) \quad (3.63)$$

where  $g_1(t)$  is a function that takes the lightning current shape into account and  $v_0(x, t)$  is the induced voltage produced by a step current as formulated in [22], which reads

$$v_{ind}^0(x, t) = \frac{\mu_0 c}{2\pi} I_0 \beta h f_0(x, t) \begin{cases} 0 & 0 \leq t \leq t_1 \\ f_1(x, t) + 1 & t_1 < t \leq t_2 \\ f_1(x, t) - f_1(x - L, t - \tau) & t > t_2 \end{cases} \quad (3.64)$$

with  $t_1 = \frac{\sqrt{x^2 + d^2}}{c}$ ,  $t_2 = \frac{\sqrt{(x-L)^2 + d^2}}{c} + T$ ,  $T = \frac{L}{c}$  and

$$f_0(x, t) = \frac{ct - x}{d^2 + \beta^2(ct - x)^2} \quad (3.65)$$

$$f_1(x, t) = \frac{x + \beta^2(ct - x)}{\xi(x, d, t)} \quad (3.66)$$

For times less than  $t_2$ , the expression (3.64) is equal to Rusck's formula (3.23) even though a different coupling model is used. This was also generally verified by Cooray in [9].

The additional contribution to the induced voltage from the horizontal electric field due to the lossy ground is given by:

$$v_{ind}^{\Delta}(x,t) = -g_1(t) * g_0(t) * v_{\Delta}(x,t) \quad (3.67)$$

where  $-g_0(t) * v_{\Delta}(x,t)$  equal to the induced voltage contribution produced by a step current. The expression of  $v_{\Delta}$  is given by Hoidalen as:

$$v_{\Delta}(x,t) = \frac{\mu_0 c}{2\pi} I_0 \beta \cdot \begin{cases} 0 & 0 \leq t \leq t_1 \\ \ln(f_2(x,t)f_0(x,t)) - \frac{1}{\beta} \ln\left(\frac{f_3(x,t)}{1+\beta}\right) & t_1 < t \leq t_2 \\ \ln\left(\frac{f_2(x,t)}{f_2(x-L,t-\tau)}\right) - \frac{1}{\beta} \ln\left(\frac{f_3(x,t)}{f_3(x-L,t-\tau)}\right) & t > t_2 \end{cases} \quad (3.68)$$

with

$$\begin{aligned} f_2(x,t) &= x + \beta^2(ct - x) + \xi(x,y,t) \\ f_3(x,t) &= \frac{1}{\sqrt{x^2 + y^2}} (\beta ct + \xi(x,y,t)) \end{aligned} \quad (3.69)$$

To analytically solve the convolution  $g_1(t) * g_0(t)$  in equation (3.67), Hoidalen choose a suitable lightning current. One such current shape is a linear rising and decreasing lightning current, reported in figure 3.17. The induced voltage terms is formulated by Hoidalen as

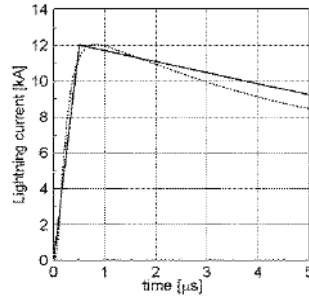


Figure 3.17: Linear rising and decreasing lightning current in Hoidalen formulation, adapted from [6].

$$\begin{aligned} v_{ind}^0(x,t) &\cong A_0(x,t) - bA_0(x,t-t_c) \\ v_{ind}^\Delta(x,t) &\cong A_\Delta(x,t) - bA_\Delta(x,t-t_c) \end{aligned} \quad (3.70)$$

where

$$A_0(x,t) = H(t) \frac{I_m \Delta t}{I_0 t_c} \left[ \sum_{i=0}^{t/\Delta t - 1} v_0(x, i\Delta t) + \frac{v_0(x,t)}{2} \right] \quad (3.71)$$

$$\begin{aligned} A_\Delta(x,t) = & -H(t) \frac{I_m}{I_0 t_c} \sqrt{\frac{\epsilon_0 \Delta t}{\pi \sigma}} \left[ \sum_{i=0}^{t/\Delta t - 1} \frac{v_\Delta(x, i\Delta t)}{\sqrt{t/\Delta t - 1}} + \right. \\ & \left. + \left( -0.22\kappa^3 + \frac{1}{6} \right) v_\Delta(x, t - \Delta t) + \left( -1.07\kappa + 0.22\kappa^3 + \frac{4}{3} \right) v_\Delta(x, t) \right] \end{aligned} \quad (3.72)$$

with  $b = t_c / [2(t_h - t_c)] + 1$ ,  $\kappa = \sqrt{\epsilon_{rg} \epsilon_0 / (\pi \sigma \Delta t)}$ ,  $\Delta t$  the time step used in the numerical integration,  $H(t)$  the unit step function,  $t_c$  the lightning current time to crest,  $t_h$  the lightning current time to half value and  $I_m$  the amplitude of return stroke current of figure 3.17.

Figure 3.18 shows the calculated induced voltage using the formula of Hoidalen for a 1 km long, 10 m high overhead line terminated with its

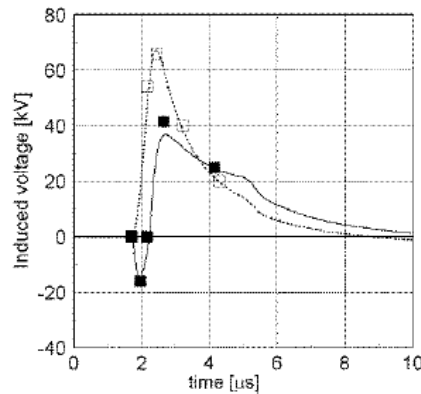


Figure 3.18: Induced voltage at the terminals A and B in overhead line terminated with its characteristic impedance. Dotted line: Hoidalen formula for lossless ground. Solid line: Hoidalen formula for lossy ground. ■: Induced voltage predicted by [22] Adapted from [6].

characteristic impedance. The lightning is located 50 m from the overhead line centre. The lightning return stroke velocity is  $1.3 \cdot 10^8$  m/s, and the current shape used is with  $t_c = 0.5 \mu\text{s}$ ,  $t_h = 20 \mu\text{s}$ ,  $I_m = 12$  kA. Moreover  $\epsilon_{rg} = 10$  and  $\sigma = 0.001 \text{ S/m}$  are assumed. In Figure 3.17 is also shown the induced voltage predicted by a numerical method [22].

### 3.5 Exact Closed Form Solution

In the previous paragraphs the most important formulae used in literature have been summarised. As detailed in the previous paragraphs, in those formulations two lightning event models are used: the first, used by Hoidalen [6], is shown in figure 3.19 a), and the second, used by Rusck [4], by Chowdhuri and Gross [5] and by Liew and Mar [7], is shown in figure 3.19 b). In both the events depicted, the lightning applies to the case of a vertical and straight lightning channel, however, in the model of figure 3.19 a) a return stroke current propagates upwards along the lightning channel initially free of charges, while in the model of figure 3.19 b), to take into account the leader effect, a negative charge is

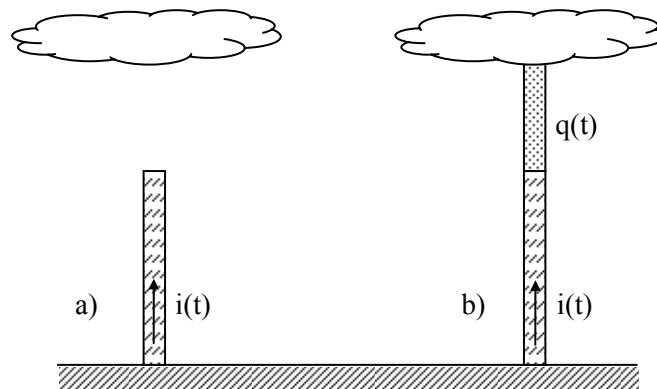


Figure 3.19: Lightning Events Models. In a) a straight and vertical return stroke current moves upwards. In b) a negative charge is uniformly distributed along the lightning path before the return stroke starts, to take into account the leader effect.

uniformly distributed along the lightning path. In both the events, we recall, that the return stroke current is assumed to be a step current which propagates along the lightning channel without any attenuation or distortion with the constant velocity  $v$  (TL model). The ground is considered to be a perfect conductor and the power line is lossless. Even if simple, these lightning event models can be considered reasonably accurate. In fact, as far as TL model, in [23] Thottappillil and Uman showed that this model is in fairly good agreement with measurements, also the lossless hypothesis for the power line is a reasonable assumption [24]. The main limitations of these models are essentially the step waveshape used for the return stroke current, which, however, overestimates the induced voltages, resulting in a safe evaluation and the perfect conductor hypothesis for the ground [24].

All the closed form solutions presented in literature have been investigated by many authors, as already discussed in the previous paragraphs. The major limitation of those investigation is the fact that the closed form solution were never compared with the only legitimate term of reference which is their corresponding *exact analytical solutions*.

For this reasons this paragraph aims, primarily, to get the *exact closed form solution* for both the lightning events of figure 3.19; in fact, no approximations will be made, and the results can be considered absolutely rigorous. Secondly to

compare the other closed form solutions with the exact one in order to highlight their accuracy.

The next sections are organised as follows: first of all the lightning electromagnetic field is evaluated for both the initially free of charges channel and for the initially charged channel, then the field to line coupling problem is analysed and the closed form solutions will be derived for both the lightning events examined. In the final part, the other closed forms presented in literature will be compared with the exact one.

### ***3.5.1 Lightning Electromagnetic Field Appraisal***

In literature, two techniques have been used for finding the electromagnetic field from a known distribution of currents and charges. One of these is the *monopole technique* (e.g. [4,5]) which has been primarily used in the power systems literature for lightning radiation calculation. The other is the *dipole technique* which is widely used in theory of antennas, but today frequently used for lightning radiation and overvoltage calculation (e.g [6,24,25]). The two techniques have been demonstrated absolutely equivalent by Rubinstein and Uman [26]. In what follows an overall analysis, in order to derive the field analytical expressions, will be carried out for both the two techniques and for both the events depicted in figure 3.19.

#### *1. Initially Free of Charge Channel: Monopole Technique*

The initially free of charges channel is considered. The geometry of the problem is shown in figure 3.20. The expression describing the current distribution for the model under study is given by

$$i(z', t) = I_0 u(t - |z'|/v) \quad (3.73)$$

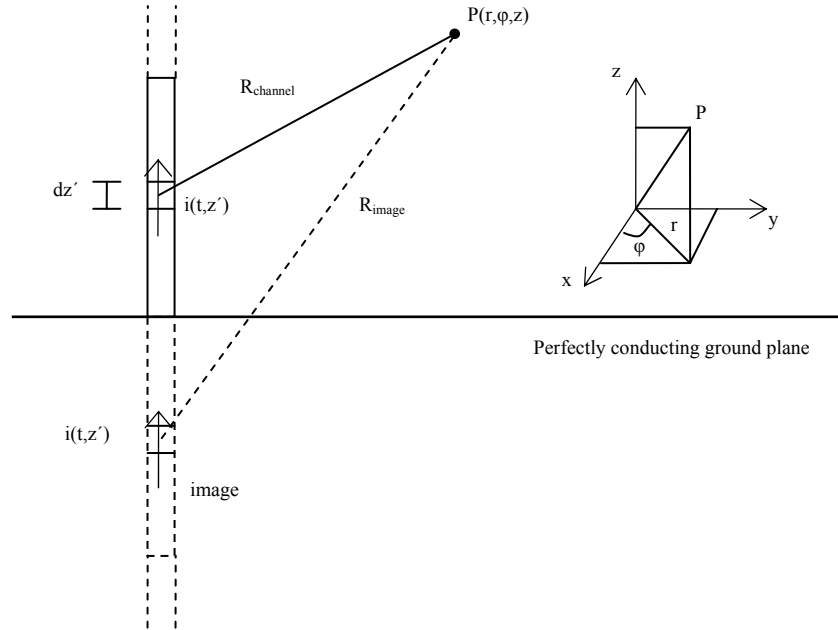


Figure 3.20: Geometry of the problem for the field evaluation.

This return stroke current, as it moves along the channel, leaves a positive charge distribution  $q$ . The relation between the current and charge distributions  $q$  is given by  $I_0 = qv$  [4].

The scalar potential  $\phi$  and the vertical component of the vector potential  $A_z$ , at the observation point  $P(r, \phi, z)$ , can be written as [4]

$$\phi(r, z, t) = \frac{1}{4\pi\epsilon_0} \int_{-\infty}^{\infty} \left[ \frac{q(z')}{R} - \frac{q(z')}{R_0} \right] dz' \quad (3.74)$$

$$A_z(r, z, t) = \frac{\mu_0}{4\pi} \int_{-\infty}^{\infty} \frac{1}{R} i(z', t - R/c) dz' \quad (3.75)$$

where  $R$  is the distance between the observation point and the source point considered and  $R_0$  is the distance between the source point considered and the point,  $P_0(r_0, \phi_0, z_0)$  in which the scalar potential is zero. As shown in figure 3.20,

$R$ , for the upper part of the channel and the image part, can be respectively written as:

$$\begin{aligned} R_{channel} &= \sqrt{(z'-z)^2 + r^2} \\ R_{image} &= \sqrt{(z'+z)^2 + r^2} \end{aligned} \quad (3.76)$$

The two integrals (3.74) and (3.75) can be split into two parts, to take into account the different contribution of the upper part of the channel and the image part. For the current, for the upper part of the channel, and for the image part, can be written, respectively,

$$\begin{aligned} i(z', t - R_{channel}/c) &= I_0 u(t - z'/v - \sqrt{(z'-z)^2 + r^2}/c) \\ i(z', t - R_{image}/c) &= I_0 u(t + z'/v - \sqrt{(z'+z)^2 + r^2}/c) \end{aligned} \quad (3.77)$$

The same applies to the charge  $q$ . Note that integrals (3.74) and (3.75) are zero when the Heaviside functions in (3.77) are zero. Then, the lower and upper limits of integrals (3.74) and (3.75) can be found by setting the argument of the Heaviside functions to zero. For the upper part channel and image part, respectively reads

$$\begin{aligned} t - \frac{z'}{v} - \frac{\sqrt{(z'-z)^2 + r^2}}{c} &= 0 \\ t + \frac{z'}{v} - \frac{\sqrt{(z'+z)^2 + r^2}}{c} &= 0 \end{aligned} \quad (3.78)$$

Solving for  $z'$ , when  $ct > \sqrt{r^2 + z^2}$ , the upper  $a(t)$  and lower  $b(t)$  limits of integrals (3.74) and (3.75) can be calculated as

$$\begin{aligned} a(t) &= \beta\gamma^2 [-(\beta z - ct) - \xi_{channel}] \\ b(t) &= \beta\gamma^2 [-(\beta z + ct) - \xi_{image}] \end{aligned} \quad (3.79)$$

with  $\xi_{channel} = \sqrt{(\beta ct - z)^2 + (r/\gamma)^2}$  and  $\xi_{image} = \sqrt{(\beta ct + z)^2 + (r/\gamma)^2}$ .

The expression of the scalar potential is then given by

$$\phi(r, z, t) = \frac{q_0}{4\pi\epsilon_0} \left[ \ln \frac{vt - z + \sqrt{(vt - z)^2 + \left(\frac{r}{\gamma}\right)^2}}{vt + z + \sqrt{(vt + z)^2 + \left(\frac{r}{\gamma}\right)^2}} + \ln \frac{z + \sqrt{z^2 + r^2}}{-z + \sqrt{z^2 + r^2}} \right] - \phi_0 \quad (3.80)$$

with

$$\phi_0 = \frac{q_0}{4\pi\epsilon_0} \left[ \ln \frac{z_0 + \sqrt{z_0^2 + r_0^2}}{-z_0 + \sqrt{z_0^2 + r_0^2}} \right] \quad (3.81)$$

The vertical component of the vector potential  $A_z$  is given by

$$A_z(r, z, t) = \frac{\mu_0}{4\pi} I_0 \cdot$$

$$\left[ \ln \frac{\beta ct - z + \sqrt{(\beta ct + z)^2 + \left(\frac{r}{\gamma}\right)^2}}{(1 + \beta) \left( -z + \sqrt{z^2 + r^2} \right)} + \ln \frac{\beta ct + z + \sqrt{(\beta ct + z)^2 + \left(\frac{r}{\gamma}\right)^2}}{(1 + \beta) \left( z + \sqrt{z^2 + r^2} \right)} \right] \quad (3.82)$$

Once that the scalar and the vector potentials are known the electromagnetic field can be calculated as

$$\vec{e}(r, z, \varphi, t) = -\vec{\nabla}\phi - \frac{\partial}{\partial t} \vec{A} \quad (3.83)$$

$$\vec{h}(r, z, \varphi, t) = \frac{1}{\mu_0} \vec{\nabla} \times \vec{A} \quad (3.84)$$

By applying equation (3.83) the radial and vertical components of the electric field read:

$$e_r^1 = \frac{\zeta_0 I_0}{4\pi\beta r} \begin{cases} 0 & 0 \leq t \leq \frac{\sqrt{r^2 + z^2}}{c} \\ \frac{\beta ct - z}{\xi_{channel}} - \frac{\beta ct + z}{\xi_{image}} + \frac{2z}{\sqrt{r^2 + z^2}} & t > \frac{\sqrt{r^2 + z^2}}{c} \end{cases} \quad (3.85)$$

$$e_z^1 = \frac{\zeta_0 I_0}{4\pi\beta} \begin{cases} 0 & 0 \leq t \leq \frac{\sqrt{r^2 + z^2}}{c} \\ \frac{1/\gamma^2}{\xi_{channel}} + \frac{1/\gamma^2}{\xi_{image}} - \frac{2}{\sqrt{r^2 + z^2}} & t > \frac{\sqrt{r^2 + z^2}}{c} \end{cases} \quad (3.86)$$

where the superscript 1 indicates the case of initially free of charge channel (figure 3.19 a)). By applying equation (3.84) the azimuthal component of the magnetic field reads:

$$h_\varphi^1 = \frac{I_0}{4\pi r} \begin{cases} 0 & 0 \leq t \leq \frac{\sqrt{r^2 + z^2}}{c} \\ \frac{\beta ct - z}{\xi_{channel}} - \frac{\beta ct + z}{\xi_{image}} & t > \frac{\sqrt{r^2 + z^2}}{c} \end{cases} \quad (3.87)$$

## 2. *Initially Free of Charge Channel: Dipole Technique*

The geometry of the problem is again shown in figure 3.19. The expression describing the current distribution for the model under study is still given by equation (3.73). The dipole technique uses infinitesimal time varying dipoles as the source of the electric and magnetic fields. Since the vector potential  $\vec{A}$  can be found from the current alone, expressing the scalar potential  $\phi$  in terms of  $\vec{A}$  allows us to write the electric field in terms of the current distribution alone. To do that the Lorentz condition can be solved for  $\phi$  [27]:

$$\phi(r, z, t) = \frac{1}{\mu_0 \epsilon_0} \int_{-\infty}^t \vec{\nabla} \cdot \vec{A} d\tau + \phi(t = -\infty) \quad (3.88)$$

Substituting (3.88) into (3.83), the electric field reads:

$$\vec{e}(r, z, t) = c^2 \int_{-\infty}^t \vec{\nabla} (\vec{\nabla} \cdot \vec{A}) d\tau - \frac{\partial \vec{A}}{\partial t} \quad (3.89)$$

where  $\phi(t = -\infty) = 0$  is assumed. Equation (3.75) can be used to write  $\vec{A}$  for an infinitesimal dipole carrying current  $i(t)$  oriented in the  $z$  direction and located at  $z'$  as shown in figure 3.20:

$$d\vec{A}(r, z, t) = \frac{\mu}{4\pi} \frac{i(t - R/c)}{R} dz' \hat{z} \quad (3.90)$$

Substituting (3.90) into (3.89) and (3.84) general expressions for the electric and magnetic fields are obtained. The process of derivation of these expressions was detailed by Uman et al. in [27]. The derived infinitesimal expressions have been already discussed in chapter 2 and reported in the expressions (2.22-2.24).

Rubinstein and Uman in [28] have derived these infinitesimal expressions for the case of a lightning step current (3.73), which read

$$de_r^1(r, z, t) = \frac{I_0 dz'}{4\pi\epsilon_0} \left[ \frac{3r(z-z')}{R^5} (t - R/c - |z'|/v) u(t - R/c - |z'|/v) + \frac{3r(z-z')}{cR^4} u(z', t - R/c - |z'|/v) + \frac{r(z-z')}{c^2 R^3} \delta(z', t - R/c - |z'|/v) \right] \quad (3.91)$$

$$de_z^1(r, z, t) = \frac{I_0 dz'}{4\pi\epsilon_0} \left[ \frac{2(z-z') - r^2}{R^5} (z', t - R/c - |z'|/v) u(z', t - R/c - |z'|/v) + \frac{2(z-z') - r^2}{cR^4} u(z', t - R/c - |z'|/v) - \frac{r^2}{c^2 R^3} \delta(z', t - R/c - |z'|/v) \right] \quad (3.92)$$

$$dh_\varphi^1(r, z, t) = \frac{I_0 dz'}{4\pi} \left[ \frac{r}{cR^4} \delta(z', t - R/c - |z'|/v) + \frac{r}{R^3} u(z', t - R/c - |z'|/v) \right] \quad (3.93)$$

The total fields can be obtained by integrating (3.91) - (3.93) between the top of the channel current path and the top of the image current path. The procedure of solving these integrals were detailed by Rubinstein and Uman [29]. The expressions derived by Rubinstein and Uman are available only for the upper part of the channel, and read:

$$e_r(r, z, t) = \frac{I_0}{4\pi\epsilon_0} \left\{ -r \left( t - \frac{z}{v} \right) \left[ \frac{1}{R_0^3} - \frac{1}{R^3} \right] + \frac{1}{vr} \left[ \frac{(a(t) - z)^3}{R^3} + \frac{z^3}{R_0^3} \right] \right\} +$$

$$- \frac{I_0 r (a(t) - z)}{4\pi\epsilon_0 c^2 R^3} \frac{1}{\left( \frac{1}{v} + \frac{(a(t) - z)}{cR'} \right)} \quad (3.94)$$

$$e_z(r, z, t) = \frac{I_0}{4\pi\epsilon_0} \left\{ \left( \frac{t}{r^2} - \frac{z}{vr^2} \right) \left[ \frac{(a(t) - z)^3}{R^3} - \frac{z^3}{R_0^3} \right] + \frac{\left( \frac{z}{v} - t \right) \frac{(a(t) - z)}{r^2} + \frac{2}{v}}{R'} \right.$$

$$\left. + \frac{\left( \frac{z}{v} - t \right) \frac{z}{r^2} - \frac{2}{v}}{R_0} - \frac{r^2}{v} \left[ \frac{1}{R^3} - \frac{1}{R_0^3} \right] \right\} - \frac{I_0 r^2}{4\pi\epsilon_0 c^2 R^3} \frac{1}{\left( \frac{1}{v} + \frac{(a(t) - z)}{cR'} \right)} \quad (3.95)$$

$$b_\varphi(r, z, t) = \frac{\mu_0 I_0 r}{4\pi r} \left[ \frac{z}{(r^2 + z^2)^{1/2}} + \frac{(a(t) - z)}{R'} \right] + \frac{\mu_0 I_0 r}{4\pi c R'^2} \frac{1}{\left[ \frac{1}{v} + \frac{(a(t) - z)}{cR'} \right]} \quad (3.96)$$

with  $R_0 = \sqrt{r^2 + z^2}$ ,  $R' = \sqrt{r^2 + (a(t) - z)^2}$  and  $a(t)$  given by (3.79). The field expressions for the image part can be obtained from (3.94)-(3.96) by changing the sign of  $z$  and by changing  $a(t)$  with  $b(t)$ , given by (3.79).

Figures 3.21, 3.22 and 3.23 show the electromagnetic field components observed at  $r = 50 \text{ m}$ ,  $z = 10 \text{ m}$  and for  $\beta = 0.4$ . In these figures the field is plotted with respect to the asymptotic value, i.e. the field produced for  $t \rightarrow \infty$ . Both the monopole and dipole techniques expressions have been plotted and, as we can see, the results are identical. The equivalence between the two approaches

was demonstrated by Rubinstein and Uman in [28]. Between the two approaches, for our analytical purposes, the monopole technique results in a more suitable analytical treatment, and will be therefore used in the following analysis.

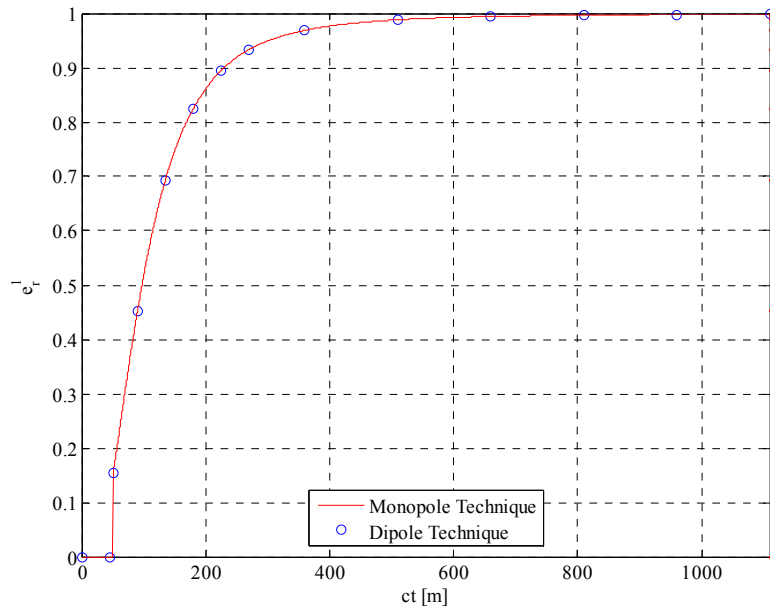


Figure 3.21: Electric field vertical component observed at  $r = 50 \text{ m}$ ,  $z = 10 \text{ m}$  and for  $\beta = 0.4$  for the model of figure 3.19 a).

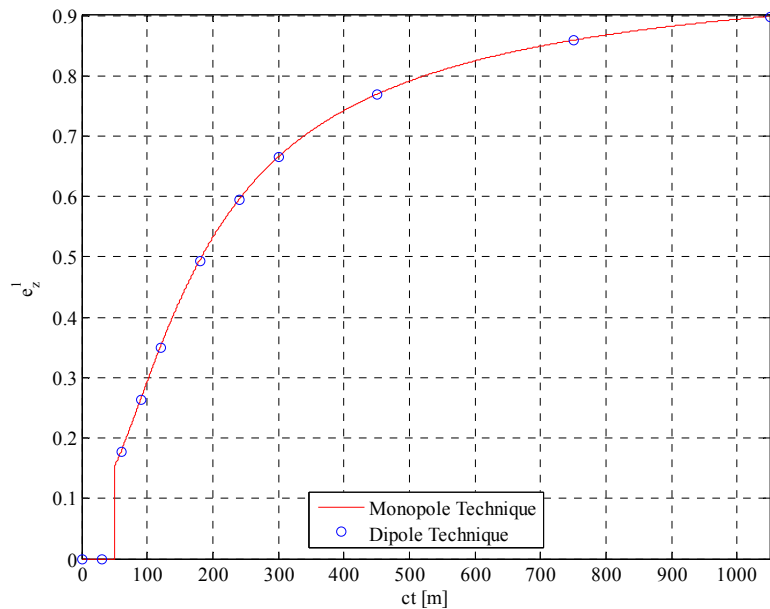


Figure 3.22: Electric field radial component observed at  $r = 50 \text{ m}$ ,  $z = 10 \text{ m}$  and for  $\beta = 0.4$  for the model of figure 3.19 a).

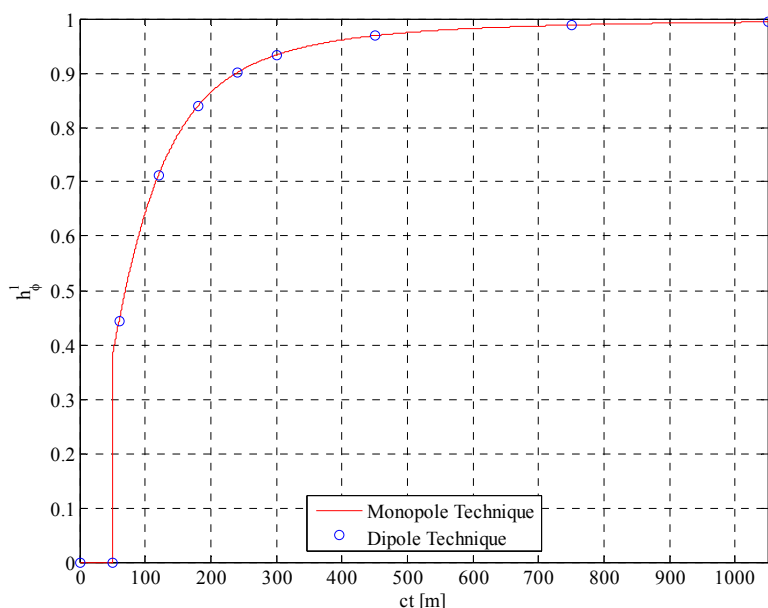


Figure 3.23: Magnetic field azimuthal component observed at  $r = 50 \text{ m}$ ,  $z = 10 \text{ m}$  and for  $\beta = 0.4$  for the model of figure 3.19 a).

In figure 3.24 the electric field is plotted for different distances and for different return stroke velocity (we recall that  $\beta = v/c$ ). In particular, figures 3.24 a) and b) show the radial and vertical component, respectively, observed at  $z = 10 \text{ m}$ ,  $r = 50 \text{ m}$  and for different values of  $\beta$ ; while figures 3.24 c) and d) show the radial and vertical component, respectively, observed at  $z = 10 \text{ m}$ , for different values of  $r$  and for  $\beta = 0.4$ . In these figures the field is again plotted with respect to the asymptotic value, i.e. the field produced for  $t \rightarrow \infty$ .

In figure 3.25 the azimuthal component of the magnetic field is plotted for different distances and for different return stroke velocity. In particular, figure 3.25 a) shows the magnetic field observed at  $z = 10 \text{ m}$ ,  $r = 50 \text{ m}$  and for different values of  $\beta$ ; while figure 3.25 b) shows the magnetic field observed at  $z = 10 \text{ m}$ , for different values of  $r$  and for  $\beta = 0.4$ . In these figures the field is again plotted with respect to the asymptotic value, i.e. the field produced for  $t \rightarrow \infty$ .

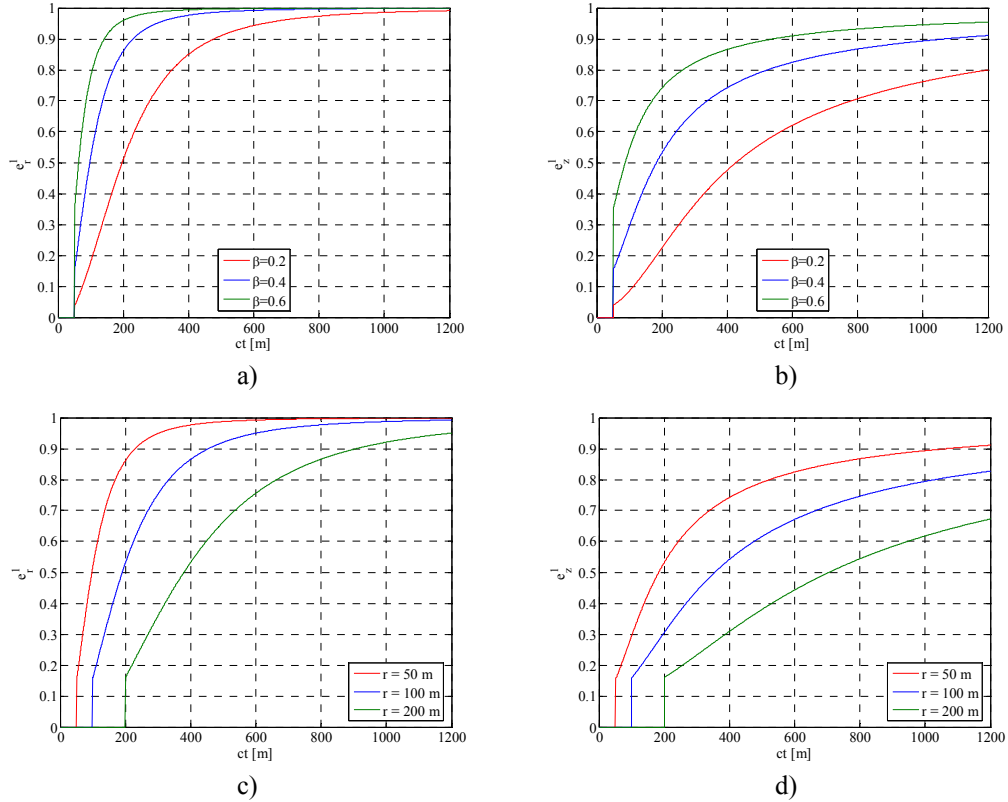


Figure 3.24: Electric field radial component observed at: a)  $z = 10$  m,  $r = 50$  m, and for different values of  $\beta$ ; c)  $z = 10$  m,  $\beta = 0.4$ , and for different values of  $r$ ; and electric field vertical component observed at: b)  $z = 10$  m,  $r = 50$  m, and for different values of  $\beta$ ; d)  $z = 10$  m,  $\beta = 0.4$ , and for different values of  $r$  (Case of figure 3.19 a).

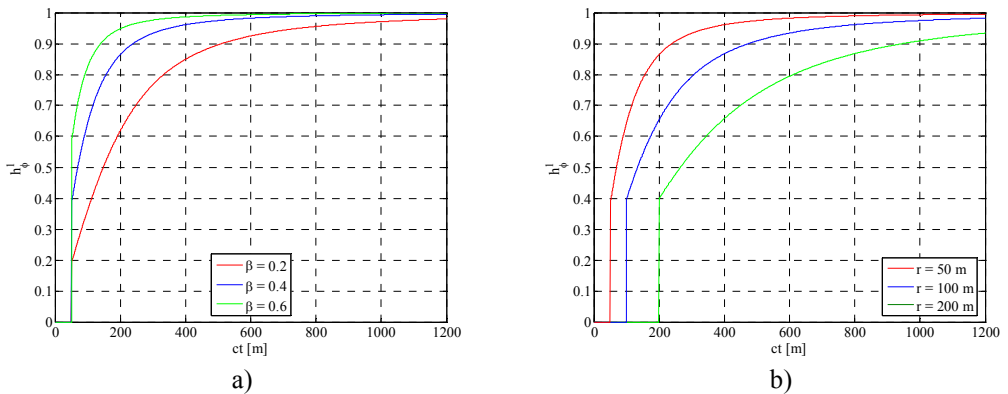


Figure 3.25: Magnetic Azimuthal component observed at  $z = 10$  m, at  $r = 50$  m and for different  $\beta$  a), and at  $z = 10$  m,  $\beta = 0.4$  and for different  $r$  c) (Case of figure 3.19 a).

### 3. *Initially Charged Channel: Monopole Technique*

The evaluation of the effects of the initially charged channel case (figure. 3.19 b)) can be carried out starting from the free of charges channel by adding the effects of an initial vertical distribution of charges  $q$ . Once the scalar potential of this distribution of charges is evaluated by applying equation (3.74), the corresponding static electric field can be easily calculated by means equation (3.83), and reads

$$e_r^s = -\frac{\zeta_0 I_0}{4\pi\beta r} \frac{2z}{\sqrt{r^2 + z^2}} \quad (3.97)$$

$$e_z^s = \frac{\zeta_0 I_0}{4\pi\beta} \frac{2}{\sqrt{r^2 + z^2}} \quad (3.98)$$

Now, the total field can be calculated by adding expression (3.97) to (3.85) and (3.98) to (3.86). Eventually, the total electric field reads

$$e_r^2 = \frac{\zeta_0 I_0}{4\pi\beta r} \begin{cases} -\frac{2z}{\sqrt{r^2 + z^2}} & 0 \leq t \leq \frac{\sqrt{r^2 + z^2}}{c} \\ \frac{\beta ct - z}{\xi_{channel}} - \frac{\beta ct + z}{\xi_{image}} & t > \frac{\sqrt{r^2 + z^2}}{c} \end{cases} \quad (3.99)$$

$$e_z^2 = \frac{\zeta_0 I_0}{4\pi\beta} \begin{cases} \frac{2}{\sqrt{r^2 + z^2}} & 0 \leq t \leq \frac{\sqrt{r^2 + z^2}}{c} \\ \frac{1/\gamma^2}{\xi_{channel}} + \frac{1/\gamma^2}{\xi_{image}} & t > \frac{\sqrt{r^2 + z^2}}{c} \end{cases} \quad (3.100)$$

where the superscript 2 indicates the case of figure 3.19 b). At last, the static distribution of charges does not produce any magnetic field, so the total one can still be evaluated by (3.87).

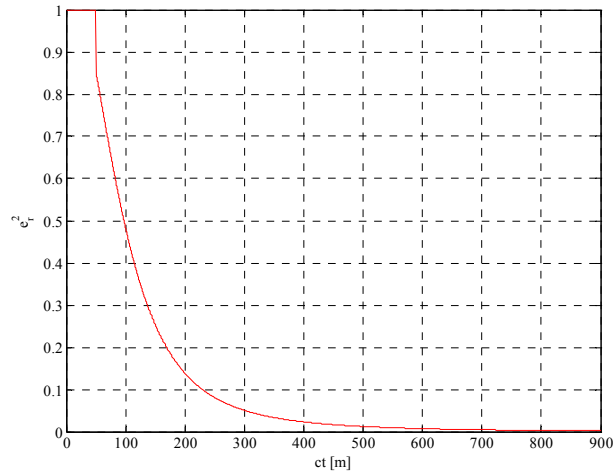


Figure 3.26: Electric field radial component observed at  $r = 50 \text{ m}$ ,  $z = 10 \text{ m}$  and for  $\beta = 0.4$  for the model of figure 3.19 b).

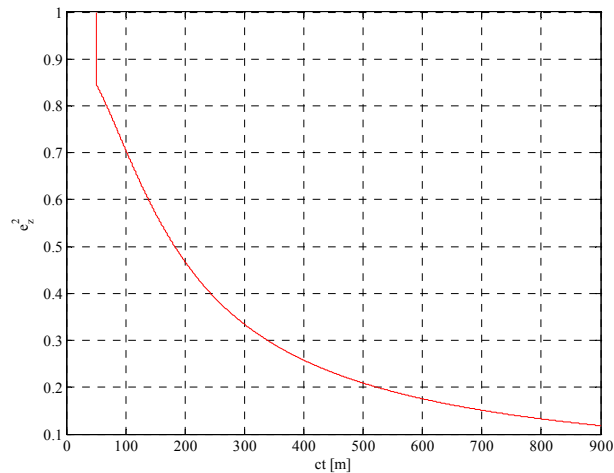


Figure 3.27: Electric field vertical component observed at  $r = 50 \text{ m}$ ,  $z = 10 \text{ m}$  and for  $\beta = 0.4$  for the model of figure 3.19 b).

At this stage we need to consider that the dipole technique gives the electromagnetic field in terms of the current distribution. Hence this technique is not able to give directly the electromagnetic field from a static distribution of charge, which can be evaluated by the usual approach for the evaluation of static fields generated by known distribution of charges.

Figures 3.26 and 3.27 show the electric field radial and vertical component, respectively, observed at  $r = 50 \text{ m}$ ,  $z = 10 \text{ m}$  and for  $\beta = 0.4$ . In these figures the field is plotted with respect to the static electric field, i.e. the field produced by the

charge deposited during the leader phase, evaluated by (3.97) and (3.98). The magnetic field is shown in figure 3.23.

### 3.5.2 Field to Transmission Line coupling

The more general and source independent approach for transmission line coupling is the Taylor et al. model [29] already detailed in chapter 2. The transmission line equations, in the time domain, are:

$$\frac{\partial}{\partial x}v(x,t) + l' \frac{\partial}{\partial t}i(x,t) = \frac{\partial}{\partial t}b_y(x,t) \quad (3.101)$$

$$\frac{\partial}{\partial x}i(x,t) + c' \frac{\partial}{\partial t}v(x,t) = -c' \frac{\partial}{\partial t} \int_0^h e_z dz$$

These equations can be equivalently rewritten in terms of only electric field components [30] as follows

$$\frac{\partial}{\partial x}v(x,t) + l' \frac{\partial}{\partial t}i(x,t) = \frac{\partial}{\partial x} \int_0^h e_z dz + [e_x(x,h,t) - e_x(x,0,t)] \quad (3.102)$$

$$\frac{\partial}{\partial x}i(x,t) + c' \frac{\partial}{\partial t}v(x,t) = -c' \frac{\partial}{\partial t} \int_0^h e_z dz$$

where  $v(x,t)$  and  $i(x,t)$  are voltage and current along the line,  $l'$  and  $c'$  are the per-unit-length inductance and capacitance parameters of the line and  $e_x$  is the line axial component of the incident electric field. The equation (3.102) applies to the case of a two conductor lossless line with the conductors lying in the  $x-z$  plane, with the reference conductor located at  $z=0$  and the other conductor located at  $z=h$ , as illustrated in figure 3.28. The solution for a matched line of length  $L$  evaluated at the near end ( $x=0$ ) reads [30]:

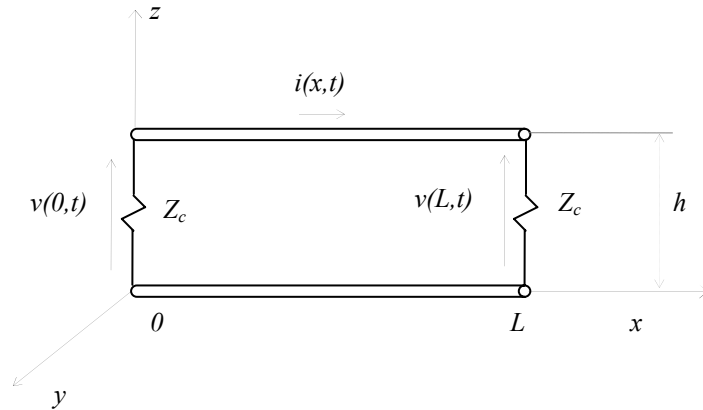


Figure 3.28: Finite length line.

$$v(0,t) - Z_c i(0,t) = v(L,t - T) - Z_c i(L,t - T) + \int_0^h e_z(0,z,t) dz - \int_0^L e_L(x,t - x/c) dx \quad (3.103)$$

where  $T = L/c$  and

$$e_L(x,t) = e_x(x,h,t) - e_x(x,0,t) \quad (3.104)$$

The solution (3.103) can be easily extended to an infinite length line. First of all we need to consider the double-finite line (figure 3.29): the total induced voltage can be obtained by adding the contribution of the left line portion  $v_l(x,t)$  to the contribution of the right line portion  $v_r(x,t)$ , which, respectively, read:

$$v_l(0,t) - Z_c i_l(0,t) = v_l(-L,t - T) - Z_c i_l(-L,t - T) + \int_0^h e_z(0,z,t) dz - \int_{-L}^0 e_L(x,t + x/c) dx \quad (3.105)$$

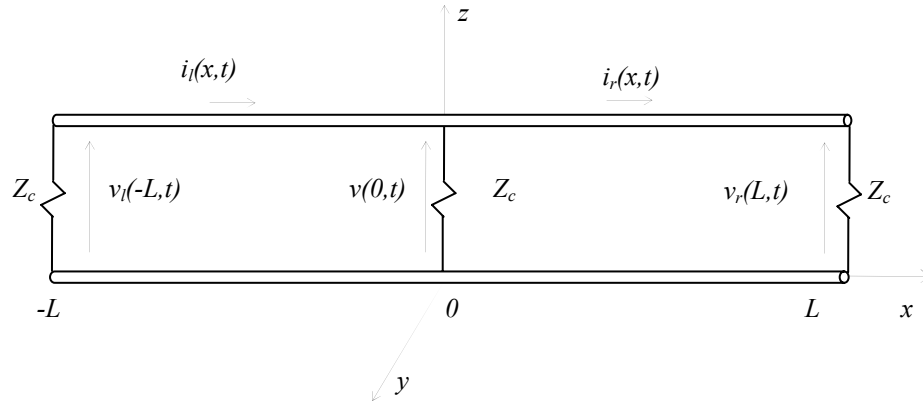


Figure 3.29: Double finite length line.

$$v_r(0,t) - Z_c i_r(0,t) = v_r(L,t-T) - Z_c i_r(L,t-T) - \int_0^h e_z(0,z,t) dz - \int_0^L e_L(x,t-x/c) dx \quad (3.106)$$

For an arbitrary abscissa  $x$ , instead of the central position  $x = 0$ , we need to consider the circuit in figure 3.30. In this instance we can write for the left and right circuits

$$v_l(x,t) - Z_c i_l(x,t) = v_l(-L,t-T) - Z_c i_l(-L,t-T) + \int_0^h e_z(x,z,t) dz - \int_{-L}^x e_L\left(\xi,t + \frac{\xi-x}{c}\right) d\xi \quad (3.107)$$

$$v_r(x,t) - Z_c i_r(x,t) = v_r(L,t-T) - Z_c i_r(L,t-T) - \int_0^h e_z(x,z,t) dz - \int_x^L e_L\left(\xi,t - \frac{\xi-x}{c}\right) d\xi \quad (3.108)$$

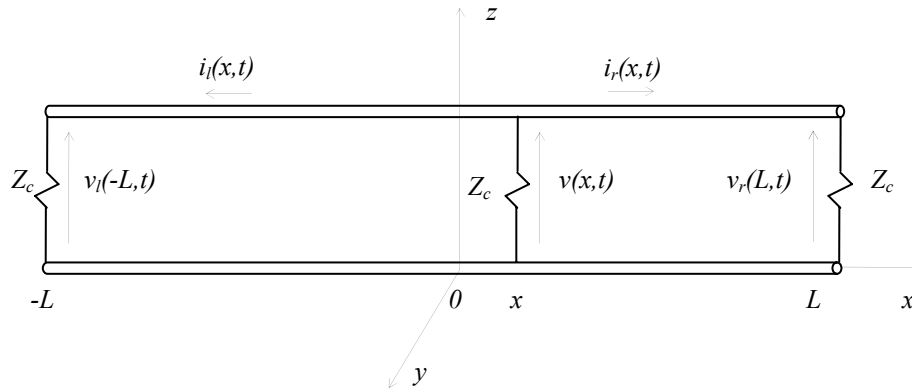


Figure 3.30: Double finite length line.

If the two circuits became two semi-infinite length lines, the terminal effects disappear and (3.107) and (3.108) became

$$v_l(x, t) = -\frac{1}{2} \int_0^h e_z(x, z, t) dz + \frac{1}{2} \int_x^{-\infty} e_L \left( \xi, t + \frac{\xi - x}{c} \right) d\xi \quad (3.109)$$

$$v_r(x, t) = -\frac{1}{2} \int_0^h e_z(x, z, t) dz - \frac{1}{2} \int_x^{\infty} e_L \left( \xi, t - \frac{\xi - x}{c} \right) d\xi \quad (3.110)$$

Considering the superposition principle of the effects produced by the two circuits, we obtain the solution at an arbitrary abscissa  $x$  for an infinite length line

$$v(x, t) = -\int_0^h e_z(x, z, t) dz - \frac{1}{2} \int_x^{\infty} e_L \left( \xi, t - \frac{\xi - x}{c} \right) d\xi - \frac{1}{2} \int_{-\infty}^x e_L \left( \xi, t + \frac{\xi - x}{c} \right) d\xi \quad (3.111)$$

### 3.5.3 Induced Voltages appraisal

In this paragraph the exact formulae for the induced overvoltage calculation will be derived both for the case of initially free of charge channel (figure 3.19 a))

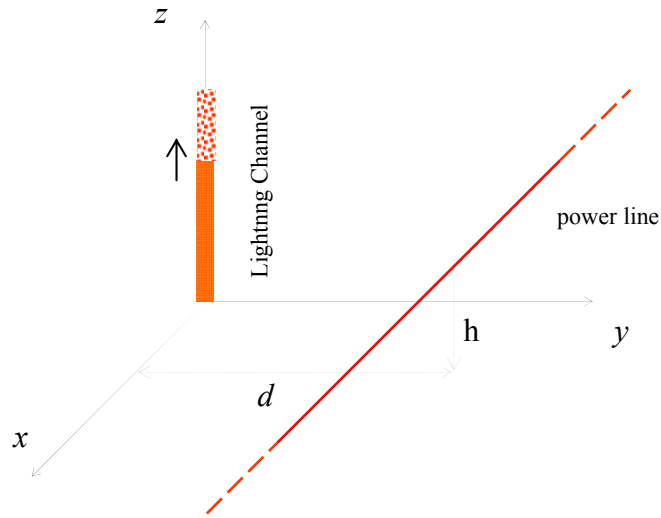


Figure 3.31: Geometry of the problem.

and for that of initially charged channel (figure 3.19 b)). The geometry of the problem is shown in figure 3.31.

First of all, we note that for the case of perfect conducting ground in (3.104) the term  $e_x(x, z = 0, t)$  is zero and so we are left only with  $e_x(x, z = h, t)$ . In order to evaluate (3.111) we need to calculate the two field components  $e_x$  and  $e_z$ . Expression of  $e_x$  results from projecting the radial field  $e_r$  along the line axis

$$e_x = \frac{x}{r} e_r \quad (3.112)$$

with  $e_r$  given by (3.85) or (3.99), while  $e_z$  given by (3.86) or (3.100).

### 1. *Initially free of charge channel*

In this case, no voltage is induced before the line is reached by the propagation of the lightning electromagnetic field. Hence, the following

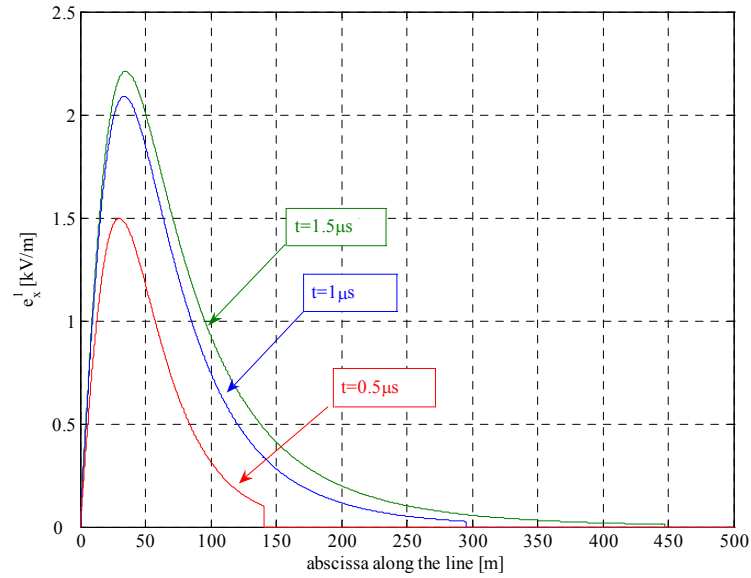


Figure 3.32: Electric field axial component exciting a 10 m height line put at 50 m far apart from the lightning channel for the event of figure 3.19 a). The field is observed for different time values and for a lightning event with  $I_0 = 10$  kA and for  $\beta = 0.4$ .

calculations will refer to  $ct > \sqrt{x^2 + d^2 + h^2}$ . Now, starting from (3.112) and (3.85), we can write

$$e_x^1 = \frac{\zeta_0 I_0}{4\pi\beta} \frac{x}{d^2 + x^2} \left( \frac{\beta ct - h}{\sqrt{(\beta ct - h)^2 + \delta^2}} - \frac{\beta ct + h}{\sqrt{(\beta ct + h)^2 + \delta^2}} - \frac{2h}{\sqrt{x^2 + d^2 + h^2}} \right) \quad (3.113)$$

with  $\delta = \sqrt{\frac{d^2 + x^2}{\gamma^2}}$ . A plot of the axial component of the electric field in figure 3.32 is shown. We have plotted the field along the line for different time values. It is worth noting the breaking effect produced by the propagation of the electromagnetic field. As far as the vertical component,  $e_z^1$  is the one given in (3.86). Now that all the field components are available, the three integrals in (3.111) can be evaluated. It is simple to evaluate the first integral in (3.111), and the solution reads

$$\int_0^h e_z^1(x, z, t) dz = \frac{\zeta_0 I_0}{4\pi\beta} \left[ \frac{1}{\gamma^2} \ln \frac{\beta ct + h + \sqrt{(\beta ct + h)^2 + \delta^2}}{\beta ct - h + \sqrt{(\beta ct - h)^2 + \delta^2}} - 2 \ln \frac{h + \sqrt{h^2 + d^2 + x^2}}{\sqrt{d^2 + x^2}} \right] \quad (3.114)$$

The two remaining integrals in (3.111), considering (3.113) become

$$\int_x^\infty e_L^1\left(\xi, t - \frac{\xi - x}{c}\right) d\xi = \int_x^{x_l} e_x^1\left(\xi, h, t - \frac{\xi - x}{c}\right) d\xi \quad (3.115)$$

$$\int_{-\infty}^x e_L^1\left(\xi, t + \frac{\xi - x}{c}\right) d\xi = \int_{x_l'}^x e_x^1\left(\xi, h, t + \frac{\xi - x}{c}\right) d\xi \quad (3.116)$$

The integration limit  $x_l$  in (3.115) is obtained by adding a time delay  $(\xi - x)/c$  to a time varying breaking point given by

$$b_l = \sqrt{(ct)^2 - d^2 - h^2} \quad (3.117)$$

This breaking point splits the line into two regions: one illuminated by the field and one not yet illuminated, while the addition counts the propagation of the field along the line. The integration limit therefore reads

$$x_l = \frac{1}{2} \frac{(ct + x)^2 - h^2 - d^2}{ct + x} \quad (3.118)$$

The same applies to the integration limit  $x_l'$  in (3.116), but the time delay this time is  $(x - \xi)/c$  and the time varying breaking point is, for symmetry reasons,  $-b_l$ . The integration limit  $x_l'$  therefore reads

$$x'_l = -\frac{1}{2} \frac{(ct-x)^2 - h^2 - d^2}{ct-x} \quad (3.119)$$

A complete description of the process for getting the solution of the integrals (3.115) and (3.116) is given in appendix A.1. The solution of (3.116) is given by

$$\int_x^{x_l} e_x^1 \left( x, h, t - \frac{\xi - x}{c} \right) d\xi = \frac{\zeta_0 I_0}{4\pi\beta} \cdot \left\{ \ln \frac{\tau_p - \beta x_l + \sqrt{(\beta x_l - \tau_p)^2 + \delta_l^2}}{\tau_m - \beta x_l + \sqrt{(\beta x_l - \tau_m)^2 + \delta_l^2}} + \ln \frac{\tau_m - \beta x + \sqrt{(\beta x - \tau_m)^2 + \delta^2}}{\tau_p - \beta x + \sqrt{(\beta x - \tau_p)^2 + \delta^2}} + \right. \\ \left. + \beta \left[ -\ln \frac{x_l - \beta \tau_m + \sqrt{(\beta x_l - \tau_m)^2 + \delta_l^2}}{x_l - \beta \tau_p + \sqrt{(\beta x_l - \tau_p)^2 + \delta_l^2}} + \ln \frac{x - \beta \tau_m + \sqrt{(\beta x - \tau_m)^2 + \delta^2}}{x - \beta \tau_p + \sqrt{(\beta x - \tau_p)^2 + \delta^2}} \right] + \right. \\ \left. + \ln \frac{-h + \sqrt{d^2 + h^2 + x^2}}{h + \sqrt{d^2 + h^2 + x^2}} + \ln \frac{h + \sqrt{d^2 + h^2 + x_l^2}}{-h + \sqrt{d^2 + h^2 + x_l^2}} \right\} \quad (3.120)$$

with  $\tau_m = \beta(ct-x) - h$ ,  $\tau_p = \beta(ct-x) + h$  and  $\delta_l = \sqrt{\frac{d^2 + x_l^2}{\gamma^2}}$ . The solution of (3.116) can be obtained by changing the sign of  $x$  in (3.120). By putting (3.116), once with  $x$  and once with  $-x$  and (3.114) in (3.111), we obtain the *exact closed form solution* for the induced voltage at an arbitrary abscissa along the line for the case of figure 3.19 a) which reads

$$v(x,t) = v_1(x,t) + v_1(-x,t) + v_2(x,t) + v_2(-x,t) \quad (3.121)$$

with

$$v_1(x,t) = \frac{\zeta_0 I_0}{8\pi\beta} \left[ \ln \frac{\tau_m - \beta x_l + \sqrt{(\tau_m - \beta x_l)^2 + \delta_l^2}}{\tau_p - \beta x_l + \sqrt{(\tau_p - \beta x_l)^2 + \delta_l^2}} + \beta \ln \frac{x_l - \beta \tau_m + \sqrt{(\beta x_l - \tau_m)^2 + \delta_l^2}}{x_l - \beta \tau_p + \sqrt{(\beta x_l - \tau_p)^2 + \delta_l^2}} - \beta \ln \frac{x - \beta \tau_m + \sqrt{(\beta x - \tau_m)^2 + \delta^2}}{x - \beta \tau_p + \sqrt{(\beta x - \tau_p)^2 + \delta^2}} \right] \quad (3.122)$$

$$v_2(x,t) = \frac{\zeta_0 I_0}{8\pi\beta} \left[ \beta^2 \ln \frac{\beta ct + h + \sqrt{(\beta ct + h)^2 + \delta^2}}{\beta ct - h + \sqrt{(\beta ct - h)^2 + \delta^2}} + \ln \frac{h + \sqrt{d^2 + h^2 + x_l^2}}{-h + \sqrt{d^2 + h^2 + x_l^2}} \right] \quad (3.123)$$

Solution (3.121) can be specified for the abscissa right in front of the lightning channel  $v^0(t) = v(0,t)$ , this particular value is used in the IEEE Standard 1410 [1].

This expression reads:

$$v^0(t) = v_1^0(t) - v_2^0(t) \quad (3.124)$$

with

$$v_1^0(t) = \frac{\zeta_0 I_0}{4\pi\beta} \left[ \ln \frac{\tau - \beta x_l + \sqrt{(\tau - \beta x_l)^2 + \delta_l^2}}{-h + \sqrt{d^2 + h^2 + x_l^2}} + \beta \ln \frac{x_l - \beta \tau + \sqrt{(\tau - \beta x_l)^2 + \delta_l^2}}{-\beta \tau + \sqrt{\tau^2 + \delta^2}} - \beta^2 \ln \left( \tau + \sqrt{\tau^2 + \delta^2} \right) \right] \quad (3.125)$$

with  $\tau = \beta ct - h$ , while  $v_2^0(t)$  is obtained by changing the sign of  $h$  in  $v_1^0(t)$ .

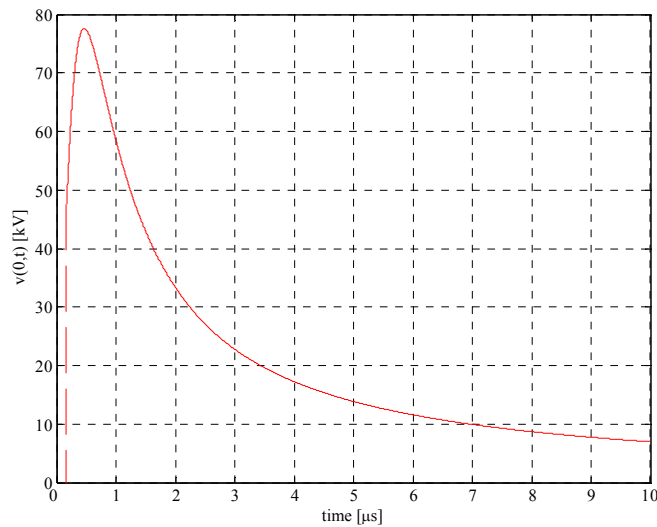


Figure 3.33. Induced voltage at  $x = 0$  of a 10 m height line put at 50 m far apart from the lightning channel, for the event of figure 3.18.a) with  $I_0 = 10$  kA and  $\beta = 0.4$ .

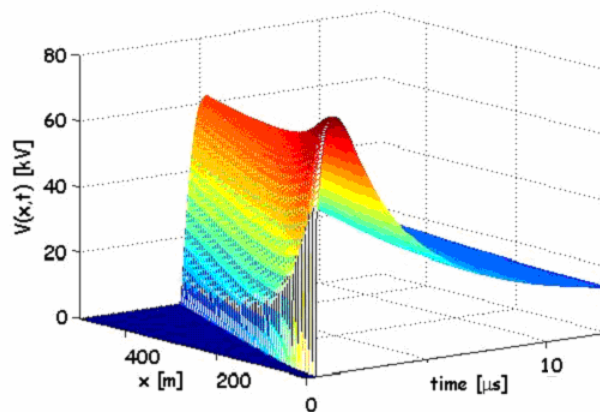


Figure 3.34: 3D plot of the induced voltage along the line for the lightning event of figure 3.33.

Figure 3.33 shows the induced voltage on a 10m height line 50m far apart from the lightning channel with  $I_0 = 10kA$  and  $\beta = 0.4$ . Figure 3.34 shows a 3D plot of the induced voltage along the line. In the plot one can see how the lightning energy is captured in the very first instants of the phenomenon, then the propagation takes place.

## 2. Initially charged channel

In this case the field  $e_x$  must be split into two contributions: the static contribution  $e_x^s$  which refers to the following range  $0 \leq ct \leq \sqrt{x^2 + d^2 + h^2}$  and is given by projecting (3.96) along the line axis, and the dynamic contribution  $e_x^d$  for  $ct > \sqrt{x^2 + d^2 + z^2}$  given by projecting (3.99) along the line axis. Hence we can write

$$e_x^s = \frac{\zeta_0 I_0}{4\pi\beta} \frac{x}{d^2 + x^2} \frac{2h}{\sqrt{d^2 + x^2 + h^2}} \quad (3.126)$$

$$e_x^d = \frac{\zeta_0 I_0}{4\pi\beta} \frac{x}{d^2 + x^2} \left( \frac{\beta ct - h}{\sqrt{(\beta ct - h)^2 + \delta^2}} - \frac{\beta ct + h}{\sqrt{(\beta ct + h)^2 + \delta^2}} \right) \quad (3.127)$$

where  $\delta$  is the same as (3.113). A plot of the axial component of the electric field is given in figure 3.35. We can observe the field along the cable for different time values. Also in this case we can observe the breaking effect produced by the propagation of the electromagnetic field.

Now we need to evaluate the three integrals in (3.111). Also in this case we will analyse the phenomenon once the field has reached the line, hence the following calculations will refer to  $ct > \sqrt{x^2 + d^2 + h^2}$ . It is simple to evaluate the first integral in (3.111), considering (3.100), and the solution reads

$$\int_0^h e_z^2(x, z, t) dz = \frac{\zeta_0 I_0}{4\pi\beta} \frac{1}{\gamma^2} \ln \frac{\beta ct + h + \sqrt{(\beta ct + h)^2 + \delta^2}}{\beta ct - h + \sqrt{(\beta ct - h)^2 + \delta^2}} \quad (3.128)$$

The two remaining integrals in (3.111), considering (3.126) and (3.127), become

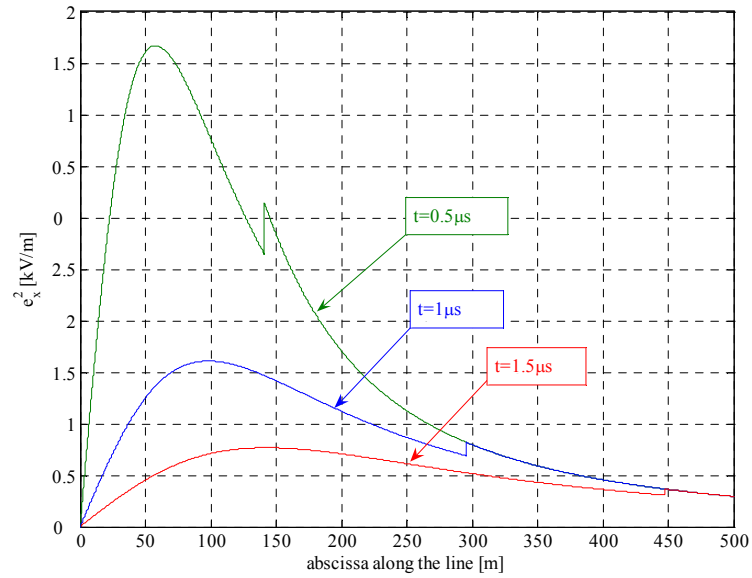


Figure 3.35: Electric field axial component exciting a 10 m height line put at 50 m far apart from the lightning channel for the event of figure 3.19 b). The field is observed for different time values and for a lightning event with  $I_0 = 10$  kA and for  $\beta = 0.4$

$$\int_x^{\infty} e_L^2 \left( \xi, t - \frac{\xi - x}{c} \right) d\xi = \quad (3.129)$$

$$\int_x^{x_l} e_x^d \left( \xi, h, t - \frac{\xi - x}{c} \right) d\xi + \int_{x_l}^{\infty} e_x^s \left( \xi, h, t - \frac{\xi - x}{c} \right) d\xi$$

$$\int_{-\infty}^x e_L^2 \left( \xi, t + \frac{\xi - x}{c} \right) d\xi = \quad (3.130)$$

$$\int_{x'_l}^x e_x^d \left( \xi, h, t + \frac{\xi - x}{c} \right) d\xi + \int_{-\infty}^{x'_l} e_x^s \left( \xi, h, t + \frac{\xi - x}{c} \right) d\xi$$

The integration limits  $x_l$  and  $x'_l$  are still given by (3.118) and (3.119). The solutions of the two integrals in (3.129) is given by

$$\begin{aligned}
 \int_x^{x_l} e_x^2 \left( x, h, t + \frac{\xi - x}{c} \right) d\xi = \frac{\zeta_0 I_0}{4\pi\beta} & \left\{ \ln \frac{\tau_p - \beta x_l + \sqrt{(\beta x_l - \tau_p)^2 + \delta_l^2}}{\tau_m - \beta x_l + \sqrt{(\beta x_l - \tau_m)^2 + \delta_l^2}} \right. \\
 & + \ln \frac{\tau_m - \beta x + \sqrt{(\beta x - \tau_m)^2 + \delta^2}}{\tau_p - \beta x + \sqrt{(\beta x - \tau_p)^2 + \delta^2}} + \ln \frac{-h + \sqrt{d^2 + h^2 + x_l^2}}{h + \sqrt{d^2 + h^2 + x_l^2}} + \\
 & \left. + \beta \left[ -\ln \frac{x_l - \beta \tau_m + \sqrt{(\beta x_l - \tau_m)^2 + \delta_l^2}}{x_l - \beta \tau_p + \sqrt{(\beta x_l - \tau_p)^2 + \delta_l^2}} + \ln \frac{x - \beta \tau_m + \sqrt{(\beta x - \tau_m)^2 + \delta^2}}{x - \beta \tau_p + \sqrt{(\beta x - \tau_p)^2 + \delta^2}} \right] \right\}
 \end{aligned}
 \tag{3.131}$$

The solution of the two integrals in (3.130) can be obtained by changing the sign of  $x$  in (3.131). The process for getting the solutions of integrals (3.129) and (3.130) is very similar to that in (3.115) and (3.116). In appendix A.1 details of this process are reported.

By putting (3.131), once with  $x$  and once with  $-x$ , and (3.128) in (3.111), we obtain the *exact closed form solution* for the induced voltage at an arbitrary abscissa along the line for the case of figure 3.19 b). It is worth noting that this solution is still given by (3.121), i.e. the induced voltage is the same both in the case of figure 3.19 a) and figure 3.19 b). This result is important since we have analytically proved the equivalence of the two lightning events of figure 3.19 when the complete approach is used. The only difference lies in the fact that for  $0 \leq ct \leq \sqrt{x^2 + d^2 + h^2}$ , i.e. when the field has not reached the line yet, theoretically, a constant value of the voltage should be considered.

In the following paragraph we can analyse the accuracy of the other closed form solution presented in literature referred to both the lightning events of figure 3.19.

### 3.6 Analysis of closed form

In this paragraph we will analyse the other closed form solution presented in literature.

#### 3.6.1 Rusck Formulae

Rusck formulae refer to figure 3.19 b). The induced voltage  $v(x,t)$  at a arbitrary line abscissa is given by (3.22) and the voltage at the point nearest to the lightning stroke ( $x = 0$ ) is given by (3.23). These two expressions find their correspondence with (3.121) and (3.124) presented in the previous paragraph. Figure 3.36 shows the voltages induced at  $x = 0$  of a line 50m far apart from the lightning channel evaluated by (3.23) and (3.124), for  $I_0 = 10kA$  and  $\beta = 0.4$ . We can see that expression (3.23) gives a steepest front and an overestimated maximum value, which can be better appreciated in the zoom presented in the figure 3.37. In figure 3.38 a plot of the peak values of the voltages induced along the line is also shown. This result is also important, since accuracy of the Rusck approach was also considered for “offset” induced voltages [10]. In this instance one can see that the Rusck expression is characterised by a small overestimate of the induced voltage for all the line abscissas.

Another interesting result is as follows: let us consider the first term of the series expansion around  $h = 0$  of (3.124):

$$v_{approx}^0(t) = \frac{\zeta_0 I_0 h}{2\pi\beta} \frac{\beta^2 ct / \gamma^2}{\left(\frac{d}{\gamma}\right)^2 + \beta^2 ct \left( ct - \sqrt{(\beta ct)^2 + \left(\frac{d}{\gamma}\right)^2} \right)} \quad (3.132)$$

as shown in Appendix A.2, we eventually get the same expression of (3.23). This means that the Rusck formula is the *first order approximation* of the exact formula (3.124), and any consideration on its accuracy and validity must be carried out in this view.

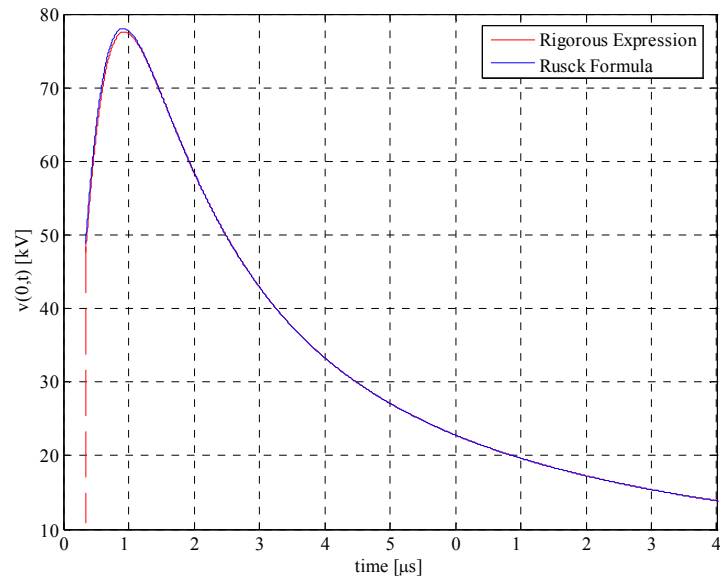


Figure 3.36 Induced voltage at  $x = 0$  of a 10 m height line put at 50 m far apart from the lightning channel with  $I_0 = 10$  kA and  $\beta = 0.4$ .

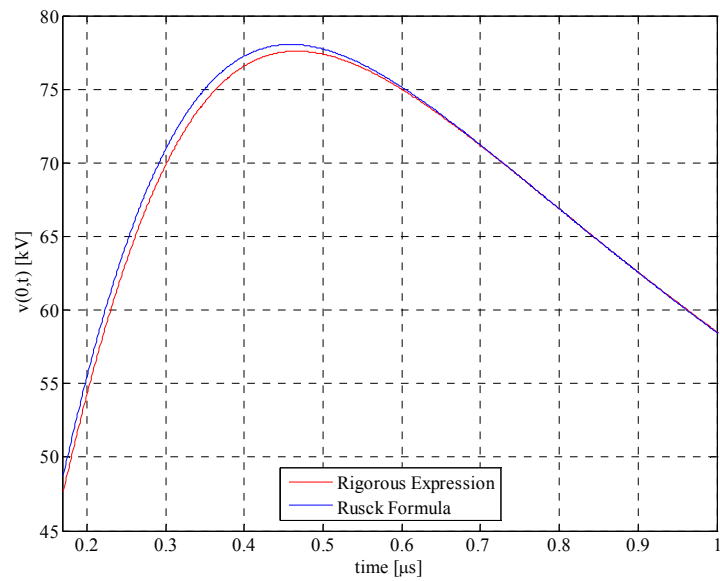


Figure 3.37: Zoom of figure 3.36 around the peak induced voltage.

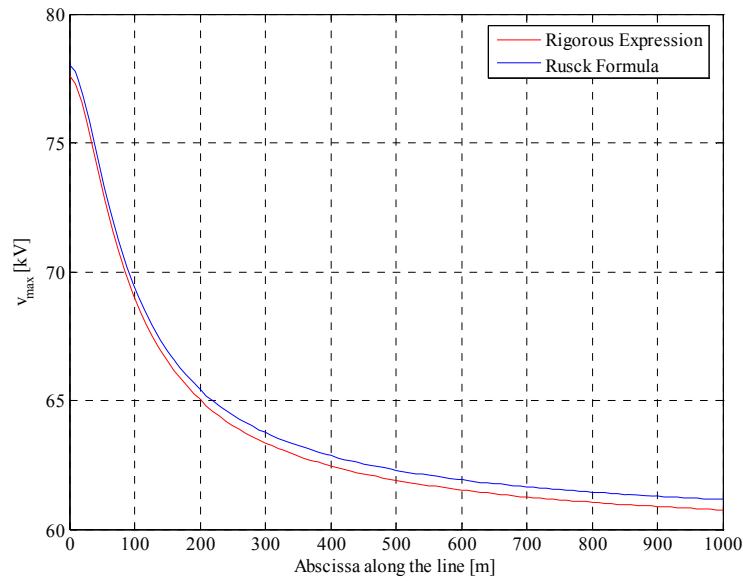


Figure 3.38: Maximum values of the induced overvoltages along a 10 m height line put at 50 m far apart from the lightning channel with  $I_0 = 10$  kA and  $\beta = 0.4$ .

### 3.6.2 Chowdhuri and Gross Formula

The Chowdhuri and Gross formula refers to figure 3.19 b). This approach refers to an initially charged channel of finite length  $h_c$ , to take into account the leader effect. The induced voltage  $v(x,t)$  at a arbitrary line abscissa is given by (3.37). Expression (3.37) finds its correspondence in our formula (3.121). We have considered formula (3.37) for  $h_c = 5$  km and the results are plotted in figure 3.39, along with our expression (3.121).

From the plots, it is clear that the missing term [11] in the model underlying the formulae lead to complete different results.

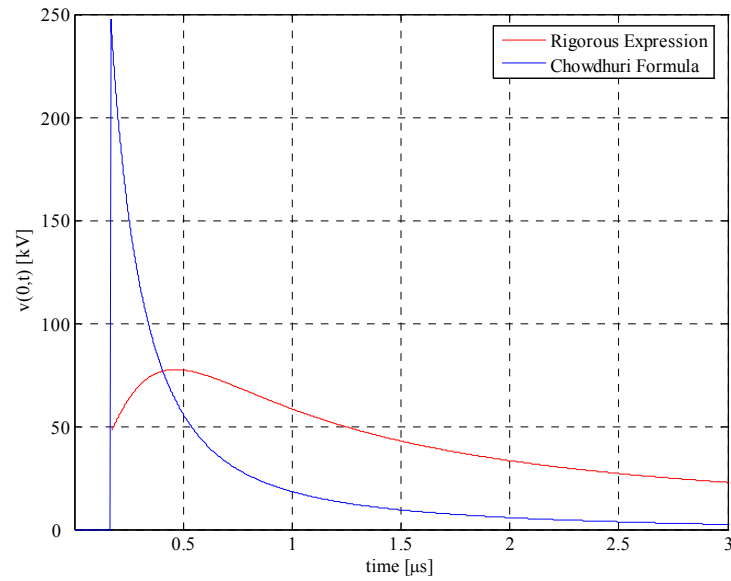


Figure 3.39: Induced voltage at  $x=0$  of a  $10\text{ m}$  height line put at  $50\text{ m}$  far apart from the lightning channel with  $I_0 = 10\text{ kA}$  and  $\beta = 0.4$ . For the Chowdhuri formula  $h_c = 5\text{ km}$ .

### 3.6.3 Liew and Mar Formulae

The Liew and Mar formula refers to figure 3.19 b). This approach refers to an initially charged channel of finite length  $h_c$ , to take into account the leader effect. The induced voltage  $v(x,t)$  at a arbitrary line abscissa is given by (3.49). Expression (3.49) finds its correspondence in our formula (3.121). We have considered formula (3.49) for  $h_c = 5\text{ km}$  and the results are plotted in figure 3.40, along with our expression (3.121).

From the plots, it is clear that the missing term [11] in the coupling model underlying the formulae leads to complete different results.

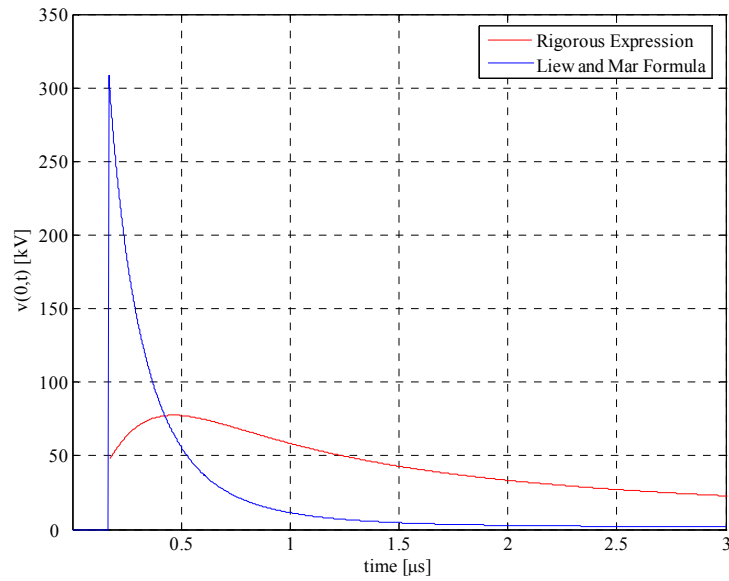


Figure 3.40: Induced voltage at  $x = 0$  of a  $10\text{ m}$  height line put at  $50\text{ m}$  far apart from the lightning channel with  $I_0 = 10\text{ kA}$  and  $\beta = 0.4$ . For the Liew and Mar formula  $h_c = 5\text{ km}$ .

### 3.6.4 Hoidalen Formulae

Hoidalen formula refers to figure 3.19 a). The voltage at the point nearest to the lightning stroke ( $x = 0$ ) is given by (3.64). This expression finds its correspondence with (3.124). A plot of (3.64) and (3.124) is presented in figure 3.41.

Since the Hoidalen approach is developed for finite length lines, we considered a suitable length line ( $300\text{ m}$ ) in order to show the “risers” effect which takes place for times greater than  $t_2$ . With a longer line this effect disappears in the graph. For  $x = 0$  the formula is identical to that of Rusck (3.23) for times less than  $t_2$ , even if calculated with another coupling model [6].

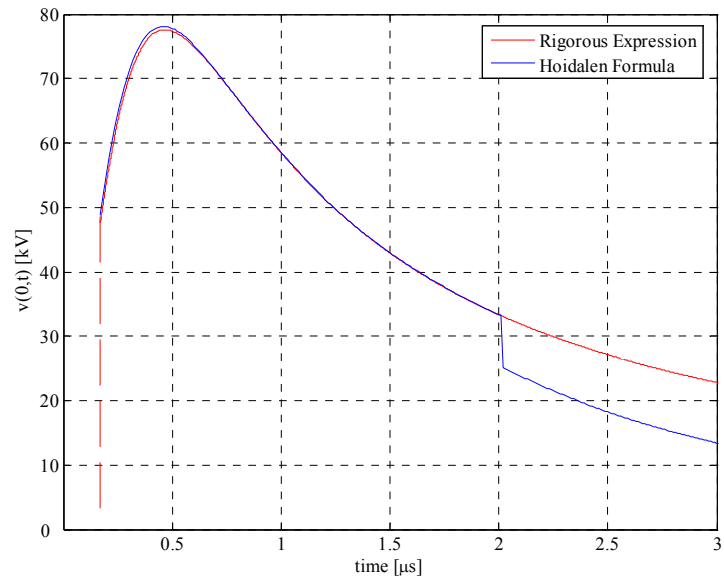


Figure 3.41: Induced voltage at  $x=0$  of a  $10\text{ m}$  height line put at  $50\text{ m}$  far apart from the lightning channel with  $I_0 = 10\text{ kA}$  and  $\beta = 0.4$ . For the Hoidalen formula  $L = 5\text{ km}$ .

## References

- [1] IEEE Guide for improving the lightning performance of electric power overhead distribution, IEEE Standard 1410, 2004.
- [2] P. Chowdhuri, "Parametric Effects on the Induced Voltages on Overhead Lines by Lightning Strokes to Nearby Ground", IEEE Trans. Power Delivery, vol.4, no.2, pp. 1185-1194, April 1989.
- [3] N.A. Katic, M.S. Savic, "Technical and economical optimisation of overhead power distribution line lightning protection", IEE Proceedings on Generation, Transmission and Distribution, Vol. 145, no. 3, pp. 239-244, May 1998.
- [4] S. Rusck, "Induced Lightning over-voltages on power transmission lines with special reference to the overvoltage protection of low-voltage networks", Trans. Royal Inst. of Tech., no. 120, pp.1-118, 1958.
- [5] P. Chowdhuri and E.T.B. Gross, "Voltage surges induced on overhead lines by lightning strokes", Proc. IEE, Vol. 114, no.12, pp. 1899-1907, Dec. 1967.
- [6] H.K. Høidalen, "Analytical Formulation of Lightning-Induced Voltages on Multiconductor Overhead Lines Above Lossy Ground", IEEE Trans. Electromagnetic Compatibility, vol.45, no.1, pp.92-100, Feb. 2003.
- [7] A.C. Liew, S.C. Mar, "Extension of the Chowdhuri – Gross Model for Lightning Induced Voltage on Overhead Lines", IEEE Trans. Power Systems, Vol. 1, no. 2, pp.240-247, 1986.
- [8] P.P. Barker, T.A. Short, A.R. Eybert-Berard and J.P. Berlandis "Induced Voltage Measurement on an experimental distribution line during nearby rocket triggered lightning flashes", IEEE Trans. Power Delivery, vol.11, no.2, pp. 980-995, April 1996.
- [9] V. Cooray "Calculating lightning-induced overvoltages in power lines. A comparison of two coupling models", IEEE Trans. Electromagnetic Compatibility, vol.36, no.3, pp. 179-182, Aug. 1994.
- [10] C.A. Nucci, F. Rachidi, M.V. Ianoz and C. Mazzetti, "Lightning-induced voltages on overhead lines", IEEE Trans. Electromagnetic Compatibility, vol.35, no.1, pp.75-86, Feb. 1993.
- [11] C.A. Nucci, F. Rachidi, M. Ianoz, C. Mazzetti, "Comparison of two coupling models for lightning-induced overvoltage calculations", IEEE Transactions on Power Delivery, vol.10, no.1, pp.330-339, Jan. 1995.
- [12] G. Cornfield, "Correspondence on reference [10]", *Proc. IEE*, vol. 119, pp. 893-894, 1972.
- [13] P. Chowdhuri, "Analysis of lightning-induced voltages on overhead lines", IEEE Trans. Power Delivery, vol.4, no.1, pp. 479-492, Jan. 1989.

- [14] P. Chowdhuri, "Lightning induced voltages on multiconductor overhead lines", IEEE Transaction on Power Delivery, vol. 5, no. 2, pp.658-667, April 1990.
- [15] H.S. Carslow, J.C. Jaeger, "Operational methods in applied mathematics", Oxford University press, 1948.
- [16] M.F. Gardner, J.L. Barnes, "Transients in linear systems", Vol.1, Wiley, 1950.
- [17] M.K. Haldar, A.C. Liew, "Alternative solution for the Chowdhuri-Gross model of lightning-induced voltages on power lines", IEE Proc., Vol. 135, Pt. C, No. 4, pp. 324-329, July 1988.
- [18] M. Rubinstein, "An approximate formula for the calculation of the horizontal electric field from lightning at close, intermediate, and long range", IEEE Trans. Electromagnetic Compatibility, vol. 38, pp. 531-535, 1996.
- [19] V. Cooray, "Horizontal fields generated by return stroke strokes," Radio Sci., vol. 27, pp. 529-537, 1992.
- [20] A. Agrawal, A. H. Price, S. Gurbaxani, "Transient response of multiconductor transmission lines excited by a nonuniform electromagnetic field", Antennas and Propagation Society International Symposium, vol.18, pp. 432-435, June 1980.
- [21] H. K. Høidalen, "Calculation of lightning induced voltages, using models", in Proc. Int. Conf. Power system Transients, Budapest, Hungary, June 20-24, pp. 359-364, 1999.
- [22] F. Rachidi, C. A. Nucci, M. Ianoz, and C. Mazzetti, "Influence of a lossy ground on lightning-induced voltages on overhead lines", IEEE Trans. Electromagnetic Compatibility, vol. 38, pp. 250-264, Aug. 1996.
- [23] R. Thottappillil and M. A. Uman, "Comparison of lightning return stroke models", *J. Geophys. Res.*, vol. 98, no. D12, pp. 22 903-22 914, 1993.
- [24] F. Rachidi, C.A. Nucci, and M. Ianoz, "Transient Analysis of Multiconductor Lines Above a Lossy Ground", IEEE Trans. Power Delivery, vol.14, no.1, pp. 294-302, Jan. 1999.
- [25] G. Diendorfer, "Induced Voltage on an Overhead Line due to nearby Lightning", IEEE Trans. Electromag. Compat., vol.32, no.4, pp. 292-299, Nov. 1990.
- [26] M. Rubinstein, M.A. Uman, "Methods for calculating the electromagnetic fields from a known source distribution: application to lightning", IEEE Trans. Electromag. Compat., vol.31, no.2, pp.183-189, May 1989.
- [27] M.A. Uman, D.K. McLain, E.P.Krider, "The electromagnetic radiation from a finite antenna", American Journal of Physics, vol.43, pp.33-38, 1975.
- [28] M. Rubinstein, M.A. Uman, "Methods for calculating the electromagnetic fields from a known source distribution: application to lightning", IEEE Trans. Electromag. Compat., vol.31, no.2, pp.183-189, May 1989.

- [29] M. Rubinstein, M.A. Uman, "Transient Electric and Magnetic Fields Associated with Establishing a Finite Electrostatic Dipole, Revisited", IEEE Trans. Electromag. Compat., vol.33, no.4, pp.312-320, November 1991.
- [30] C. Taylor, R. Satterwhite, C. Jr. Harrison, "The response of a terminated two-wire transmission line excited by a nonuniform electromagnetic field", IEEE Trans. on Antennas and Propagation, vol.13, no.6, pp. 987-989, Nov 1965.
- [31] C.R. Paul, "Analysis of Multiconductor Transmission Lines", Wiley-Interscience, John Wiley & Sons, Inc. New York, NY, USA, 1994.

## **CHAPTER 4**

### **APPLICATION TO MV DISTRIBUTION SYSTEMS FOR IMPROVING THE QUALITY OF POWER SUPPLY**

Distribution line outages due to indirect lightning strokes is one important cause of disturbances in distribution systems. The overvoltages induced by lightning on an overhead line, in fact, can cause phase to ground and phase to phase flashovers that need, for their removal, the use of recloser breakers. In the case of distribution networks the use of these breakers causes a temporal decrease of consumers voltage feeding, known as *voltage sags*. The duration of these sags depends on the cycle type of the recloser breakers, which, in turn, depends on the fault removal time. The trouble caused to customers, because of the susceptibility of some loads, may be very severe even in the case of transient faults, i.e. those which disappear after the opening and high speed reclosure of protective breakers. Hence, it is useful and important to reduce the frequency of the occurrence of faults caused by such indirect strokes.

To improve the lightning performances of overhead distribution lines, traditionally, distribution line designers use guides containing information on methods for improving system reliability and power quality or improving protection schemes, such as the use of additional reclosures or sectionalizers. By means of these methods designers may exercise control over structure material and geometry, shielding, amount of insulation, grounding, and placement of arresters.

An important tool to evaluate the lightning performances of the distribution lines, is the IEEE 1410 guide [1]. This guide is dedicated to suggest methods to estimate expected frequency of occurrence of faults due to indirect lightning of an overhead distribution line, and to suggest improvements options for lightning protections. To estimate this expected frequency of occurrence of faults the proposed method is divided into two parts:

1. evaluation of the overvoltages induced on an overhead line by an indirect lightning;
2. statistical evaluation of the behaviour of the overhead distribution line to estimate the expected frequency of lightning faults.

As far as point 1) the IEEE method suggests the Rusck formula (3.25) for the calculation of the lightning induced overvoltages, presented and discussed in chapter 3. This formula gives the maximum value of the induced voltage.

As far as point 2) the problem of the estimation of the occurrence of the lightning faults presents many uncertainties due to the random nature of the lightning phenomenon [2-4]. Hence, to obtain an estimation of the occurrence of lightning faults, a statistical treatment of the data is needed. The IEEE method follows the procedure presented by Chowdhuri in [5].

Concerning the statistical procedure, the IEEE method deals with two random variables of the lightning phenomenon: the peak value of the lightning current  $I_0$ , and the point of impact of the stroke location. Using the analytical results presented in chapter 3, we will carry out a statistical analysis which is an improvement of the IEEE method since it considers, besides the other parameters, also the return stroke velocity  $v$  as a random variable. In fact, while it is considered fixed in [1] ( $120 \text{ m}/\mu\text{s}$ ), in this work it is considered, as it must be, a random variable [4,6-9].

The chapter is organised as follows: in paragraph 4.1 the random behaviour of the lightning parameters will be analysed; the IEEE method for the lightning

performance evaluation will be summarised in paragraph 4.2; an improved procedure to evaluate the expected frequency of the lightning faults will be presented in paragraph 4.3. In paragraph 4.4, the procedure will be extended to the operating phase of distribution networks for improving the quality of power supply by means of the real-time data providing by lightning detection systems. Hence in paragraph 4.5 some recent advances in instrumentation that can be used to detect and locate cloud-to-ground lightning are summarised.

#### **4.1. Lightning parameters**

The calculation of induced overvoltages is affected by three simultaneous random variables (e.g. see equations (3.121) or (3.25)): the lightning peak current  $I_0$ , the distance between the lightning stroke point and the line  $y$ , and the return stroke velocity  $v$ . According to [1,4] the statistical variation of the lightning parameters can be approximated by standard probability distributions: the random variables  $I_0$  and  $v$  are lognormally distributed, whereas  $y$  is uniformly distributed. In [1], in order to propose a simplified approach, the lightning peak current, instead of lognormally distributed, is assumed to have the probabilistic distribution given by the expression [10]

$$P(I \geq i_0) = \frac{1}{1 + (i_0/31)^{2.6}} \quad (4.1)$$

This expression is calculated for the values of median value  $\mu = 31.1kA$  and standard deviation  $\sigma = 0.484kA$ , which are typical values [10]. We underline that (4.1) is a reasonable approximation of the corresponding lognormal distribution for a wide range of values [10].

As far as the return stroke velocity  $v$  we said that in [1] this is assumed constant to the value  $120m/\mu s$ . However, a constant value is far from the physical situation, where the return stroke velocity must be instead considered a random variable [4,6-9].

For this reason the random nature of the velocity will be assumed in what follows. For any random variable  $Z$ , the lognormal probability density function can be expressed as:

$$f_z(z, \mu, \sigma) = \frac{1}{z\sigma\sqrt{2\pi}} \exp\left\{-\frac{1}{2}\left(\frac{\ln z - \mu}{\sigma}\right)^2\right\} \quad (4.2)$$

where  $\mu$  and  $\sigma^2$  are, respectively, mean and variance of the associated normal distribution of  $Z$ . The mean value  $\mu_z$  and standard deviation  $\sigma_z$  of the random variable  $Z$  are given by:

$$\mu_z = \exp(\mu + 1/2\sigma^2) \quad (4.3)$$

$$\sigma_z^2 = \exp 2(\mu + \sigma^2) - \exp(2\mu + \sigma^2)$$

In particular, according to [4], the mean velocity is assumed equal to  $\mu_v = 76.43m/\mu s$  and the standard deviation equal to  $\sigma_v = 51.01m/\mu s$ .

As far as the distance between the lightning impact point at the ground and the line, a uniform distribution is assumed. For an interval  $[a, b]$ , this kind of distribution is expressed as

$$f_y(y, a, b) = \frac{1}{b - a} \quad (4.4)$$

with mean and variance given by

$$\mu_y = \frac{a+b}{2} \tag{4.5}$$

$$\sigma_y^2 = \frac{(b-a)^2}{12}$$

The lightning impact point is assumed within an interval  $[a, b]$ , considering  $a$  the closest point to the line and  $b$  the further point. The interval between  $a$  and  $b$  must be wide enough to include all the indirect lightning events that can cause an insulation flashover. Furthermore, as far as the closest point  $a$ , we need to consider that a stroke close to the line can strike either line conductors or ground, depending on the peak current of the return stroke. The Electrogeometric Model, proposed in [11] allows the calculation of the minimum distance below which a lightning stroke will strike directly the line. Figure 4.1 shows the application of the Electrogeometric Model which allows to evaluate whether a stroke will be direct or indirect.

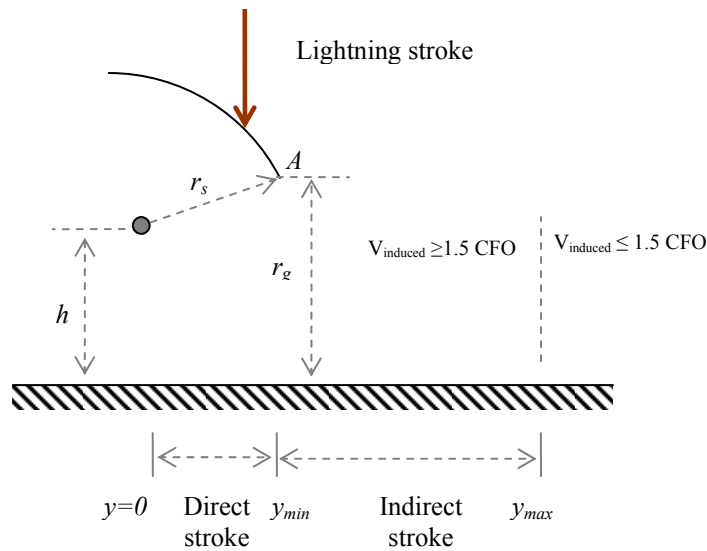


Figure 4.1: The Electrogeometric Model.

If the return stroke channel is vertical, a stroke, with a current peak  $I_0$ , will strike the phase if its final path is to the left of the intersection point  $A$ , being the arc centred on the phase and having radius  $r_s$ , calculated by means of the following expression

$$r_s = \alpha I_0^\gamma \quad (4.6)$$

with  $r_s$  the striking distance to the conductor, and  $\alpha = 10$ ,  $\gamma = 0.65$  [1]. So the minimum distance,  $y_{min}$ , is given by

$$y_{min} = \begin{cases} \sqrt{r_s^2 - (\beta r_s - h)^2} & \beta r_s > h \\ r_s & \beta r_s \leq h \end{cases} \quad (4.7)$$

where  $\beta = 0.9$  [1].

An important parameter is the ground flash density per  $\text{km}^2$  and year,  $N_g$ ; in fact, the reliability of a distribution line is dependent on its exposure to lightning. To determine exposure, the annual number of flashes per unit time needs to be known. This number is the ground flash density  $N_g$  and may be estimated from the keraunic level, using the following equation [12]

$$N_g = 0.04 T_d^{1.25} \quad \text{flashes}/\text{km}^2 / \text{yr} \quad (4.8)$$

where  $T_d$  is the number of thunderstorm days per year, (the keraunic level). Another estimate of ground flash density  $N_g$  may be obtained from thunderstorm hour records [13], as shown by the following equation

$$N_g = 0.054T_h^{1.1} \quad (4.9)$$

where  $T_h$  is the number of thunderstorm hours per year. Eventually, estimates of average ground flash density may also be obtained directly from lightning detection network data or from flash counters. If enough years are present, this has the advantage of identifying regional variations. Figure 4.2 shows the Italian isokeraunic map with the typical value of ground flash density.

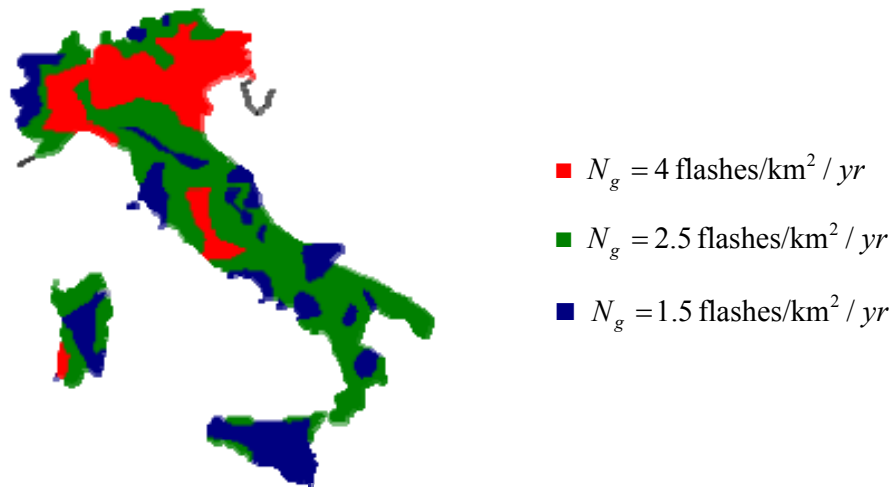


Figure 4.2 Italian isokeraunic map.

## 4.2. The IEEE Method

In this paragraph the procedure used to infer the lightning performance of a distribution line in the IEEE Guide 1410 [1] is summarised. In this guide the maximum value of the lightning induced voltages are calculated using the Rusck formula (3.25), which reads:

$$v_{\max} = \frac{\zeta_0 I_0 h}{4\pi d} \left[ 1 + \beta \frac{1}{\sqrt{2 - \beta^2}} \right] \quad (4.10)$$

Using (4.10) and by means of a statistical analysis, the IEEE method evaluates the flashover rate of the line. The results are presented in the form of a graph of flashover rate versus the insulation level of the line, i.e. the *critical flashover*. Even though the designers may be more familiar with the *basic impulse insulation level* (BIL) of a given combination of insulating materials, the results in the IEEE 1410 Guide, are given in terms of the *critical flashover* (CFO) of these combinations. The CFO is defined as the voltage level at which statistically there is a 50% chance of flashover and a 50% chance of withstand. This value is a laboratory-definable point. If a Gaussian distribution of flashover data is assumed, then any specific probability of withstand may be statistically calculated from the CFO mean value and the standard deviation [1].

The statistical procedure can be summarised as follows: the amplitude of the return stroke current is varied from 1 to 200 kA in intervals of 1 kA. For each current value, both the minimum distance  $y_{min}$ , for which lightning will not divert to the line, and the maximum distance  $y_{max}$ , at which the stroke may produce an insulation flashover are calculated. The number of annual flashover per km of distribution line  $F_p$  is obtained as the summation of the contributions from all intervals considered as expressed by [5]

$$F_p = 2 \sum_{i=1}^{200} (y_{max}^i - y_{min}^i) N_g P_i \quad (4.11)$$

where  $P_i$  is the probability of current peak to be within interval  $i$ ; it is determined as the difference between the probability for current to be equal or larger than the lower limit and the probability for current to reach or exceed the higher limit of the interval. For the probabilistic distribution of the lightning current peak, the expression (4.1) is adopted while the value of the return stroke velocity  $v$  is chosen equal to  $120m/\mu s$ .

The minimum distance  $y_{min}$  is evaluated by means of equation (4.7), while the maximum distance  $y_{max}$  for every peak current interval is the maximum

distance for which lightning stroke may produce insulation flashover (figure 4.1). According to [1], the minimum overvoltage which can produce an insulation flashover is assumed  $v_{\min} = 1.5 \times \text{CFO}$ . The 1.5 factor is an approximation that accounts for the turnup in the insulation volt-time curve. This approximation is used for induced voltage, shield wire, and arresters-spacing calculations. These voltages are assumed to have much shorter duration waveshape than the standard  $1.2/50 \mu\text{s}$  [1].

The results for an ungrounded overhead 10 m high line are shown in figure 4.3. The ungrounded circuit does not have a grounded neutral wire or a shield wire, such as a typical Italian MV distribution network. In the figure 4.3 also the results relevant to a grounded neutral or shielding wire are reported. These results are obtained in [1] from the preceding ones by applying a scale factor of 0.75 to the induced voltages.

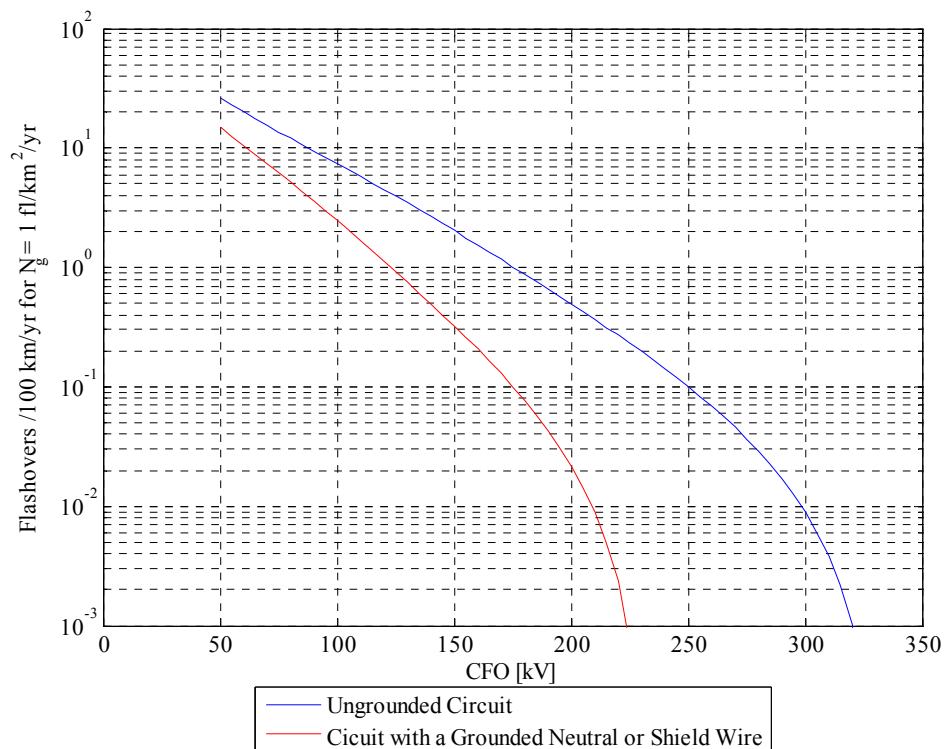


Figure 4.3: Number of annual induced flashover versus critical flashover. The curves are obtained by applying the IEEE method.

From figure 4.3 we note that induced voltage flashover frequency may dramatically increase for low levels of insulation. The values are normalised for a ground flash density of  $N_g = 1 \text{ flashes/km}^2 / \text{yr}$ .

### 4.3. Method Based on Monte Carlo Technique

In this paragraph we use a procedure for the evaluation of the distribution line performances based on the application of the Monte Carlo technique. This technique has already adopted by others authors, e.g. [14].

In this procedure the lightning induced voltages will be evaluated using equation derived in chapter 3, which reads:

$$v^0(t) = v_1^0(t) - v_2^0(t) \quad (4.12)$$

with

$$v_1^0(t) = \frac{\zeta_0 I_0}{4\pi\beta} \left[ \ln \frac{\tau - \beta x_l + \sqrt{(\tau - \beta x_l)^2 + \delta_l^2}}{-h + \sqrt{d^2 + h^2 + x_l^2}} + \beta \ln \frac{x_l - \beta\tau + \sqrt{(\tau - \beta x_l)^2 + \delta_l^2}}{-\beta\tau + \sqrt{\tau^2 + \delta^2}} - \beta^2 \ln(\tau + \sqrt{\tau^2 + \delta^2}) \right] \quad (4.13)$$

and  $v_2^0(t)$  obtained by changing the sign of  $h$  in  $v_1^0(t)$ , and the other symbols meaning already given in (3.124).

The Monte Carlo technique is a statistical process, which operates generating casual variables (i.e.  $I_0$ ,  $v$ ,  $d$ ) and produces as result the probability function of the output variable (i.e.  $v_{max}$ ). Monte Carlo simulation is a widely used computational method already used in many power system applications. In this

study we generate a significant number of events, each characterised by the following random variables:

- o the peak value of the lightning current  $I_0$  ;
- o the return stroke velocity  $v$  ;
- o the position of the stroke location with respect to the line.

Now we will first make a comparison between the statistical method based on our formula (4.12) and the IEEE method based on the Rusck formula, when the same probability distribution of the lightning current (4.1), the same values of return stroke velocity ( $120m/\mu s$ ), and the same lateral distance expression (4.7) are assumed.

The results of the comparison are shown in figure 4.4. A 10 m height line has been considered and  $N_g = 1 \text{ flashes/km}^2/\text{yr}$ . The plot shows that, for this case, the two methods predict basically the same results.

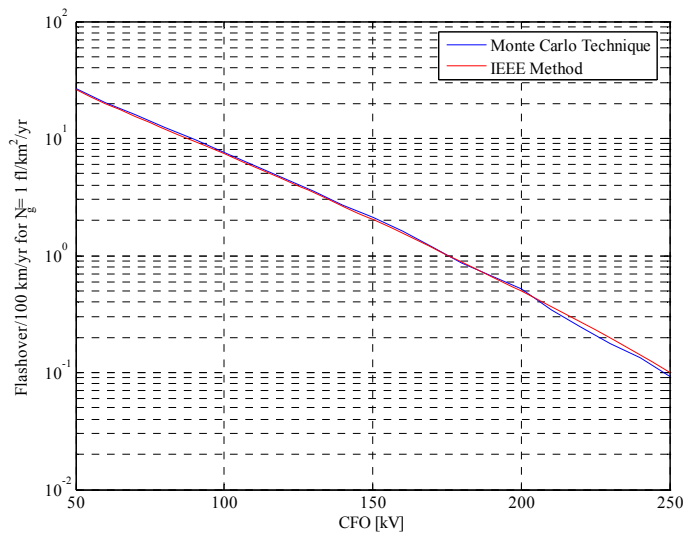


Figure 4.4: Number of annual induced flashover versus critical flashover.

We have then repeated our computation by setting the return stroke velocity as a lognormal probability density function of mean  $\mu_v = 76.43m/\mu s$  and standard deviation  $\sigma_v = 51.01m/\mu s$ . The results are presented in figure 4.4, along with the results computation with constant return stroke velocity  $v = 120m/\mu s$ .

Figure 4.5 shows that by considering the return stroke velocity as a random variable, the expected number of annual induced flashover decreases.

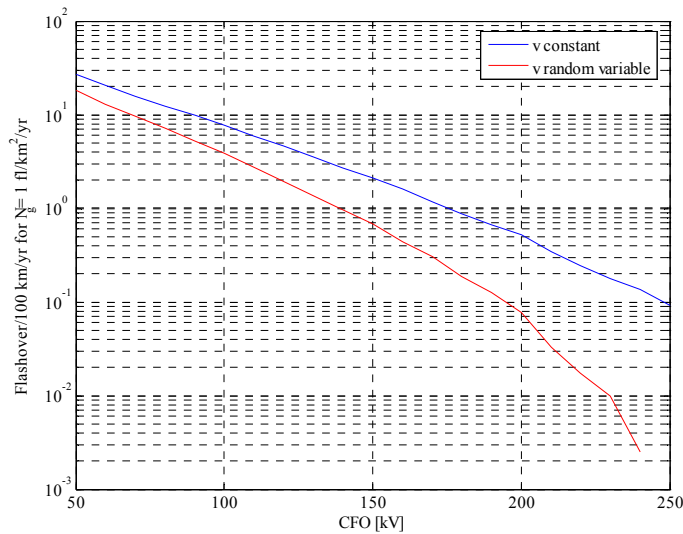


Figure 4.5: Number of annual induced flashover versus critical flashover.

#### 4.4. Application to operating condition of MV Distribution Network

Lightning Detection Network are used in order to obtain accurate data on the time, location, amplitude, and polarity of the individual return strokes in cloud-to-ground flashes. In power system operation, data providing by lightning detection networks are usually stored and used for the classification of faults on transmission and distribution systems and the evaluation of the performance of various methods that are used in lightning protection, as discussed in the first part of this chapter. The knowledge of the time, location, and peak current of each return stroke provides a valuable empirical database with which to address the key

issues. A comprehensive review on lightning detection network, with some useful observations on the use of lightning data by power utilities, is presented in [15].

The lightning detection network data can be used to understand and quantify the performance of transmission and distribution systems that are exposed to lightning. Figure 4.6 shows an “*asset exposure map*” for a power line. The number of these events characterizes the exposure of the line to nearby and direct lightning strikes during the observation time.

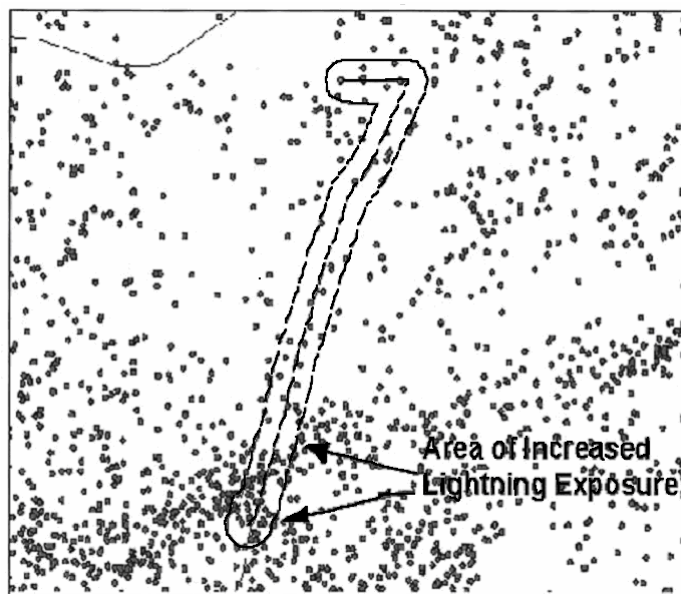


Figure 4.6: A map of the could to ground strokes that struck in the region of power line, adapted from [16].

Real-time lightning data can also be combined with online monitoring of circuit breakers, relays, and/or substation alarms to improve operations and minimize damage. Typical practice is to clear nonpersistent faults, such as lightning, with an instantaneous circuit breaker or relay operation. During lightning storms, however, multiple strokes, improper relay reclosures, or temporary faults that persist for the duration of the breaker sequence can cause feeder lockouts. Such lockouts can be restored by reclosing the feeder breaker, but an important concern at the time of lockout is whether or not the fault is permanent or whether it was caused by lightning. The real-time lightning data

provide this information, giving utilities a powerful tool both for averting damage to and speeding the restoration of their systems. In this view real-time data can also be useful to define an optimal control strategy of distribution network for improving the quality of service. In fact these data can be used to evaluate the location, amplitude, and polarity of the individual return strokes that, in real time, by means of a statistical procedure, provide a probability distribution of the expected induced overvoltages. For example the use of procedure presented in paragraph 4.3, provide a expected frequency of induced voltages occurrence.

As application now we will evaluate this occurrence by means of a statistical method based on our formula (4.12), when the probability distribution of the lightning current (4.1) is assumed, and the return stroke velocity is assumed lognormally distributed with probability density function of mean  $\mu_v = 76.43m/\mu s$  and standard deviation  $\sigma_v = 51.01m/\mu s$  and considering  $N_g = 1 \text{ flashes}/\text{km}^2 / \text{yr}$ . In figure 4.7 and 4.8 the expected occurrence  $f_{v_{\max}}$  of the induced voltages maximum value  $v_{\max}$  on the line is plotted.

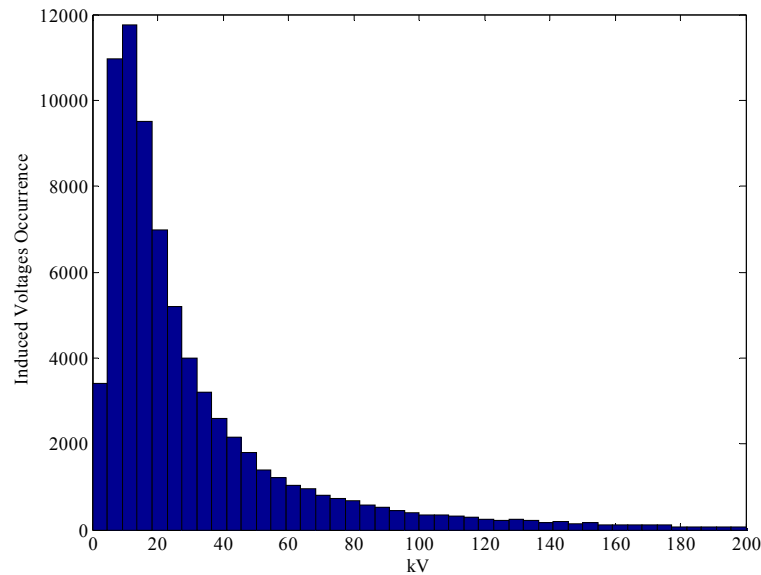


Figure 4.7: occurrence of the induced voltages maximum value for an interval 2 km centred on the line.

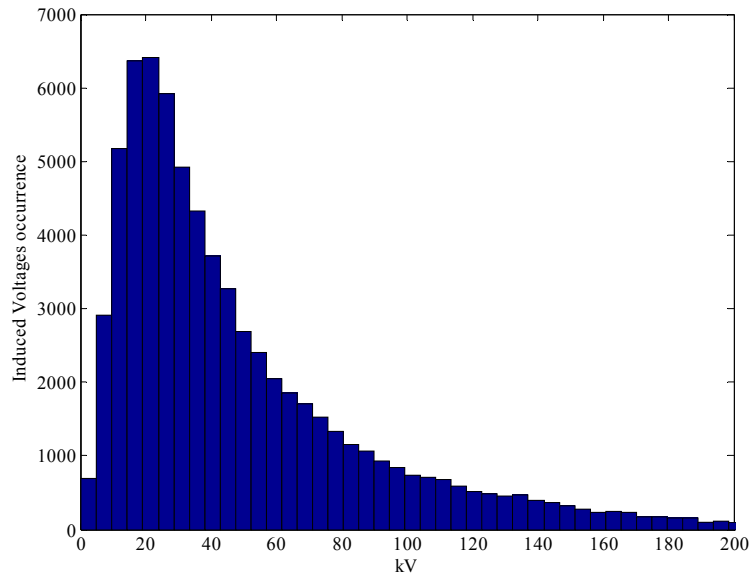


Figure 4.8: occurrence of the induced voltages maximum value for an interval 1 km centred on the line.

Figure 4.7 refers to an area wide 2 km centred on the line and figure 4.8 refers to an area wide 1 km centred on the line. For both the figure we have generated  $8 \cdot 10^4$  events for the Monte Carlo technique.

From the expected occurrence  $f_{v_{\max}}$  of  $v_{\max}$  we can also evaluate, for each area, the cumulative probability function  $F_{v_{\max}}$  of  $v_{\max}$  by means of

$$F_{v_{\max}}(v^*) = \int_0^{v^*} f_{v_{\max}}(v) dv \quad (4.14)$$

$F_{v_{\max}}$  allows us to determine different area around the line each characterised by a  $F_{v_{\max}}$  (figure 4.9). Eventually, if the CFO of the line is known, this information provide also the probability of flashover (e.g. with the same procedure defined in the previous paragraph) or fault hazard.

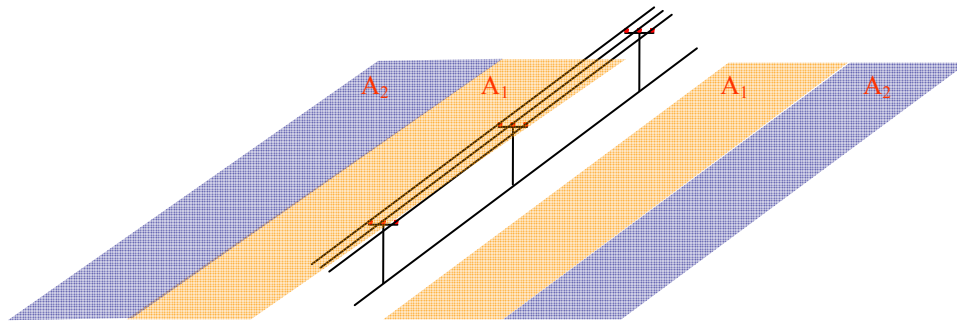


Figure 4.9: Each area around the line is characterised by a fault hazard.

In conclusion, the data provided by the lightning detection network can give, in real time, the feature of the lightning parameters. By means of these data we are able to evaluate the actual fault hazard for each area around the line. Consequently, by the tracking of the lightning storm, a preventive alarm can be given to improve operations in substation for minimize damage.

## References

- [1] IEEE Guide for improving the lightning performance of electric power overhead distribution, IEEE Standard 1410, 2004.
- [2] “Guide to Procedure for Estimating the Lightning Performance of Transmission Lines”, CIGRE Brochure, No. 63, October 1991.
- [3] “Characterization of Lightning Applications in Electric Power Systems”, CIGRE Brochure, No. 172, December 2000.
- [4] Lightning and Insulator Subcommittee of the T&D Committee: “Parameter of Lightning Strokes: A Review”, IEEE Transaction on Power delivery, vol. 20, No. 1, January 2005.
- [5] P. Chowdhuri, “Estimation of flashover rates of overhead power distribution lines by lightning strokes to nearby ground”, IEEE Transactions on PWDR, Vol. 4, No. 3, pp. 1982-1988, July 1989.
- [6] B. F. J. Schonland, and H. Collens, “Progressive lightning”, Proc. Royal Society, Vol. 143, Ser. A, pp. 354-674, 1934.
- [7] J.S. Boyle, R. E. Orville, “Return stroke velocity measurements in multi stroke lightning flashes”, J. Geophys. Res., vol. 81, No 24, pp. 4461-4466, August 1976.
- [8] V. P., Idone, R. E. Orville, “Lightning return stroke velocities in the Thunderstorm Research International Program (TRIP)”, J. Geophys. Res., Vol. 87, No. C7, pp. 4903-4916, June 1982.
- [9] B. F. J. Schonland, D. J. Mlan, H. Collens, “Progressive lightning II”, Proc. Royal Society, vol. 152, Ser. A, pp. 595-625, 1935.
- [10] J.G. Anderson, “Lightning performance of transmission line”, in Palo Alto (Ed.): “Transmission Line Reference Book 345 kV and above”, (CA: Elect. Power Res. Inst. , ch. 12, 2nd ed), 1987.
- [11] IEEE Working Group Report, “Calculating the Lightning Performance of Distribution Lines”, IEEE Trans. Power Delivery, vol. 5, no. 3, pp. 1408-1417, Jul 1990.
- [12] R.B. Anderson, A.J. Eriksson, “Lightning parameters for engineering application”, Electra, No. 69, 1980.
- [13] D.R. MacGorman, M.W. Maier, W.D. Rust, “Lightning strike density for the contiguous United States from thunderstorm duration records”, Report to U.S. Nuclear Regulatory Commission, NUREG/CR-3759, 1984.
- [14] A. Borghetti, C.A. Nucci, M. Paolone, “Lightning performances of distribution lines: sensitivity to computational methods and to data”, IEEE Power Engineering Society Winter Meeting, Vol. 2, pp. 796-798, 2001.

- [15] K. L. Cummins, E. P. Krider, and M. D. Malone, “The U.S. National Lightning Detection Network and Applications of Cloud-to-Ground Lightning Data by Electric Power Utilities”, IEEE Trans. on Electromagnetic compatibility, vol. 40, no. 4, November, 1998.
- [16] D. L. Van House, K. L. Cummins, and J. V. Tuel, “Applications of the U.S. National Lightning Detection Network in line reliability and fault analysis”, in Proc. CIGRE Int. Workshop Line Surge Arresters Lightning, Rio de Janeiro, Brazil, Apr. 1996.

## CONCLUSIONS

In recent years, in literature many efforts have been directed to improve the knowledge of the lightning phenomenon and its effects on power circuits. In particular, many numerical approaches have been proposed for the evaluation of the overvoltages induced on an overhead line by indirect lightning. Also closed form solutions have been proposed and it is important to underline that they are very important both in the design phase, in parametric evaluation and sensitivity analysis. All the closed form proposed so far presented in literature are approximated and/or incomplete as shown in the thesis. The first significant contribution of the thesis has been that of obtaining the *exact closed form solution*, overcoming errors and/or approximations in the closed form solutions so far available in literature. Another contribution has been that of using our exact formulation to check the accuracy of the other closed form solutions, so definitively closing a still on-going international debate. We also believe we made a contribution both for the statistical evaluation of lightning effects and to show a possible implementation during the operational phase of the results we have obtained.

## APPENDIX A.1

In this appendix details are given for the process for getting integrals (3.115), (3.116), (3.129) and (3.130) of chapter 3.

### A.1.1 Integral (3.115)

Integral (3.115) is

$$\int_x^{x_f} e^{i\left(\xi, h, t - \frac{\xi - x}{c}\right)} d\xi \quad (\text{A.1-1})$$

Now, by considering the field expression (3.85) and (3.112), we can split this integral into three parts:

$$\int_x^{x_f} \frac{\beta ct + \beta x - \beta \xi - h}{\sqrt{(\beta ct + \beta x - \beta \xi - h)^2 + \frac{d^2 + \xi^2}{\gamma^2}}} \frac{\xi}{d^2 + \xi^2} d\xi \quad (\text{A.1-2})$$

$$\int_x^{x_f} \frac{\beta ct + \beta x - \beta \xi + h}{\sqrt{(\beta ct + \beta x - \beta \xi - h)^2 + \frac{d^2 + \xi^2}{\gamma^2}}} \frac{\xi}{d^2 + \xi^2} d\xi \quad (\text{A.1-3})$$

$$\int_x^{x_f} \frac{2h}{\sqrt{\xi^2 + d^2 + h^2}} \frac{\xi}{d^2 + \xi^2} d\xi \quad (\text{A.1-4})$$

First we deal with integrals (A.1-2) and (A.1-3) which can be written as

$$\int_x^{x_l} f(\xi) d\xi = \int_x^{x_l} \frac{\tau_h - \beta\xi}{\sqrt{(\tau_h - \beta\xi)^2 + \frac{d^2 + \xi^2}{\gamma^2}}} \frac{\xi}{d^2 + \xi^2} d\xi \quad (\text{A.1-5})$$

where  $\tau_h = \tau_m$  in (A.1-2) and  $\tau_h = \tau_p$  in (A-3), with  $\tau_m = \beta(ct - x) - h$ ,  $\tau_p = \beta(ct - x) + h$ . Integral (A.1-5) can be brought to a standard form [1], and the solution reads

$$\begin{aligned} \int_x^{x_l} f(\xi) d\xi = \ln \frac{\tau_h - \beta x + \sqrt{(\beta x - \tau_h)^2 + \delta^2}}{\tau_h - \beta x_l + \sqrt{(\beta x_l - \tau_h)^2 + \delta_l^2}} + \\ + \beta \left[ \ln \frac{x - \beta \tau_h + \sqrt{(\beta x - \tau_h)^2 + \delta^2}}{x_l - \beta \tau_h + \sqrt{(\beta x_l - \tau_h)^2 + \delta_l^2}} \right] \end{aligned} \quad (\text{A.1-6})$$

As far as integral (A.1-4), it is easy to evaluate it

$$\begin{aligned} \int_x^{x_l} \frac{2h}{\sqrt{\xi^2 + d^2 + h^2}} \frac{\xi}{d^2 + \xi^2} d\xi = \\ = \ln \frac{h + \sqrt{d^2 + h^2 + x_l^2}}{-h + \sqrt{d^2 + h^2 + x_l^2}} + \ln \frac{-h + \sqrt{d^2 + h^2 + x^2}}{h + \sqrt{d^2 + h^2 + x^2}} \end{aligned} \quad (\text{A.1-7})$$

In conclusion, the solution of (A.1-1) is obtained by evaluating (A.1-6), once for  $\tau_h = \tau_m$  and once for  $\tau_h = \tau_p$ , by evaluating (A.1-7), and then by adding these three contributions. The final result reads

$$\begin{aligned}
 \int_x^{x_l} e_x^1 \left( x, h, t - \frac{\xi - x}{c} \right) d\xi &= \frac{\zeta_0 I_0}{4\pi\beta} \\
 & \left\{ \ln \frac{\tau_p - \beta x_l + \sqrt{(\beta x_l - \tau_p)^2 + \delta_l^2}}{\tau_m - \beta x_l + \sqrt{(\beta x_l - \tau_m)^2 + \delta_l^2}} + \ln \frac{\tau_m - \beta x + \sqrt{(\beta x - \tau_m)^2 + \delta^2}}{\tau_p - \beta x + \sqrt{(\beta x - \tau_p)^2 + \delta^2}} + \right. \\
 & + \beta \left[ - \ln \frac{x_l - \beta \tau_m + \sqrt{(\beta x_l - \tau_m)^2 + \delta_l^2}}{x_l - \beta \tau_p + \sqrt{(\beta x_l - \tau_p)^2 + \delta_l^2}} + \ln \frac{x - \beta \tau_m + \sqrt{(\beta x - \tau_m)^2 + \delta^2}}{x - \beta \tau_p + \sqrt{(\beta x - \tau_p)^2 + \delta^2}} \right] + \\
 & \left. + \ln \frac{-h + \sqrt{d^2 + h^2 + x^2}}{h + \sqrt{d^2 + h^2 + x^2}} + \ln \frac{h + \sqrt{d^2 + h^2 + x_l^2}}{-h + \sqrt{d^2 + h^2 + x_l^2}} \right\}
 \end{aligned} \tag{A.1-8}$$

### A.1.2 Integral (3.116)

Integral (3.116) is

$$\int_{x_l}^x e_x^1 \left( \xi, h, t + \frac{\xi - x}{c} \right) d\xi \tag{A.1-9}$$

this integral, also, by considering (3.85) and (3.112), can be split in three parts:

$$\int_{x_l}^x \frac{\beta c t - \beta x + \beta \xi - h}{\sqrt{(\beta c t - \beta x + \beta \xi - h)^2 + \frac{d^2 + \xi^2}{\gamma^2}}} \frac{\xi}{d^2 + \xi^2} d\xi \tag{A.1-10}$$

$$\int_{x_l}^x \frac{\beta c t - \beta x + \beta \xi + h}{\sqrt{(\beta c t - \beta x + \beta \xi - h)^2 + \frac{d^2 + \xi^2}{\gamma^2}}} \frac{\xi}{d^2 + \xi^2} d\xi \tag{A.1-11}$$

$$\int_{x'_l}^x \frac{2h}{\sqrt{\xi^2 + d^2 + h^2}} \frac{\xi}{d^2 + \xi^2} d\xi \quad (\text{A.1-12})$$

To solve this integral, we show that it can be brought to the same form of integral (A.1-2). Infact, by changing the sign of  $\xi$  and  $x$  in (A.1-10), we obtain the integral

$$-\int_x^{-x'_l} \frac{\beta ct + \beta x - \beta \xi - h}{\sqrt{(\beta ct + \beta x - \beta \xi - h)^2 + \frac{d^2 + \xi^2}{\gamma^2}}} \frac{\xi}{d^2 + \xi^2} d\xi \quad (\text{A.1-13})$$

with the integration limit  $-x'_l$  (given in (3.119))

$$-x'_l = \frac{1}{2} \frac{(ct + x)^2 - h^2 - d^2}{ct + x} \quad (\text{A.1-14})$$

We note that the R.H.S. of (A.1-14) is the same as (3.118). Then, the integral (A.1-13) is the same of (A.1-2), and the solution of (A.1-13) is the same solution of (A.1-2) evaluated by changing the sign of  $x$ .

We can also find, with an analogous process, that the solutions of (A.1-11) and (A.1-12) are the same of (A.1-3) and (A.1-4), respectively, evaluated by changing the sign of  $x$ . In conclusion, the solution of integral (24) is obtained by changing the sign of  $x$  in (A.1-8).

### A.1.3 Integral (3.129)

The integral (3.129) is

$$\int_x^{x'_l} e_x^d \left( \xi, h, t - \frac{\xi - x}{c} \right) d\xi + \int_{x'_l}^{\infty} e_x^s \left( \xi, h, t - \frac{\xi - x}{c} \right) d\xi \quad (\text{A.1-15})$$

First, we evaluate the solution of the first integral in (A.1-15). By considering the field expressions (3.126) and (3.127), it can be split in two parts: (A.1-2) and (A.1-3), already been evaluated in this Appendix, and the solutions are given by adding (A.1-6), evaluated for  $\tau_h = \tau_m$ , to the same (A.1-6), this time evaluated for  $\tau_h = \tau_p$ . The second integral in (A.1-15) is easy to evaluate it, and the solution reads

$$\int_{x_l}^{\infty} \frac{2h}{\sqrt{\xi^2 + d^2 + h^2}} \frac{\xi}{d^2 + \xi^2} d\xi = \ln \frac{-h + \sqrt{d^2 + h^2 + x_l^2}}{h + \sqrt{d^2 + h^2 + x_l^2}} \quad (\text{A.1-16})$$

In conclusion, the solution of (3.129) is obtained by evaluating (A.1-6), once for  $\tau_h = \tau_m$  and once for  $\tau_h = \tau_p$ , by evaluating (A.1-16), and then by adding these three contributions. The final result is reported reads

$$\begin{aligned} \int_x^{x_l} e_x^2 \left( x, h, t + \frac{\xi - x}{c} \right) d\xi = & \zeta_0 I_0 \left\{ \ln \frac{\tau_p - \beta x_l + \sqrt{(\beta x_l - \tau_p)^2 + \delta_l^2}}{\tau_m - \beta x_l + \sqrt{(\beta x_l - \tau_m)^2 + \delta_l^2}} \right. \\ & + \ln \frac{\tau_m - \beta x + \sqrt{(\beta x - \tau_m)^2 + \delta^2}}{\tau_p - \beta x + \sqrt{(\beta x - \tau_p)^2 + \delta^2}} + \ln \frac{-h + \sqrt{d^2 + h^2 + x_l^2}}{h + \sqrt{d^2 + h^2 + x_l^2}} + \\ & \left. + \beta \left[ -\ln \frac{x_l - \beta \tau_m + \sqrt{(\beta x_l - \tau_m)^2 + \delta_l^2}}{x_l - \beta \tau_p + \sqrt{(\beta x_l - \tau_p)^2 + \delta_l^2}} + \ln \frac{x - \beta \tau_m + \sqrt{(\beta x - \tau_m)^2 + \delta^2}}{x - \beta \tau_p + \sqrt{(\beta x - \tau_p)^2 + \delta^2}} \right] \right\} \end{aligned} \quad (\text{A.1-17})$$

#### A.1.4 Integral (3.130)

The integral in (3.130) is

$$\int_{x'_l}^x e_x^d \left( \xi, h, t + \frac{\xi - x}{c} \right) d\xi + \int_{-\infty}^{x'_l} e_x^s \left( \xi, h, t + \frac{\xi - x}{c} \right) d\xi \quad (\text{A.1-18})$$

By considering the field expressions (3.126) and (3.127), we note that also the first has already been evaluated in this Appendix. It can be split into two parts (A.1-10) and (A.1-11) and the solution is given by adding (A.1-6), evaluated for  $\tau = \tau_m$  and  $-x$ , to the same (A.1-6), evaluated, this time, for  $\tau = \tau_p$  and  $-x$ .

The second integral in (3.130) is

$$\int_{-\infty}^{x'_l} \frac{2h}{\sqrt{\xi^2 + d^2 + h^2}} \frac{\xi}{d^2 + \xi^2} d\xi \quad (\text{A.1-19})$$

To solve this integral we show that it can be brought to the same form of integral (A.1-16). Infact, by changing the sign of  $\xi$  and  $x$  in (A.1-16), we obtain the integral

$$- \int_{-x'_l}^{\infty} \frac{2h}{\sqrt{\xi^2 + d^2 + h^2}} \frac{\xi}{d^2 + \xi^2} d\xi \quad (\text{A.1-20})$$

By considering (A.1-13), we can observe that (A.1-20) is the same of the integral in (A.1-14). Then, the solution of (A.1-20) is given by changing the sign of  $x$  in the R.H.S. of (A.1-16). In conclusion, the solution of (3.130) is obtained by changing the sign of  $x$  in (A.1-17).

## References

- [1] I. S. Gradshteyn and I. W. Ryzhik, "Table of integral, series, and products", New York: Academic, 1980.

## APPENDIX A.2

### A.2.1 Derivation of the Rusck Formula

In this appendix we derive the formula of Rusck (3.23) from the exact closed form solution (3.124). This solution is

$$v^0(t) = v_1^0(t) - v_2^0(t) \quad (\text{A.2-1})$$

with  $v_1^0(t)$  and  $v_2^0(t)$  given in (3.125). First of all we evaluate the first term of the series expansion around  $h = 0$  of  $v_1^0(t)$  in (A.2-1). To do that we consider (3.125) and we split it in three parts as

$$v_1^0(t) = v'(t) + v''(t) + v'''(t) \quad (\text{A.2-2})$$

with

$$v'(t) = \frac{\zeta_0 I_0}{4\pi\beta} \ln \frac{\tau - \beta x_l + \sqrt{(\tau - \beta x_l)^2 + \delta_l^2}}{-h + \sqrt{d^2 + h^2 + x_l^2}} \quad (\text{A.2-3})$$

which first term of the series expansion around  $h = 0$  is zero.

The second term of (A.2-2) is

$$v''(t) = \frac{\zeta_0 I_0 h}{4\pi} \ln \frac{x_l - \beta\tau + \sqrt{(\tau - \beta x_l)^2 + \delta_l^2}}{-\beta\tau + \sqrt{\tau^2 + \delta^2}} \quad (\text{A.2-4})$$

which first term of the series expansion is

$$\left. \frac{\partial v''(t)}{\partial h} \right|_{h=0} = \frac{\zeta_0 I_0 h}{4\pi} \frac{\beta \left( -ct + \sqrt{(\beta ct)^2 + (d/\gamma)^2} \right)}{\beta^2 ct \left( -ct + \sqrt{(\beta ct)^2 + (d/\gamma)^2} \right) - (d/\gamma)^2} \quad (\text{A.2-5})$$

The third term of (A.2-2) is

$$v'''(t) = -\frac{\zeta_0 I_0 h}{4\pi} \beta \ln \left( \tau + \sqrt{\tau^2 + \delta^2} \right) \quad (\text{A.2-6})$$

which first term of the series expansion is

$$\left. \frac{\partial v'''(t)}{\partial h} \right|_{h=0} = \frac{\zeta_0 I_0 h}{4\pi} \frac{\beta}{\sqrt{(\beta ct)^2 + (d/\gamma)^2}} \quad (\text{A.2-7})$$

By adding (A.2-7) to (A.2-5) the first term of the series expansion of  $v_1^0(t)$  is obtained. Now, according to (A.2-1) we have to evaluate the first term of the series expansion of  $v_2^0(t)$  which is, however, obtained by changing the sign of  $h$  in  $v_1^0(t)$ . It can obviously be evaluated still by adding (A.2-5) to (A.2-7). Hence, the first term of the series expansion around  $h = 0$  of (A.2-1) is

$$\left. \frac{\partial v^0(t)}{\partial h} \right|_{h=0} = \frac{\zeta_0 I_0 h}{2\pi\beta} \frac{\beta^2 ct / \gamma^2}{\left(\frac{d}{\gamma}\right)^2 + \beta^2 ct \left( ct - \sqrt{(\beta ct)^2 + \left(\frac{d}{\gamma}\right)^2} \right)} \quad (\text{A.2-8})$$

Now, we show that this expression can be brought to the same form of the Rusck formula (3.23). First we rewrite (A.2-8) in a more suitable form that is

$$\left. \frac{\partial v^0(t)}{\partial h} \right|_{h=0} = \frac{\zeta_0 I_0 h}{4\pi d^2} \frac{2\beta ct}{1 + (\beta ct / d)^2} \left( \frac{(1 + (\beta ct / d)^2)(1 - \beta^2)}{1 - \beta^2 + \beta^2 \frac{ct}{d} \left( \frac{ct}{d} - \sqrt{1 + \left(\frac{\beta ct}{d}\right)^2} - \beta^2 \right)} \right) \quad (\text{A.2-9})$$

After some algebraic manipulation to the numerator and denominator of the term in the brackets we obtain

$$\left. \frac{\partial v^0(t)}{\partial h} \right|_{h=0} = \frac{\zeta_0 I_0 h}{4\pi d^2} \frac{2\beta ct}{1 + (\beta ct / d)^2} \left( 1 + \frac{\beta^2 \frac{ct}{d} \left[ \sqrt{1 + \left(\frac{\beta ct}{d}\right)^2} - \beta^2 - \left(\frac{\beta^2 ct}{d}\right) \right]}{1 - \beta^2 + \beta^2 \frac{ct}{d} \left( \frac{ct}{d} - \sqrt{1 + \left(\frac{\beta ct}{d}\right)^2} - \beta^2 \right)} \right) \quad (\text{A.2-10})$$

This expression can easily be brought to a simpler form which reads

$$\left. \frac{\partial v^0(t)}{\partial h} \right|_{h=0} = \frac{\zeta_0 I_0 h}{4\pi d^2} \frac{2\beta ct}{1 + (\beta ct/d)^2} \left( 1 + \frac{\beta^2 \frac{ct}{d} \left[ (1 - \beta^2) \left( 1 + \left( \frac{\beta ct}{d} \right)^2 \right) \right]}{(1 - \beta^2) \left[ \left( 1 + \left( \frac{\beta ct}{d} \right)^2 \right) \sqrt{1 + \left( \frac{\beta ct}{d} \right)^2 - \beta^2} \right]} \right) \quad (\text{A.2-11})$$

At last, by a trivial simplification, we obtain a simple expression which reads

$$\left. \frac{\partial v^0(t)}{\partial h} \right|_{h=0} = \frac{\zeta_0 I_0 h}{4\pi d^2} \frac{2\beta ct}{1 + (\beta ct/d)^2} \left( 1 + \beta^2 \frac{ct/d}{\sqrt{1 + \beta^2 \left[ \left( \frac{ct}{d} \right)^2 - 1 \right]}} \right) \quad (\text{A.2-12})$$

which is exactly the same of (3.23) given by Rusck.